A theoretical and empirical framework for measuring minimum conductance, an understudied plant drought trait

By
Huw F. T. Irlam

Presented in fulfilment of the requirements for the degree of

Master of Science (MSc) in Biological Sciences

by dissertation

In the Department of Biological Sciences

UNIVERSITY OF CAPE TOWN

December 2024



Supervisor: Adam G. West[1]
Co-supervisor: Robert P. Skelton[2]

[1]*Department of Biological Sciences, University of Cape Town, South Africa*

[2]*School of Animal, Plant and Environmental Science, University of the Witwatersrand, South Africa*

Acknowledgements

I thank the Du Plessis family and Cape Nature for allowing access to the Jonaskop site, and the team at Drie Kuilen Nature Reserve for graciously hosting the ongoing field experiments at that site. I am grateful to Tiaan Fortune, Amy Irlam, Hannah Rees, James Irlam, and Uzair Hendricks for their direct assistance in my fieldwork and lab work. Good company and an extra pair of hands can often make all the difference. I'm thankful also to Matthew Arens for providing pressure-volume curve tools, code, and know-how. To the members of West Lab throughout 2023 and 2024, your willing assistance and friendly collaboration made for a world of difference. I'd like to thank Neil Bredekamp, Derick September, and George Pietersen for graciously equipping me with a new skillset in electronics, even if it ultimately was not directly used in the final version of this thesis. I couldn't have completed this degree without the support of many friends and family who helped me stay grounded through the highs and lows of an undertaking such as this. Many thanks go to Robert Skelton for providing his vulnerability data, for his valuable feedback as a co-supervisor, and also for sharing his wealth of knowledge and boundless enthusiasm for plants. Finally, I owe the deepest gratitude to Adam West for not only being a responsive and constructively critical supervisor, but also for his constant encouragement and relentless commitment to creating a positive working environment for all whom have the pleasure of working with him.

Table of Contents

Figures & Tables

Figures

Tables

List of Abbreviations

Abbreviation	Full Term/Definition
BA	Bark area
CFR	Cape Floristic Region
CS	Carbon Starvation
DIM	Drought Induced Mortality
e_s	saturation vapour pressure
g	total plant conductance
g_{cuti}	conductance through an isolated nonstomatal cuticle
g_{bark}	minimum conductance measured through the bark
g_{min}	minimum leaf conductance
g_{res}	residual conductance which is equal to gmin + gbark
g_s	measured stomatal conductance
g_{smax}	maximum stomatal conductance
HF	Hydraulic Failure
LA	Leaf Area
LAI	Leaf Area Index
LMA	Leaf Mass per Area
MLD	Mass Loss of Detached leaves method for acquiring gmin
NSC	non-structural carbohydrates
p-v curve	pressure-volume curve
RH	percent relative humidity
RWC	percent relative water content
SMRI	Stomatal Margin Retention Index, the time taken to cross the SSM
$SMRI_{\Psi crit}$	specifically the SMRI measured until a specified Ψcrit threshold
SPAC	soil-plant-atmosphere continuum
SSM	stomatal safety margin
$SSM_{\Psi crit}$	SSM defined until a specified Ψcrit threshold
tHF	time to Hydraulic Failure
TLP	turgor loss point
VPD	vapour pressure deficit
Ψ_{crit}	critical water potential threshold associated with DIM
Ψ_{50}	water potential at the critical threshold of 50% embolism
Ψ_{88}	water potential at the critical threshold of 88% embolism
Ψ_{95}	water potential at the critical threshold of 95% embolism
Ψ_{gs90}	water potential at 90% stomatal closure
Ψ_{tlp}	water potential at turgor loss point

Abstract

In light of increased drought frequency and intensity due to climate change, knowledge of how plant drought tolerance is affected is important for understanding plant vulnerability to these changes. Minimum conductance (g_{min}) describes the residual rate of water loss by a plant through its leaves when it has closed its stomata in order to minimise that water loss rate. This includes contributions to water loss through incompletely closed or leaky stomata, the waxy cuticle layer, or through wounding and scarring. This understudied conductance parameter is a critical piece to understanding plant dry-down time to death. However, definitions of this trait have historically been inconsistent leading to non-standardised methods for measurement, which lack an underlying theoretical basis. This obscures assessment of the existing variability and sensitivity of this important trait.

In this thesis, clear definitions for minimum conductance are provided. A theory-based and biologically meaningful framework for measuring this trait over the stomatal safety margin is proposed. There is a focus on standardisation of existing methods, while increasing applicability and reproducibility on plants with a variety of morphologies. Using this framework, an assessment of minimum conductance was carried out on three characteristic and well-studied plant families of the Cape Floristic Region, namely Proteaceae, Ericaceae, and Restionaceae, to improve our understanding of drought response in these groups while demonstrating how this framework helps to improve minimum conductance measurements. Results showed a diverse response of minimum conductance values indicative of diverse drought strategies. This highlights the importance of including accurate values of minimum conductance in models predicting plant mortality under changing climate conditions.

Chapter 1:
Literature Review - Understanding Plant Drought Response

1.1 Vulnerability to drought

1.1.1 Climate change

The anthropogenic climate crisis is predicted to continue increasing global temperatures and disruptions to rainfall patterns, leading to increased frequency, duration and severity of heat waves and drought events (Jentsch, Kreyling and Beierkuhnlein, 2007; Allen *et al.*, 2010; Trenberth, 2011; Dai, 2013). On a global scale, plant communities are vulnerable to these changes (Choat *et al.*, 2012; Brodribb *et al.*, 2020). Assessing this vulnerability is key to understanding the effects climate change will have on plant communities.

The risks an ecosystem or species faces of population decline, reductions in fitness, losses of genetic diversity, or of extinction define the extent of their vulnerability to climate change effects. Understanding vulnerability means understanding its three main facets. Exposure is the extent to which a particular climate change effect will be experienced by the ecosystem. This is driven by rate of change and magnitude of the climate change effect being experienced (Dawson *et al.*, 2011). In the case of drought, this would be how rapid the onset of drought was and the intensity and duration of the drought event. Sensitivity refers to the extent species are affected by the onset of climate change effect. For example, this is how badly affected species are by a drought event. This is mediated by species' dependence on prevailing conditions, their ecophysiology, presence of refugia or micro-habitats, and life history, among other factors.

Adaptive capacity then refers to the ability of species to adapt to the change, be it by evolving ways to persist amidst the change, or by shifting habitats. Effectively, how the species copes moving into the future. This can depend on many factors such as phenotypic plasticity, inherent genetic diversity, life history, dispersal ability, or the availability and nature of niches in alternative environments.

While many past assessments of vulnerability have assessed well the exposure aspect of vulnerability based on climate-envelope models, there is a need for a synthesis of empirical, observational, and mechanistic models to fully understand vulnerability to climate change (Dawson *et al.*, 2011). Providing a mechanistic understanding of plant response to drought is

thus an important contribution to our knowledge of sensitivity and adaptive capacity to drought events under climate change.

1.1.2 CFR diversity

The Cape Floristic Region (CFR) in south-western South Africa is home to the smallest, yet most diverse floral kingdom in the world, hosting over 8500 species within only 90 000 km^2 (Allsopp, Colville and Verboom, 2014). This diversity stems primarily from a history of climatic stability amidst what was otherwise large scale climatic change during the Last Glacial Maximum (Dynesius and Jansson, 2000; Colville *et al.*, 2020), topographic and edaphic variability driven by mild tectonic uplift (Cowling *et al.*, 2015), and a gradient of rainfall reliability (Cowling *et al.*, 2005, 2017) which has led to the creation of a vast array of diverse microhabitats and refugial landscapes (Keppel *et al.*, 2012). However, the region is forecast to face exposure to increased frequency and intensity of drought due to climate change (Tadross, Jack and Hewitson, 2005; Hewitson and Crane, 2006). Understanding vulnerability to climate effects such as drought in such a complex and species rich landscape is thus especially important (West *et al.*, 2012; Allsopp, Colville and Verboom, 2014).

1.2 Understanding plant function and failure

1.2.1 Holistic understanding of the Soil-Plant-Atmosphere Continuum (SPAC)

An understanding of sensitivity of plants to drought conditions and their adaptive capacity to deal with it, helps determine how they will fare under changing climate scenarios. To do this, we require a detailed mechanistic understanding of soil hydrology, climatology, plant physiology, and plant ecology, as well as the interactions that occur between them. These aspects are generally understood through the concept of the soil-plant-atmosphere continuum (SPAC). This model outlines the water, mass, and energy exchanges, and feedback mechanisms that exist between these three aspects. Attempts at modelling SPAC processes, known as SPAC models, have in the past focused primarily on either water acquisition and soil hydrology (root models) or on water transport and plant stem physiology (xylem models) (Deng, 2015). While both types have been developed for different purposes, the need has arisen to combine these aspects as well as incorporate new parameters to holistically understand how water deficit leads to physiological consequences on the plant (Anderegg, Anderegg and Berry, 2013).

1.2.2 Modelling time to hydraulic failure (tHF)

In order to predict plant drought induced mortality (DIM), complex models such as the SurEau model were developed (Cochard *et al.*, 2020). Using this model, time to hydraulic failure (tHF) has been shown to be the most relevant parameter for predicting the effects of drought on tree mortality rates (Cochard, 2021). As this is a model aimed at being holistic, its complex nature requires the combination of multiple traits in order to simulate the real SPAC. These traits include soil hydrological parameters such as soil volume and water content, as well as climate variables like vapour pressure deficit (VPD), temperature, and wind speed. There are also many physiological traits considered, such as those relating to stomatal regulation, residual transpiration, hydraulic conductance and capacitance, xylem embolism vulnerability, leaf area, leaf shedding, root density, and root/shoot ratio (Cochard, 2021; Petek-Petrik *et al.*, 2023). Plant physiology underpins the mechanisms by which DIM occurs in the plant and as such requires careful consideration.

1.2.3 Plant water transport mechanisms

There are two main avenues by which plants face risk of drought induced mortality (DIM), which we can understand through the SPAC model. These are the risk of hydraulic failure (HF) through excessive xylem embolism, and the risk of carbon starvation (CS) through depletion of non-structural carbohydrates (NSC) (McDowell *et al.*, 2008). While recent studies suggest HF may be far more influential than CS (Malone *et al.*, 2024), mediating these risks regardless requires regulation of water transport through the plant.

Plant water transport through the SPAC is primarily explained by cohesion-tension theory (Dixon and Joly, 1997) and occurs through several mechanisms outlined below (Tyree and Zimmermann, 2002; Sack and Holbrook, 2006). The typical plant is rooted in soil containing moisture and grows above the soil surface, establishing contact with the atmosphere. A pathway along which water can travel from soil to atmosphere is created through the plant by absorptive roots, hollow conduit structures, and stomatal cells. Because of the higher vapour pressure deficit in the atmosphere, at the leaf-atmosphere interface vaporisation of water in the leaf occurs and the vapour is lost through the open stomata in the process of transpiration. The negative pressure (water potential) gradient created between the top of the plant and the soil creates tension on the water column, effectively pulling water into the conduits. Water transport is then assisted by cohesive forces between the water molecules and conduit walls, as well as by osmotic gradients in cells, which allows for water containing soil nutrients to be distributed up through the plant. At the leaf surface, stomata open and close in response to environmental

stimuli, regulating transpiration and thus performing various functions within the plant, such as carbon supply, and temperature regulation by evaporative cooling. By serving as the opening between the plant and atmosphere, stomata allow for acquisition of the components necessary for photosynthesis.

1.2.4 Hydraulic Failure vs Depletion of NSC

However, the stomata must ensure that the water demand from the leaves does not exceed the supply capacity from the soil. Failure to do so results in the increasing negative pressure on the plant water column inducing air through the porous conduit walls. The arrival of these air bubbles combined with the negative pressure can act as a catalyst for the pressurised liquid inside the conduit to vaporise, thus expanding the air bubbles which can propagate up the length of the conduit, causing embolism (Sperry, Donnelly and Tyree, 1988; Lens *et al.*, 2013). The water column within these embolised conduits is broken, which reduces the plant's ability to transpire. As conduits embolise, the conductivity of the xylem can decrease irreparably (Sperry, Donnelly and Tyree, 1988; Tyree and Zimmermann, 2002; Choat *et al.*, 2012). The remaining functional conduits can quickly become unable to sustain the water needs of the plant's living tissues, leading to cell death and whole plant mortality via hydraulic failure (HF) (Mantova *et al.*, 2022, 2023; McDowell *et al.*, 2022). Thus, under drought conditions, the stomata are faced with the dilemma of when to remain open and when to close. Remaining open retains plant productivity and cooling but risks hydraulic failure. Conversely, closing the stomata reduces the risk of hydraulic failure, but comes with a trade-off of increased leaf temperature, and halting current water transport which thus restricts plant productivity via photosynthesis (Flexas and Medrano, 2002). The longer that photosynthesis is halted, the greater the risk becomes that the plant will deplete its store of NSCs, i.e. energy stores, and suffer death by carbon starvation.

1.2.5 The iso-/anisohydric framework

Plants have however been observed to have evolved xylem which can tolerate a wide variety of water potentials (Ackerly, 2004; Martínez-Vilalta *et al.*, 2014), with some drought tolerant species able to withstand severely negative water potentials. This observed productivity-safety trade-off led to the previously held notion of isohydric vs anisohydric strategies to regulate water status (Tardieu *et al.*, 1997; Tardieu and Simonneau, 1998; McDowell *et al.*, 2008). Anisohydric plants were predicted to have lower stomatal regulation, keeping stomata open for longer periods under drought-like conditions, thus maintaining photosynthesis for longer periods. These plants operating on the cusp of the plant's hydraulic supply capacity would not

risk CS allowing them to thrive under drought (Cruiziat, Cochard and Améglio, 2002; Sperry, 2004). However, they would have a low or non-existent difference between the point of stomatal closure and the onset of embolism (decreased hydraulic safety) and little way to mitigate runaway water loss to prevent loss of xylem function, and thus had resistant xylems to deal with accrued embolism. By contrast, isohydric plants would have tight stomatal control to prevent loss of xylem function, and a large distance between the point of stomatal closure and the onset of embolism (increased hydraulic safety) but would risk CS under drought conditions (McDowell *et al.*, 2008). The mechanism driving stomatal closure was not well understood and it was suggested that stomatal closure may occur as a response to xylem embolism (Sperry, Donnelly and Tyree, 1988; Nardini and Salleo, 2000). Under this framework, it was also suggested that plants may have accumulated embolisms and regularly undergone periods of repair (Zufferey *et al.*, 2011; Trifilò *et al.*, 2015).

The iso-/anisohydric framework was influential and resulted in many years of research furthering understanding of water and carbon relations in plants (Martinez-Vilalta *et al.*, 2019). This increased understanding has led to more recent findings which alter how we understand observed plant behaviours. Plant behaviour under drought was found to rather exist as continuum between isohydric and anisohydric strategies (Klein, 2014; Martínez-Vilalta *et al.*, 2014). Other studies showed that tight stomatal control under drought did not necessarily equate to decreased productivity nor reduced carbon acquisition under drought (Martínez-Vilalta and Garcia-Forner, 2017) and that droughted plants are more commonly under threat of hydraulic failure than at risk of carbon starvation (Adams *et al.*, 2017; Malone *et al.*, 2024). In fact, it was found that the definitions for isohydry and anisohydry were inconsistent across the literature, thus reducing the validity of the distinctions themselves (Meinzer *et al.*, 2016; Martínez-Vilalta and Garcia-Forner, 2017; Hochberg *et al.*, 2018).

It has also been shown that the occurrence of stomatal closure seems to precede the onset of embolism consistently across a vast array of species (Cochard and Delzon, 2013; Cardoso *et al.*, 2018; Creek *et al.*, 2020), thus suggesting maintenance of higher hydraulic safety than previously thought in so-termed “anisohydric” species. Stomatal closure seems to in fact be physiologically limited by cell turgor at a water potential of around -4 to -4.5 MPa (Martin-StPaul, Delzon and Cochard, 2017), as no species has ever had a point of stomatal closure reported beyond that point, despite the apparent benefits that it could have for productivity during drought under the iso-/anisohydric framework. Additionally, recent studies show that hydraulic factors tend to act as the main constraints on plant survival under drought rather than

carbon limitation (Malone *et al.*, 2024). The focus of subsequent research on plant drought mortality has thus further been placed on hydraulic traits and function, and how they interact.

1.2.6 Hydraulic strategies

Adaptive hydraulic strategies have arisen in plants as combinations of diverse traits and responses to drought conditions, but which can display similar ecological behaviours (Pivovaroff *et al.*, 2016; Choat *et al.*, 2018; Volaire, 2018). These formed behaviours are linked to key hydraulic thresholds such as the points of stomatal closure or lethal xylem embolism (Bartlett *et al.*, 2016; Ziegler *et al.*, 2023).

Attempts to quantify hydraulic vulnerability have led to a better understanding of these key thresholds and the distance between them, termed the stomatal safety margin (SSM) (Delzon and Cochard, 2014; Skelton, West and Dawson, 2015; Martin-StPaul, Delzon and Cochard, 2017). Mortality occurs at a water potential associated with a critical level of conductivity loss due to embolism, termed the critical water potential threshold (Ψ_{crit}) (Blackman *et al.*, 2019; Petek-Petrik *et al.*, 2023). This value was found to be around 50% embolism (Ψ_{50}) in gymnosperms (Brodribb and Cochard, 2009) and 88-95% (Ψ_{88} or Ψ_{95}) in angiosperms (Resco *et al.*, 2009; Urli *et al.*, 2013; Li *et al.*, 2015), although many other factors may also significantly influence these values. The identification of a restrictive physiological boundary for stomatal closure (termed Ψ_{gs90}, the water potential at 90% stomatal closure) (Martin-StPaul, Delzon and Cochard, 2017) means that stomatal behaviour is more constrained than previously thought. Plants with embolism resistant conduits capable of tolerating more negative water potentials tend to close their stomata at similar values to those with less resistant conduits. As such, the distance between stomatal closure (Ψ_{gs90}) and Ψ_{crit}, i.e. the SSM, tends to be larger in these embolism resistant species (Martin-StPaul, Delzon and Cochard, 2017). This larger SSM suggests that the mechanisms by which embolism-resistant species survive drought do not centre around continued productivity at low water potentials. Rather stomata close "early" but their ability to tolerate negative water potentials through resistant xylem allows them to maximise their SSM. This can contribute to late embolism onset which conveys a lowered risk of hydraulic failure (Sperry, 1995; Martin-StPaul, Delzon and Cochard, 2017; Petek-Petrik *et al.*, 2023). It has been repeatedly shown that a large SSM correlates strongly with increased survival under drought (Chen *et al.*, 2019; Petek-Petrik *et al.*, 2023; Ziegler *et al.*, 2023). However, these static hydraulic thresholds indicate only the dehydration tolerance level of the plant and lack the ability to alone predict the time to hydraulic failure (tHF) (Blackman *et al.*, 2019; Ziegler *et al.*, 2024).

1.2.7 Tolerance and Avoidance strategies

These hydraulic strategies typically increase tHF by two main mechanisms. Tolerance strategies promote tolerance of low levels of tissue hydration in cells, while avoidance strategies limit water loss from stored water pools to avoid cell dehydration (Choat *et al.*, 2018; Volaire, 2018; Cochard, 2021). Plants employ aspects of both strategies to deal with tissue dehydration under drought conditions. In tandem with the tolerance thresholds of the SSM, avoidance strategies regulate the time taken to reach dehydration and plant death (Ziegler *et al.*, 2024).

The rate at which water loss occurs across the SSM affects how quickly the water potential declines. This rate is generally termed minimum or residual conductance (the so-called "g_{min}"). This rate is determinant on many physiological characteristics but will also be affected by the following factors.

Firstly, loss of water is affected by the total area from which water can be lost from the plant once the stomata are closed. This allometric parameter typically incorporates the leaf area, but also any surface of the plant capable of losing water such as the bark area. This parameter can vary over time as leaf shedding is an important adaptation in many plants (drought-deciduous plants) to reduce transpirational demand during periods of water stress (Bucci *et al.*, 2005). Secondly, the vapour pressure deficit (VPD) of the atmosphere affects how strong the force drawing water out from the leaf is. Finally, the hydraulic capacitance of the plant describes the total amount of internally stored water available to be lost from tissues in the leaves, stems, or roots. The magnitude of this storage can buffer decreases in water potential in the water column (Pineda-García, Paz and Meinzer, 2013; Salomón *et al.*, 2017).

The aforementioned form the basis of the parameters considered in the construction of several models of plant time-to-death. One such model is the t_{crit} model (Blackman *et al.*, 2016, 2019), where t_{crit} is the time taken to desiccate from stomatal closure to lethal water stress levels using excised branches. The parameters mentioned in the preceding paragraph can be measured for any individual specimen and are combined in this model to predict t_{crit} such that a certain value for t_{crit} may be obtained through several differing combinations (Blackman *et al.*, 2016). This combination of interacting traits helps to explain numerous observations of differing survival rates amongst plants with similar Ψ_{crit} values (Dayer *et al.*, 2020), as well as the existence of variable Ψ_{crit} values in plants living in similar conditions (Martínez-Vilalta *et al.*, 2014).

In order for comparisons to be made, normalisation needs to occur. Allometric and capacitance parameters tend to vary not only between species, but also scale with plant size in such a way that larger plants will have more storage capacity per unit leaf area (Scholz *et al.*, 2011). Conversely, the rate of water loss when normalised, is independent of plant size, which makes this trait particularly helpful for comparison between individuals or species. While minimum conductance has been measured in different forms in the past, only thanks to these recent advancements has it been illuminated as particularly useful in models of tHF such as SurEau.

1.3 Understanding minimum conductance

1.3.1 Clarification of definitions

The term 'g_{min}' has been attributed several definitions of minimum conductance in the past. Table 1 summarises the differing definitions as currently understood (adapted from Duursma *et al.*, 2019).

TABLE 1: Differing definitions of g_{min}

Variable	***Definition***
g_{cuti}	Conductance through an isolated nonstomatal cuticle
g_{min}	Minimum conductance measured via mass loss of detached leaves
g_{bark}	Minimum conductance measured through the bark
g_{res}	Residual conductance which is equal to $g_{min} + g_{bark}$
g_{dark}	Night-time conductance, or conductance after significant dark adaptation
g_e	Epidermal conductance, formerly used name for many types of minimum conductance
g_0	Intercept in the Ball-Berry-type stomatal conductance model, that is, g_s when photosynthesis (A_n) approaches zero

Much attention has historically been paid to cuticular conductance (g_{cuti}), a function of the permeability of the waxy leaf cuticle (Kerstiens, 1996; Riederer and Muller, 2008; Fernández *et al.*, 2017; Schuster, Burghardt and Riederer, 2017), but without consideration for the contribution of stomata. Contemporary drought response models (Blackman *et al.*, 2016, 2019; Martin-StPaul, Delzon and Cochard, 2017; Petek-Petrik *et al.*, 2023) most commonly use the leaf minimum conductance (g_{min}), defined as the rate of water loss from specifically the leaf past the point of stomatal closure (Blackman *et al.*, 2016, 2019; Duursma *et al.*, 2019; Petek-Petrik *et al.*, 2023). It thus excludes contributions to total conductance (g) from the stomata

(g_s) but includes contributions from g_{cuti}, as well as contributions from incompletely closed stomata (be they damaged or naturally leaky) or from additional wounding of the leaf. It is standardised per unit leaf area (LA) and by vapour pressure deficit (VPD) to allow for comparison (although it is notable that the g_{min} definition used by (Blackman *et al.*, 2016, 2019) excludes VPD from the g_{min} term, even though it still corrects for it in their model of plant time-to-death). Some studies include also the contribution from bark, the lenticular conductance (g_{bark}) (Blackman *et al.*, 2016; Billon *et al.*, 2020; Ziegler *et al.*, 2024). When leaf and bark contributions are both considered, this is distinguished as the residual conductance (g_{res}). In species which show vulnerability segmentation, that is when leaf xylem is significantly more vulnerable than stem xylem, the distinction between g_{min}, g_{bark}, and g_{res} is most important (Ziegler *et al.*, 2024). These species are often drought-deciduous, an adaptation to significantly reduce total g_{res} (Wolfe, Sperry and Kursar, 2016; Blackman *et al.*, 2019; Levionnois *et al.*, 2021) by dropping the g_{min} component of g_{res} and "switching" to g_{bark}, which is a much lower water loss rate, to conserve the xylem within their stem.

In this thesis, I have taken particular care to refer to g_{res} and g_{min} separately even when they are spoken about together, as they represent potentially different values relevant in different contexts. 'Minimum conductance' is used to refer to both or either values.

1.3.2 Function in context

To understand the importance of minimum conductance as a trait contributing to whole plant drought resistance, we need to understand how it functions in context with other aspects of tolerance and avoidance strategies.

Let us consider in Fig. 1 two whole plants (Red and Blue) with the same water potential at point of stomatal closure (Ψ_{gs90}) but differing critical water potentials (Ψ_{crit}), and thus differing stomatal safety margins (SSM). Initially, both plants are fully hydrated and maintain a natural daily flux around roughly zero water potential in their xylem. Upon the onset of a drought event, both plants' stomata will begin to close to minimise water loss. However, the plant will continue to lose water through incompletely closed stomata, through the waxy cuticle layer, through its bark, or through any damaged or scarred tissue. This is the minimum conductance from the whole plant (g_{res}). Water potentials will begin to fall until they reach a critical value beyond which the plant cannot recover, i.e., the critical water potential (Ψ_{crit}). In Fig. 1A, the rate at which the plants lose water is identical and thus the blue plant crosses its shorter SSM and reaches its less negative Ψ_{crit} sooner than the red plant, thus resulting in a shorter time to

cross the stomatal safety margin and thus a shorter time to death by hydraulic failure (tHF). Hydraulic thresholds like Ψ_{gs90} and Ψ_{crit} clearly play an important role in determining tHF. However, in Fig. 1B when we alter the rate at which water is lost post-stomatal closure, i.e., the g_{res}, this can significantly alter the time taken to cross the SSM and the resulting tHF.

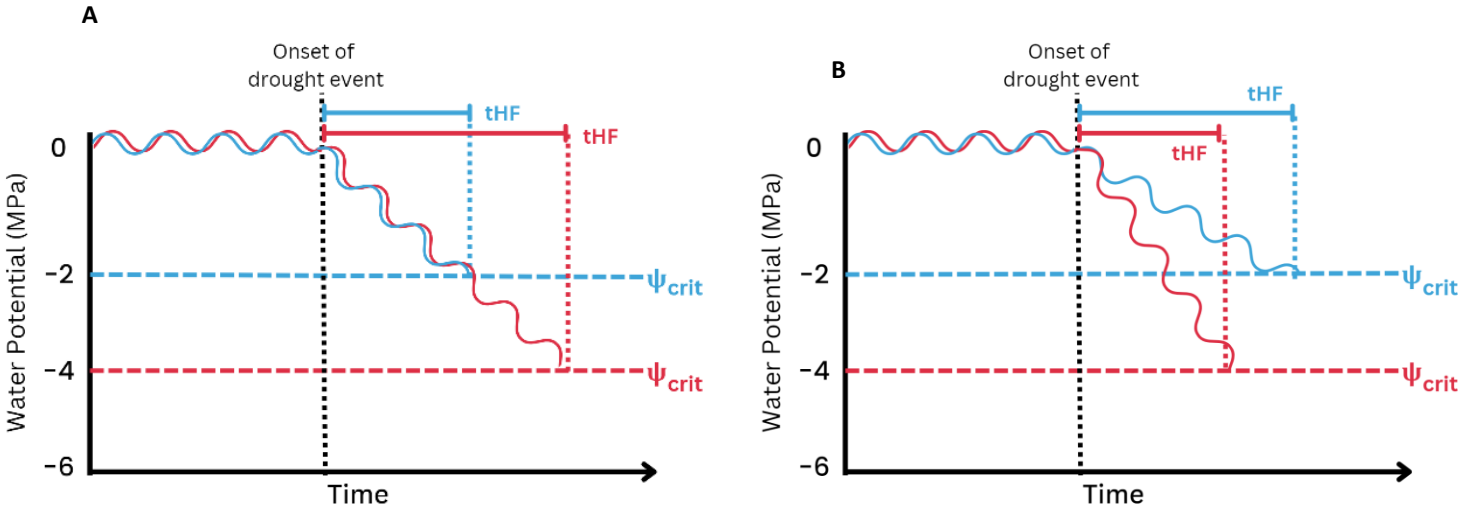

Figure 1: Simplified model showing plant dry-down time to death: A) Two separate plants function well above their critical water potentials (Ψ_{crit}). Upon the onset of a drought event, given the same rate of water loss (g_{res}), the plant with a more negative Ψ_{crit} survives longest (it has the longer time to hydraulic failure – tHF). B) Given differing rates of water loss (g_{res}), survival times are not solely dependent on Ψ_{crit}, and a plant with less negative Ψ_{crit} may survive longest.

1.3.3 Stomatal Margin Retention Index (SMRI)

The time taken to cross the SSM seems to be a theoretically important metric that combines the static points of stomatal closure and critical xylem embolism with the dynamic residual rate of conductance. As such, Petek-Petrik *et al.* (2023) proposed formalising this metric as an integrative index they dubbed the 'stomatal margin retention index' or 'SMRI$_{\Psi 50}$'. They used Ψ_{50} as they were working on gymnosperms (Brodribb and Cochard, 2009), but this trait can be genericised as SMRI$_{\Psi crit}$ or simply SMRI. They used g_{min} as they were working on leaves. SMRI$_{\Psi crit}$ (MPa m^2 s mmol^{-1}) was derived according to the following equation:

$$SMRI_{\Psi crit} = \frac{SSM_{\Psi crit}}{g_{min}} \qquad \text{Eqn. 1)}$$

where, SSM$_{\Psi crit}$ is the stomatal safety water potential (MPa), and g_{min} is minimum conductance of leaves (mmol m^{-2} s^{-1}).

To test the power of this index, they measured the correlation between Ψ_{crit}, SSM, g_{min}, and SMRI$_{\Psi 50}$ on normalised plant time-to-death using the SurEau model for four conifer species

with differing levels of embolism resistance. All these traits showed significant positive correlations with time-to-death, but $SMRI_{\Psi 50}$ had the strongest correlation (Table 2).

TABLE 2: Time to death can be predicted most accurately using SMRI (data from Petek-Petrik et al. 2023).

Trait correlation to normalised time to death (tHF)

Trait	*Model fit (R^2)*	*Significance*
g_{min}	0.69	P<0.05
Ψ_{50}	0.78	P<0.05
$SSM_{\Psi 50}$	0.89	P<0.05
$SMRI_{\Psi 50}$	0.96	P<0.05

While analyses across a broader species range are now called for, $SMRI_{\Psi crit}$ is promising as its constituent traits do not scale with plant size (Petek-Petrik *et al.*, 2023). This makes it a comparable integrative trait for drought performance across individuals and species.

As g_{res} or g_{min} is a term in the denominator of the $SMRI_{\Psi crit}$ equation, variance in its estimation can cause significant shifts in the value of $SMRI_{\Psi crit}$. As such, accurate determination of g_{res} or g_{min} is key to successfully estimating this important integrative trait.

1.4 Thesis structure

This thesis focuses on estimation of the minimum conductance, g_{res} or g_{min}, and its use and implications. Chapter 2 takes a critical look at the current methods used to determine this trait, and assesses their accuracy, shortcomings, and applicability to diverse plant growth forms. Chapter 3 builds upon the insights of Chapter 2 to make recommendations for an updated framework for determination of g_{res} or g_{min} with biological meaning, before then applying the framework to assess any further shortcomings. Chapter 4 compares g_{res} and g_{min}, and stomatal margin retention index SMRI measured on diverse species within the Cape Floristic Region (CFR), building on our knowledge of these groups, while also informing us about what global patterns may look like. Chapter 5 acts as a summary of the thesis as a whole and will present the final refined framework recommended for use in determination of minimum conductance (g_{res} or g_{min}).

Chapter 2:
Assessing methodological challenges and limitations in estimating minimum conductance

2.1 Introduction

Measures of minimum conductance are important dehydration avoidance traits which contribute to the hydraulic strategies of plants experiencing desiccating conditions. Practically speaking, they can act as a predictor of plant time to death via hydraulic failure (tHF), but even more importantly are a constituent in several more powerful integrative traits for predicting tHF, such as t_{crit} (Blackman *et al.*, 2016, 2019) or stomatal margin retention index (SMRI) (Petek-Petrik *et al.*, 2023), and are crucial to more complex models, such as SurEau (Cochard *et al.*, 2020).

This importance has only been properly acknowledged relatively recently in the literature surrounding plant drought and hydraulic function, and thus few data have been collected specifically for these purposes as of yet. In the biomes of the Cape Floristic Region (CFR), hydraulic data only exist for tolerance traits such as determination of resistance to embolism and safety margins (Jacobsen *et al.*, 2007, 2009; Skelton, West and Dawson, 2015; Skelton *et al.*, 2023) or avoidance traits such as stomatal regulation (Skelton *et al.*, 2023) without consideration of the rate at which these thresholds are approached during drought. As such, determining minimum conductance would greatly assist in understanding fully the drought response of plants in this floral biodiversity hotspot.

2.2 Shortcomings of current methods

Understanding the diversity in plant drought response requires studying species with varying morphologies and physiologies across differing ecological contexts. Robust methods are those which are capable of accounting for this diversity. It is in this way that current methods face challenges. But to understand these challenges, it is important to establish what the currently accepted methods are.

The commonly used method to acquire g_{min} is that of Mass Loss of Detached leaves (MLD) (Sack and Scoffoni, 2010; Blackman *et al.*, 2019; Duursma *et al.*, 2019; Petek-Petrik *et al.*, 2023; Ziegler *et al.*, 2024). Simply put, this involves removing leaves from a sample, sealing the cut, and recording mass loss over time as they dry out. Plotting a dry-down curve of mass loss over time, one theoretically obtains a curvilinear relationship with three distinct phases (Duursma *et al.*, 2019) (see Fig. 2):

1. Initial phase where the stomata are open so initial water loss is high.
2. Transitional phase where rate of water loss decreases as stomata begin to close.
3. Linear phase where rate of water loss stabilises at a constant rate once stomata are as closed as possible (Hygen, 1951). This continues until leaf relative water content (RWC) is close to zero.

The g_{min} (mmol m^{-2} s^{-1}) can then be calculated according to the following equation:

$$g_{\min} = \frac{slope \times \frac{atmospheric\ pressure}{VPD}}{leaf\ area} \quad \text{Eqn. 2)}$$

Atmospheric pressure (kPa) can be measured or determined based on altitude, while Vapor Pressure Deficit (VPD, kPa) is a function of the recorded temperature and humidity within the dry-down environment during the dry-down period (Sinclair and Ludlow, 1986). The g_{min} is normalised based on leaf area (m^2). Finally, 'slope' (mmol s^{-1}) refers to the "linear part of the leaf mass versus time curve" (Petek-Petrik *et al.*, 2023), referring to phase 3 above, i.e. the region of constant rate of mass loss (Duursma *et al.*, 2019). However, there are issues and shortcomings to these methods, both previously acknowledged, and those I have found in my attempts to emulate them.

2.2.1 Non-simple leaf shapes and non-excisable leaves

The MLD method is performed on detached leaves, requiring study species with leaves that are easily detachable, sealable at the site of detachment, and large enough to register mass loss on a portable balance. Many arid-adapted species, for example, possess leaf morphologies that do not meet these criteria, presenting an issue for widespread application of the MLD method, unless we reconsider some of these parameters.

This issue has been tackled in the past and adaptations have been made for use of shoots. For example, the DroughtBox is a programmable climate-controlled chamber designed for automatically measuring mass loss of a desiccating sample attached within (Billon *et al.*, 2020). Such a tool is suitable for recording small changes in mass and has been used to obtain

measurements from both leaves and small branches and shoots. This device was tested using shoots to generate residual conductance (g_{res}) values. It is thus possible to perform dry-down experiments on branches in the same way as in the MLD method to generate g_{res} instead of g_{min} values. It is however unclear to what extent g_{min} and g_{res} are comparable, as assessing their similarity is dependent on additional knowledge regarding morphology and leaf shedding behaviour (Wolfe, Sperry and Kursar, 2016; Blackman *et al.*, 2019; Levionnois *et al.*, 2021; Ziegler *et al.*, 2024).

2.2.2 Non-linearity of curve shapes

Delineating the 'linear phase' of the curve is crucial for the minimum conductance calculation in the MLD method. These methods rely on a curve in which a linear phase is clearly observable. However, repeated observation, as shown in later results of this chapter (see examples in Fig. 2), indicates that dry-down curves display a variety of shapes, with many appearing closer to non-linear exponential decay curves than linear ones. In this is the case, it is difficult or even entirely not possible to visually distinguish where a 'linear' section starts or ends. While often not displayed in figures in the literature, all dry-down curves will attenuate as RWC gets low. Even if curves appeared more linear, it would still be subjective as to where the start and endpoints for that linear section were to be defined. Inaccuracy may be induced by a "misjudgement" in start or endpoint, potentially being exacerbated by poor data density or noisy data. Smoothing the data could help mitigate these potential effects. It is unclear how sensitive these start- and endpoints are to error, nor is there currently a more accurate estimate to set the standard.

The starting point of the "linear section" (see Fig. 2) is defined by behaviour indicative of stomatal closure, which has a physiological meaning, making it a likely good estimate, although how precise is not well known. However, the endpoint of the third "linear" phase is defined only by RWC reaching "near-zero" values. This definition is vague and does not have a robust physiological meaning.

As a curve becomes less linear as it approaches zero, the section chosen to be the "linear section" and calculate g_{res} should have an increased influence on the outputted g_{res} value. It is unclear the extent of the difference that "slope selection" would have on g_{res}, but without robust and standardised methods to delineate which section of the curve to use, it is logical to believe that generated g_{res} or g_{min} values could vary extensively. An endpoint with physiological meaning (such as the starting point) would allow for a consistent point to be chosen.

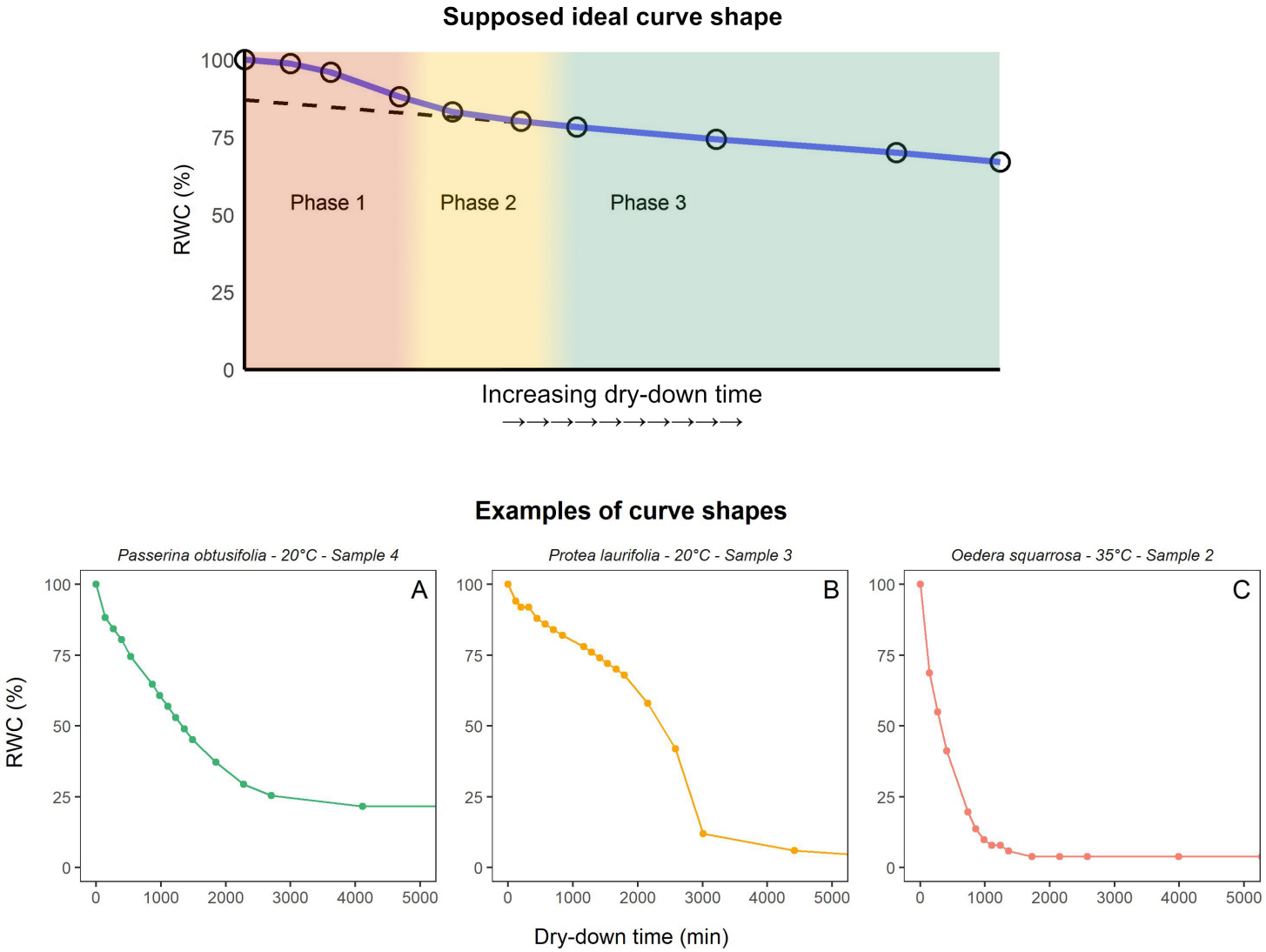

Figure 2: Above: Desired curve shape reported in the literature (example data from Duursma et al., 2019). Note the difficulty to distinguish between phases and the cutoff before the curve attenuates at 0% RWC. Below: Dry-down curve examples of three study species showing diverse curve shape: A) Curve with a flatter, more linear section, B) Curve shape experiencing a rapid increase in dry-down (artefact), C) Curve displaying a non-linear curve shape.

2.2.3 Lack of standardisation

As indicated previously, there has been uncertainty and confusion as to the definition of g_{min} and much nuance has either been overlooked and/or conflated (Duursma *et al.*, 2019). In a meta-analysis it was found that, because conductance measurements have in the past been taken for many different purposes under the name 'minimum conductance' or similar supposedly equivalent terms, a lack of standardisation in the methods used, and the parameters measured is commonplace (Duursma *et al.*, 2019). For example, many studies quantifying minimum conductance were excluded due to lack of VPD or humidity data, which are essential for generating comparable data. This has led to g_{min} values which have different units and are thus non-comparable. There is also inconsistency in necessity of performing certain steps in the methods, and a lack of standardisation of experimental conditions, lighting, wind presence, sealing of cuts, timing of start of the experiment after cuts have been made, and number of weight measurements obtained (Sack and Scoffoni, 2010; Duursma *et al.*, 2019).

2.2.4 Experimental artefact

One such consequence of poorly defined methods may be artefact induced during the dry-down process (Heinsoo and Koppel, 1998; Duursma *et al.,* 2019). It is not uncommon to observe a stark increase in observed rate of water loss at some point after leaf detachment (Fig. 2B). It is likely that certain conditions, especially those of rapid dry-down cause the leaf epidermis to dry excessively, with adjacent shrunken cells pulling the stomata open in a phenomenon known as 'mechanical advantage' (Buckley, 2005). It is thus recommended to dry samples out slowly under low light and low VPD conditions (Duursma *et al.*, 2019) to limit the occurrence of this phenomenon. However, the extent to which this phenomenon has affected prior studies is unknown. It is possible that a more targeted "slope selection" to identify the linear phase could reduce the number of problematic curves.

2.2.5 Leaf area determination

As it is a part of the g_{res} and g_{min} calculation, leaf area (LA) determination is also an important parameter to establish consistent and reproducible methods for. All methods for LA estimation for minimum conductance involve a step where projected leaf area is measured by taking a scan of the sample, a so called planimetric method. However, method inconsistency is common in the literature. For example, some studies measure LA prior to dry-down treatment (fresh LA) (James, Lawn and Cooper, 2008; Blackman *et al.*, 2019), while others scan after samples have been dried (dry LA) (Petek-Petrik *et al.*, 2023). This inconsistency is a problem as leaves tend to shrink by varying amounts based on morphology as they lose water content, changing their outputted LA. Deciding when to consistently measure LA is thus critical to obtain comparable g_{res} or g_{min} values.

How one handles that scanned LA is also important when comparing g_{res} or g_{min} across species, e.g., g_{res} or g_{min} calculated from projected and double-sided leaf areas will differ by a factor of two. There also exists the issue of how to handle non-flat leaves or small branches, as a vertical scan will not capture this structure accordingly.

In order to decide on when to measure LA and what methods to employ, we must consider both the biological significance of LA for minimum conductance measurements as well as practical concerns for measurement.

2.2.6 Lack of patterns and potential plasticity

Despite great potential to significantly influence plant time to death, no significant trends were found between g_{min} and climate variables nor other leaf traits measured in over 40 studies analysed together (Duursma *et al.*, 2019). Similar lack of correlation was found in a

compilation of g_{cuti} and g_{min} values (Schuster, Burghardt and Riederer, 2017). While some trends were found in g_{min} values when broken down by taxonomic order, only the extreme ends of the distribution showed significant difference from each other (Duursma *et al.*, 2019). Lack of major discernible patterns in a trait such as g_{min} which seems to be evolutionarily important for plant survival is surprising.

Part of this confusing lack of correlation could lie in the fact that g_{min} may not necessarily be a static trait, but rather has a potential for plasticity. Studies have shown that leaf age (Jordan and Brodribb, 2007), altitude (DeLucia and Berlyn, 1984; Herrick and Friedland, 1991; Anfodillo, Di Bisceglie and Urso, 2002; Fernández *et al.*, 2017), drought stress (Bengtson, Larsson and Liljenberg, 1978; James, Lawn and Cooper, 2008; Blackman *et al.*, 2019), instantaneous changes in temperature (Schuster *et al.*, 2016; Drake *et al.*, 2018), and changes in growing temperature (Duursma *et al.*, 2019) may result in acclimatisation of g_{min}. This plasticity may very well affect how minimum conductance responds to increasing droughts, heatwave events, or other climate shifts brought about by the current anthropogenic climate crisis.

However, lack of methods standardisation may cause significant variance in values that has the potential to occlude trends in these findings. This may also hinder our ability to interpret existing measures of minimum conductance in the literature and thus the ability to utilise them in models such as t_{crit} or SurEau to predict plant mortality rates under changing climate. It begs the question: Does the observed variance in measured g_{min} arise from real plasticity or from inconsistency in measurement? This further demonstrates the need for standardised methods and measurement practices (Duursma *et al.*, 2019).

2.3 Aim

An investigation of the extent to which the above shortcomings posed a concern was required in order to work towards more robust methods for g_{min} and g_{res} determination.

The aim of the upcoming analysis was to 1) show that curve shapes often do not appear to be linear, 2) find a robust way to minimise the effects of noisy or density poor data when selecting a slope while accounting for a diversity of curve shapes, 3) assess how sensitive g_{min} or g_{res} may be to differences in slope selection, and 4) assess whether high vapour pressure deficit (VPD) during measurement causes decreased data quality and is problematic for determination of g_{min} and g_{res}. As such, g_{min} or g_{res} measurements were taken on 14 morphologically diverse species from the arid extent of the Renosterveld and Mountain Fynbos habitats in the Cape Floristic Region (CFR).

2.4 Methods

2.4.1 Study area

The location for this investigation was the Drie Kuilen Nature Reserve, a semi-arid mountainous shrubland and winter rainfall region of the CFR. Of the <300mm mean annual precipitation, roughly 65% occurs in winter (van Blerk *et al.*, 2021). The vegetation present results from the existence of a mosaic of shale and sandstone substrate. While both soils are relatively poor, the sandstone is especially leached, typical of substrate from the Table Mountain group. The vegetation is classified as Matjiesfontein Shale Renosterveld and Langeberg Sandstone Fynbos (Mucina and Rutherford, 2006). This site represents the arid extent of both ecotones.

Sampling took place at two separate sites, each representing one of the distinct ecotones: a Renosterveld site (33° 35' 14.26" S, 20° 0' 47.19" E, 1100m above sea level), and a Fynbos site (33° 35' 41.63" S, 19° 59' 13.79" E, 1240m above sea level) located within a kilometre of each other.

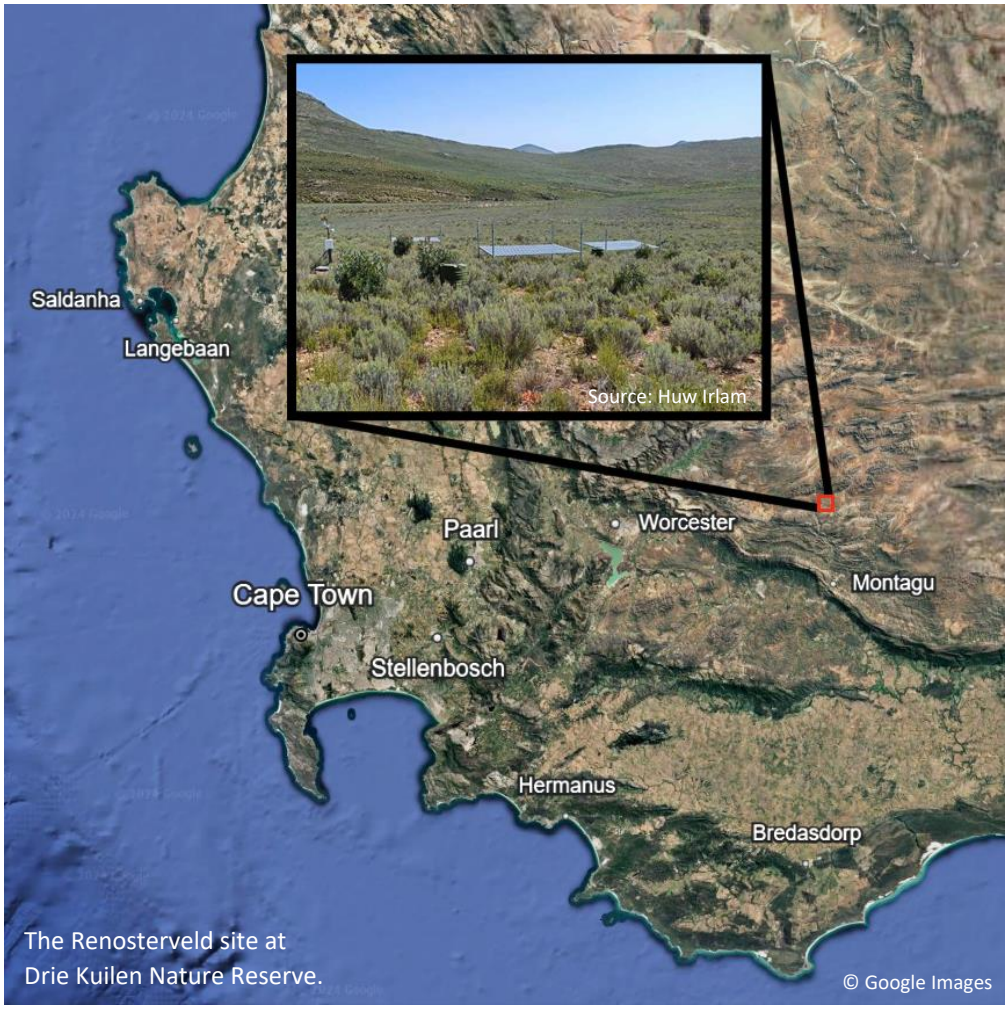

The Renosterveld site at Drie Kuilen Nature Reserve.

2.4.2 Study species and Sampling

The species selected were morphologically diverse and represented common genera and/or growth forms within the two ecotones (Table 3). Two sampling runs were performed across the two study sites. The sample collection at the Renosterveld Site occurred on 27 October and 24 November 2023, while sample collection at the Fynbos Site occurred on 24 November 2023. In each run seven individuals were collected, of which six were used, with one serving as a backup.

All samples were taken from healthy-looking individuals at the base of a branch of the plant and kept hydrated with the stem in water, allowing for rehydration, and stored at 10°C until experimentation began (Run 1 began on 1 Nov, and Run 2 began on 27 Nov). Each individual plant had four samples taken from it, one to be used in each of four temperature treatments (discussed below). Fully expanded shoots were selected for most species and cut at the base of a node. Flowers were avoided where possible but were removed if present. Cuts were sealed with contact adhesive. As shoots were used, g_{res} values were obtained for these species. The exception to this was all *Protea* species which had individual leaves large enough to be dried down individually according to the standard MLD method and as such g_{min} was obtained.

TABLE 3: Species measured at the Renosterveld and Fynbos sites

Site	***Collected***	***Family***	***Species***
Renosterveld	Run 1,	Asteraceae	*Dicerothamnus rhinocerotis* (L.f.) Koek.
	27 Oct 2023	Proteaceae	*Protea laurifolia* H.Buek ex Meisn.
		Aizoaceae	*Ruschia multiflora* Schwantes
		Thymelaeacae	*Passerina obtusifolia* Thoday
		Asteraceae	*Oedera squarrosa* (L.) Anderb. and K.Bremer
	Run 2,	Scrophulariaceae	*Microdon polygaloides* Druce
	24 Nov 2023	Campanulaceae	*Wahlenbergia nodosa* (H.Buek) Lammers
		Peraceae	*Clutia rubricaulis* Eckl. ex Sond.
Fynbos	Run 2,	Boraginaceae	*Lobostemon decorus* Levyns
	24 Nov 2023	Fabaceae	*Aspalathus shawii* L.Bolus
		Scrophulariaceae	*Selago dolosa* Hilliard
		Rutaceae	*Agathosma capensis* Druce
		Proteaceae	*Protea lorifolia* (Knight) Fourc.
		Proteaceae	*Protea repens* (L.) L.

2.4.3 Experiments

In order to vet the effects of high VPD on data quality, four temperature treatments were performed at 20°C, 25°C, 35°C, and 40°C. The experiments for 20°C, 35°C, and 40°C were performed in temperature controlled phytotron chambers, while the 25°C experiment was performed in a constant temperature room. VPD was not able to be controlled directly.

For each treatment for each species, six samples from different individuals were imaged using a scanner (Epson Perfection V850 Pro) to obtain leaf area planimetrically. Using ImageJ (Schneider, Rasband and Eliceiri, 2012), one-sided leaf area was determined. Threshold range was automatically detected but adjusted if necessary to include the visible stem and leaves while excluding shadow as best as possible.

For certain samples in the first run, leaf area scans were taken post-desiccation. In these cases, scans of extra samples were taken pre- and post-desiccation. The loss in leaf area over the dry-down process was then determined on a per-species basis and used to empirically set a calibration factor that was applied to the relevant scans (see Table S1).

The six samples for each species were then placed on labelled trays and placed into their respective treatment rooms. Temperature and relative humidity (RH) were monitored in each room using a logger (either Lascar EL-USB-2 or EL-USB-2+) placed in the room (see Table S2). The rooms were kept in darkness to facilitate closing of stomata. A two-place decimal balance (AND HT-120) for measuring mass was placed outside of each phytotron chamber or within the constant temperature room for the 25°C treatment. An initial mass measurement was taken prior to placing specimens under treatment conditions, then roughly every 1-2 hours afterward for the first day, with intervals growing larger overnight and as rate of dry-down decreased. Measurements were halted once constant mass was reached. Dried samples were then placed in labelled paper bags and placed into an 80°C oven to dry further for approximately 96hrs. Relative water content (RWC) of the samples at each measurement point along the dry-down curve was calculated as such:

$$RWC\ (\%) = 100\left(\frac{fresh\ weight - dry\ weight}{turgid\ weight - dry\ weight}\right) \qquad \text{Eqn. 3)}$$

where ‘fresh weight’ is the measured weight of the sample at any measurement point, ‘turgid weight’ is the weight of the sample when fully hydrated before the dry-down began, and ‘dry weight’ is the final weight of oven-dried samples.

2.4.4 Data analysis

Mass loss data were collected using a Google Sheets spreadsheet and smartphone, then downloaded as a csv file and imported into R using the packages *readxl* (Wickham, Bryan, *et al.*, 2023) and *lubridate* (Grolemund and Wickham, 2011).

Temperature and humidity data were downloaded from the loggers as txt files and collated into a csv file using R base functions and the packages *dplyr* (Wickham, François, *et al.*, 2023) and *tidyverse* (Wickham *et al.*, 2019). These data were averaged over the course of the dry-down time and used to calculate the mean VPD for each treatment (see Table S2). An exception was the 40°C data in Run 2, where the logger data became corrupted and the Run 1 data were instead used. Saturation vapour pressure (e_s) and subsequently VPD were calculated according to the equations and values found in Campbell and Norman, 2000:

$$e_s(T) = a \exp\left(\frac{bT}{T+c}\right) \quad \text{Eqn. 4)}$$

where $e_s(T)$ is the saturation vapour pressure in kPa at a given temperature T in °C, $a = 0.611\ kPa, b = 17.502$, and $c = 240.97°C$.

$$VPD = e_s(T)\ (1 - RH) \quad \text{Eqn. 5)}$$

where RH is percent relative humidity, and VPD is in kPa.

Leaf area (LA) data were collated into a csv file and also read into R. Table S1 was also created for correcting LAs taken on desiccated samples (as mentioned above) and for transforming one-sided LA into total LA based on leaf morphology according to the motivation column.

All data analysis was then done in R Studio (R Core Team, 2020). Mass loss over time was normalised using relative water content (RWC) to obtain graphs displaying the change in RWC over time (Fig. 3). An exponential decay function was fitted to each curve of the form:

$$y = A * e^{-k*x} + (100 - A) \quad \text{Eqn. 6)}$$

where y = percent RWC (%), x = dry-down time, while the curve-fitting parameters A and k were obtained using the package *minpack.lm* (Elzhov *et al.*, 2023). The term "$+(100 - A)$" was added to ensure the curve intersected the y-axis at 100% RWC.

This was done to smooth the data such that it could be plotted at desired intervals which did not match up with the exact RWC at which measurements were taken. This also minimised the effect of noisy data.

Using these fitted RWC (y) values from the model, the parameters necessary for g_{res} and g_{min} calculation were generated at RWC values at 10% intervals (i.e. 100% RWC, 90% RWC, etc.) g_{res} or g_{min} was then calculated at each RWC "bin" (i.e. using only values 100-90% RWC, then 90-80% RWC, etc.) Graphs displaying change in g_{res} or g_{min} at differing RWC bins (Fig. 4) were then plotted using the packages *ggpubr* (Kassambara, 2023), *gridExtra* (Auguie and Antonov, 2017), *multcompView* (Graves and Dorai-Raj, 2024), and/or *cowplot* (Wilke, 2024).

2.5 Results and Discussion

2.5.1 Curve shape

The difficulty of accurately defining the linear section of a dry-down curve is apparent when looking at the linearity of the curves (Fig. 3). Samples seemed to display a variety of slopes but were all non-linear to some degree. Some had flatter sections closer to that described in the literature (e.g., Fig. 2A, 2B) Some slopes seemed to experience a rapid increase in dry-down rate (e.g., Fig. 2B), likely due to the aforementioned artefact resulting from forced-open stomata. This displays the limitations encountered when attempting to define by eye the linear portion of the slope across diverse curves.

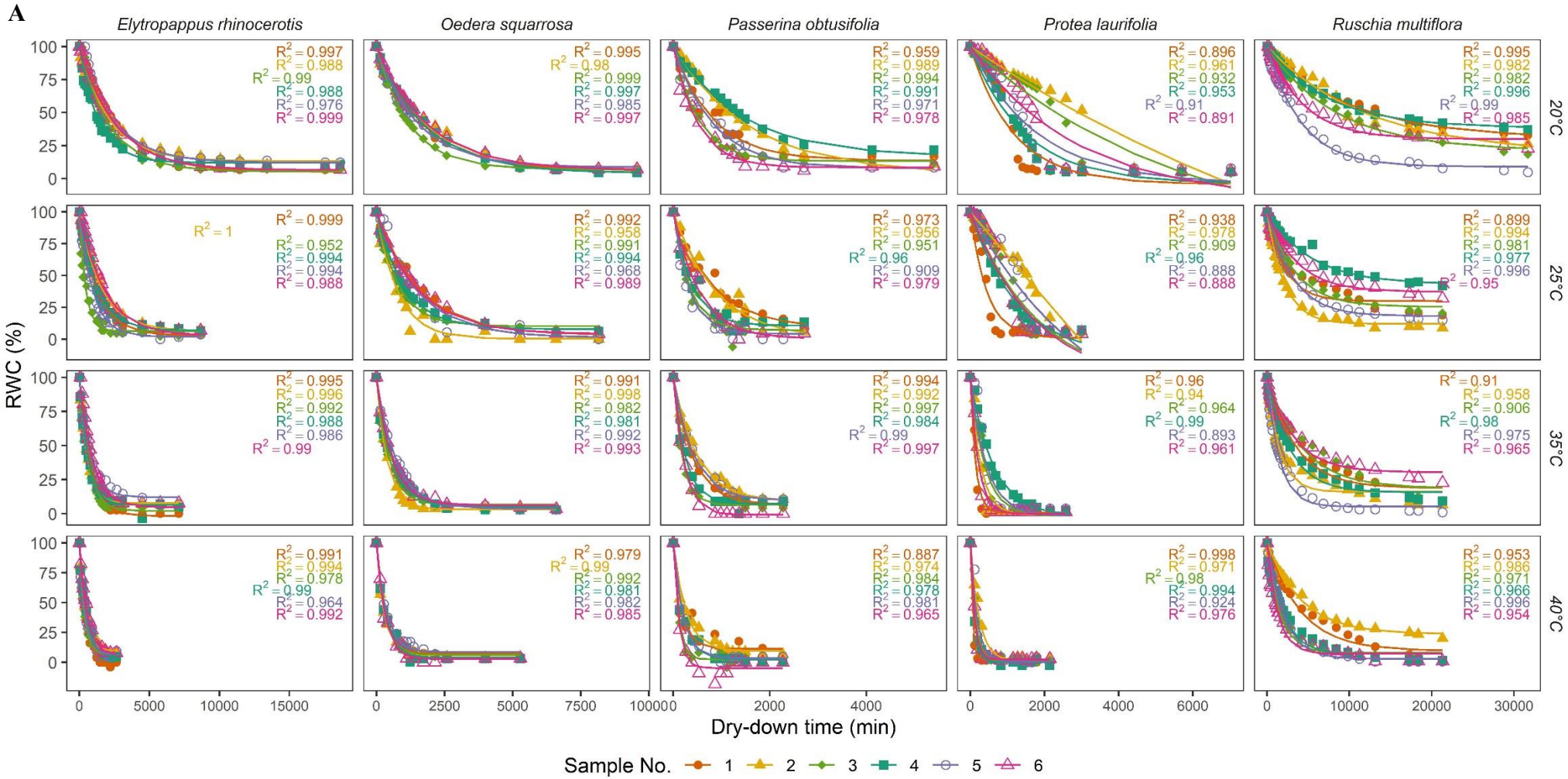

Figure 3A: Dry-down curves showing the decrease in relative water content (RWC) with time in Run 1 study species, fitted with the saturating model (Eqn. 6). Associated R^2 values are displayed. Eqn. 6: $y = A * e^{-k*x} + (100 - A)$

B

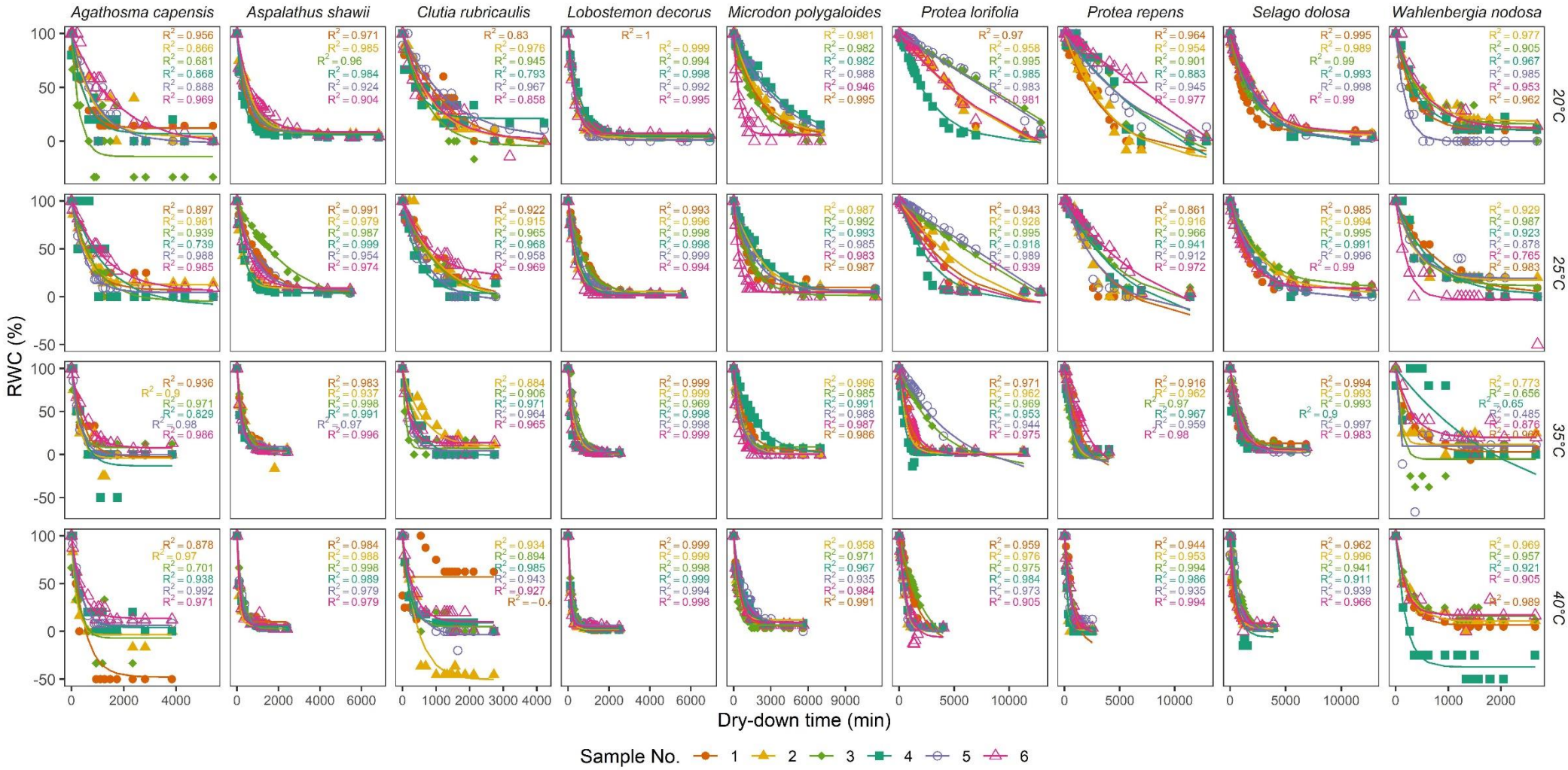

Figure 3B: Dry-down curves showing the decrease in relative water content (RWC) with time in Run 2 study species, fitted with the saturating model (Eqn. 6). Associated R^2 values are displayed. Eqn. 6: $y = A * e^{-k*x} + (100 - A)$

2.5.2 Success of model fitting

Despite diverse curve shapes, the exponential decay model from Eqn. 6, $y = A * e^{-k*x} + (100 - A)$, was capable of fitting the observed data remarkably well. R^2 values associated with fitting the exponential decay model to dry-down curves as in Fig. 3 were assessed across all runs to determine how successfully the model fitted the observed dry-down patterns. Table 4 includes data from Run 1 and 2 assessed in this chapter, but also from Run 3 (Chapter 3 and 4). With over 81% of samples being successfully fitted by the model at the 0.95 R^2 level, and over 97% being fitted at the 0.90 R^2 level, this model offers a promising approach to smoothing curves from diverse, and potentially somewhat noisy dry-down datasets.

The species with the least strong model fitting scores tended to include: 1) those where only leaves were measured (*P. laurifolia, P. lorifolia*, *P. repens*), and 2) those which had tiny leaves and thus small total masses, even with stems included (*W. nodosa*, *C. rubricaulis*, *A. capensis*). The former may have been as a result of standalone leaves with less stored water being more vulnerable to rapid dry-down inducing mechanical advantage and diverging from the exponential decay fit, whilst the latter is likely due to observably noisy data (Fig. 3B) stemming from their small masses measured only with two-place decimal balances. Despite this, the model fitted even observably poor data sets with high R^2 values.

It is important to note that some curves represented in Fig. 3 have negative relative water content (RWC) values. This is due to methodological error when determining weight, often due to equipment noise when dealing with low mass samples. The curve shapes are still real, they have just been incorrectly transformed below the 0% RWC threshold. As the purpose of Fig. 3 is to illustrate success of the model at fitting curve shape, these values were not excluded. It is important to note that a good model fit should not be taken at face value and that negative values should be excluded from actual analysis of the values.

TABLE 4: Success rate of fitted model by species, $y = A * e^{-k*x} + (100 - A)$

Site	Species	Leaf or shoot	% Samples with R^2 >0.95	% Samples with R^2 >0.90
Drie Kuilen, Renosterveld	*Dicerothamnus rhinocerotis*	Shoot	100	100
	Oedera squarrosa	Shoot	100	100
	Ruschia multiflora	Shoot	87.5	100
	Passerina obtusifolia	Shoot	91.67	100
	Protea laurifolia	Leaf	54.17	100
	Microdon polygaloides	Shoot	95.83	100
	Wahlenbergia nodosa	Shoot	47.83	78.26
	Clutia rubricaulis	Shoot	47.83	86.96
Drie Kuilen, Fynbos	*Lobostmon decorus*	Shoot	100	100
	Aspalathus shawii	Shoot	87.5	100
	Selago dolosa	Shoot	83.33	100
	Agathosma capensis	Shoot	45.83	87.5
	Protea lorifolia	Leaf	75	100
	Protea repens	Leaf	62.5	100
Jonaskop	*Cannomois congesta*	Shoot	100	100
	Erica monsoniana	Shoot	100	100
	Protea repens (shoots)	Leaf	94.44	100
	Protea repens (leaves)	Leaf	94.44	100
		Average	81.55	97.37

TABLE 5: Success rate of fitted model by temperature, $y = A * e^{-k*x} + (100 - A)$

Temperature treatment	% Samples with R^2>0.95	% Samples with R^2>0.90
20°C	84.26	97.22
25°C	72.62	97.62
35°C	82.24	95.33
40°C	82.24	98.13
Average	80.34	97.07

2.5.3 Sensitivity to linear slope selection

Values for g_{res} and g_{min} should differ depending on the section of the slope selected as linear. Values for g_{res} and g_{min} computed using binned RWC sections of the modelled slope show variation in the sensitivity of different species to changes in the RWC interval used for calculation of g_{res} and g_{min} and are shown to differ by one to two orders of magnitude at bin extremes (Fig. 4A & B).

RWC is more likely to be a common physiological set point than time. Therefore, RWC acts as a way to standardise dry-down time across the many species. Because of the shape of the exponential decay function fit in Fig. 3 (Eqn. 6), g_{res} and g_{min} scaled linearly with the RWC interval used in their determination. The more linear the dry-down curve, the less steep the slope of the predicted g_{res} or g_{min} in Fig. 4, i.e. sensitivity of g_{res} and g_{min} to "slope selection" was variable. Therefore, it is clear that "slope selection" is important for g_{res} and g_{min} determination, especially if the species produces steeper dry-down curve.

2.5.4 Temperature effect on data quality

An increase in poor data quality and presence of outliers will result in lower R^2 values. Thus, Table 5 was collated from data from Run 1 and 2 assessed in this chapter, but also from Run 3 (Chapter 3 and 4), to assess whether higher temperatures produced erroneous data more than lower temperatures as these are proxies for overall VPD which is said to promote artefact and poor data.

However, there was no observable pattern in success rate of the fitted model (Eqn. 6) across temperatures at either the 0.95 R^2 level nor the 0.90 R^2 level. The temperature with the lowest fit was 25°C, potentially due to less stable wind conditions in the measurement environment (see 3.7 - Critiques and Improvements). Over 80% of samples had an R^2 above 0.95 with over 97% having an R^2 above 0.90, indicating good fit overall. These results thus vouch that the model-fitting approach is a fair one when measuring g_{res} and g_{min} at higher temperatures and VPD, such as in comparative studies.

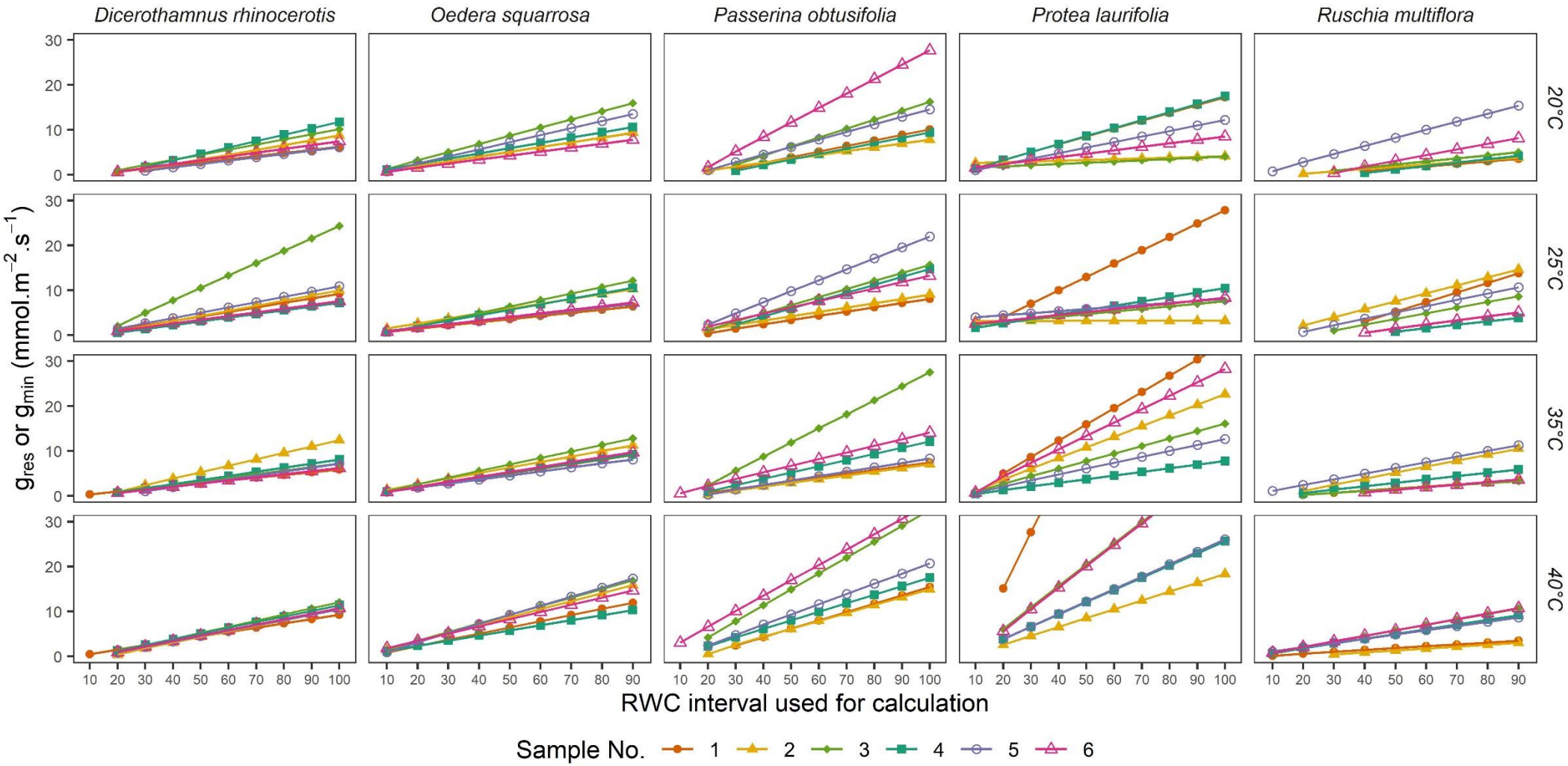

Figure 4A: The linear increase in g_{res} and g_{min} values calculated between differing RWC bins for Run 1 species. The steepness of each slope indicates how sensitive the g_{res} or g_{min} is to the RWC interval used to select the linear portion of the slope in its calculation. A RWC interval of '10' represents the interval of 0-10% RWC (Note: Some extreme values are cut off to allow for better visual representation of less steep slopes.)

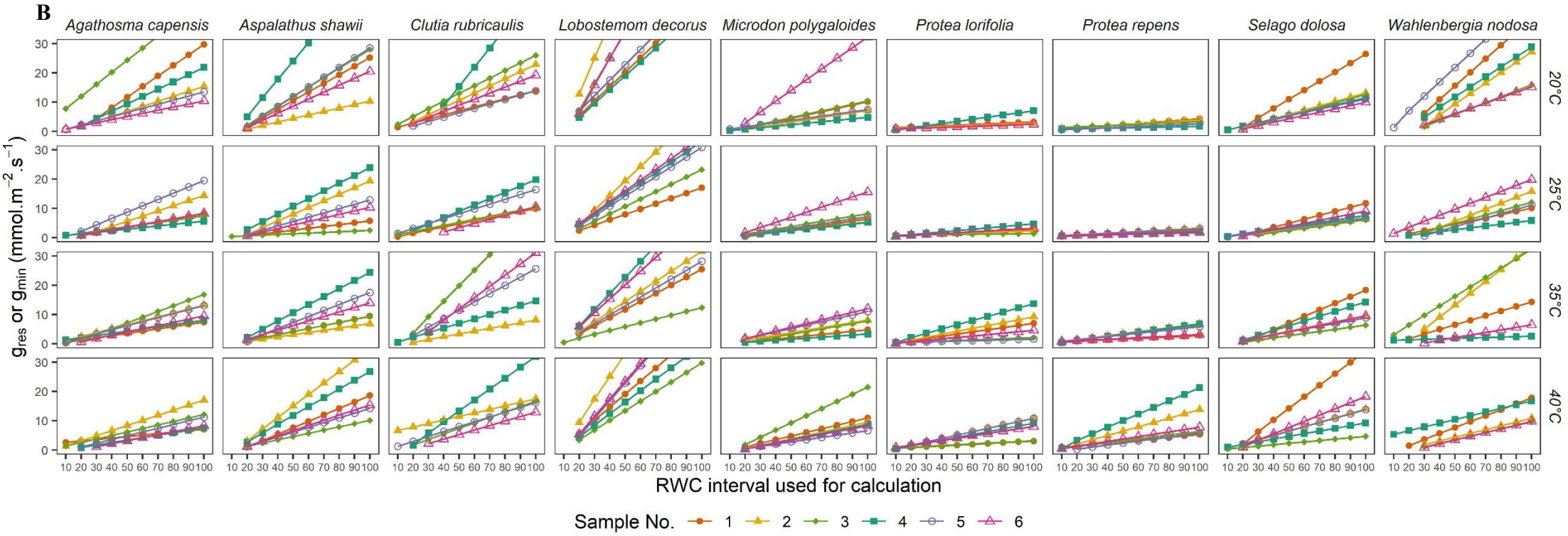

Figure 4B: The linear increase in g_{res} and g_{min} values calculated between differing RWC bins for Run 2 species. The steepness of each slope indicates how sensitive the g_{res} or g_{min} is to the RWC interval used to select the linear portion of the slope in its calculation. A RWC interval of '10' represents the interval of 0-10% RWC (Note: Some extreme values are cut off to allow for better visual representation of less steep slopes.)

2.6 Conclusion

The chosen model (Eqn. 6) was able to fit the diversity of curve shapes (Fig. 3) exceedingly well (Table 4) which allowed us to negate the effect of outliers while determining linear slope sections on non-linear curves. It also showed us that any experimental artefact induced in the form of rapid dry-down sections did not have a powerful effect on the ability of the model to fit data. Difference in measurement temperature also did not have an effect on model fit due to artefact. Values of g_{res} or g_{min} were shown to have varying levels of sensitivity to the slope interval used in their calculation (Fig. 4A & B).

This suggests that the approach of applying the exponential decay model is a robust one capable of dealing with datasets dealing with a variety of curve shapes, data of varying quality, and data from different measurement temperatures. What remains is to determine what the selected linear section to be used in g_{res} and g_{min} determination should be.

Chapter 3:
Theoretical framework for determining minimum conductance across a diverse set of species

The variance in curve shape and sensitivity to the selection of the linear section used to calculate minimum conductance, g_{res} and g_{min} (shown in Chapter 2), support the notion that a more robust, standardised, and reproducible method for g_{res} and g_{min} determination is needed. To do this while accounting for as much variation in plant morphology and physiology as possible, I propose the need to establish a framework that takes into account the physiological processes occurring in the plant during a drought event over which minimum conductance is the determining factor for plant time-to-death.

3.1 When is minimum conductance relevant?

To identify the linear section of the dry-down curve, let us consider where along this curve minimum conductance is most relevant, i.e. where g_{res} has the largest impact on plant survival (g_{min} fulfils the same function in this theoretical discussion and so g_{res} will be used to demonstrate the point).

Let us consider a plant under different scenarios of water stress (Fig. 5). The g_{res} always forms a component of the total conductance of the plant as it is effectively the uncontrollable water loss component. The exact g_{res} may be determined by several parameters such as cuticular thickness and chemical composition, and may fluctuate with prevailing environmental conditions. However, for the purposes of this scenario, let us use an average g_{res} at all times. When unstressed, the total conductance through a plant (g_s) for the course of a day will be large, of which only a small fraction of which will be the uncontrolled g_{res}. Let us term this the g_{res} fraction. The impact of that g_{res} fraction on the total conductance of the plant throughout the course of the day will be tiny (Fig. 5A). For example, for the conifer *Cupressus sempervirens* the g_{min} (measured on leaves only) is 2.47 ± 0.14 mmol.m^{-2}.s^{-1} out of the maximum stomatal conductance (g_{smax}) of 180.62 ± 17.53 mmol.m^{-2}.s^{-1} (Petek-Petrik *et al.*, 2023): a g_{res} fraction of only ~1.37%. Thus, during active transpiration, g_{res} is relatively unimpactful.

In a scenario with decreased water availability, the plant exerts control over its stomata and closes them in response to the water conditions. The total g_s integrated over the course of the day will be lower, but the fractional contribution of the uncontrolled conductance (g_{res}) to the total conductance will be larger, i.e. the g_{res} fraction will be higher (Fig. 5B). As water stress

continues to increase, so too will the g_{res} fraction increase.

When under maximum water stress, the plant's stomata will close as far as possible and the g_{res} fraction approaches 100% of the total conductance (Fig. 5C). Under this scenario, the rate of water loss from minimum conductance is what wholly determines when the plant will reach its critical water potential where it faces lethal levels of embolism (Ψ_{crit}). Uncontrolled conductance is thus most relevant under maximum water stress when stomata are closed, hence g_{res} is defined after the point of stomatal closure (g_{s90}). Before stomatal closure, it would not be possible to say that the total measured conductance (g_s) was equal to the residual conductance (g_{res}).

The start point of the 'linear phase' of the mass loss versus time curve (dry-down curve) is currently defined in the minimum conductance methods at the point of stomatal closure, albeit it is determined visually based on curve shape. This makes physiological sense as g_{res} is not the determining factor driving desiccation before the point of stomatal closure.

The question remains of how to define the endpoint of the dry-down curve in a similar manner. The plant continues to lose water at a certain rate (g_{res}) until it reaches its critical water potential threshold (Ψ_{crit}) and is unable to recover, ultimately leading to plant death (Fig. 1). However, the plant will continue to lose water past this point of no return, as this loss is driven by the prevailing environmental conditions and high VPD associated with the drought conditions. When we define the "linear part of the slope" of the dry-down curve, we should be wary of including this period of time where the plant's water potential has already fallen below Ψ_{crit}. From an evolutionary perspective, any survival benefits granted by a reduced g_{res} only have an effect when the plant is still able to recover from the drought stress. To put it another way, it doesn't matter what the plant's g_{res} is after it has passed the point of no return (Ψ_{crit}). Therefore, to obtain a biologically relevant g_{res}, we should not include in the g_{res} calculation the latter section of the mass loss curve which corresponds to the period after which the plant has passed this fatal threshold (Ψ_{crit}) (Fig. 6).

Thus, I argue that one should be taking g_{res} or g_{min} readings between stomatal closure (Ψ_{gs90}) and the critical water potential threshold (Ψ_{crit}), i.e. across the stomatal safety margin (SSM), as this has a biological and evolutionary meaning. This is also logical when we consider that the stomatal margin retention index ($SMRI_{\Psi crit}$) is the time taken for a plant to cross the SSM. It follows then that to find the rate at which the SSM is crossed, we should measure the rate of water loss (g_{res} and g_{min}) across the SSM.

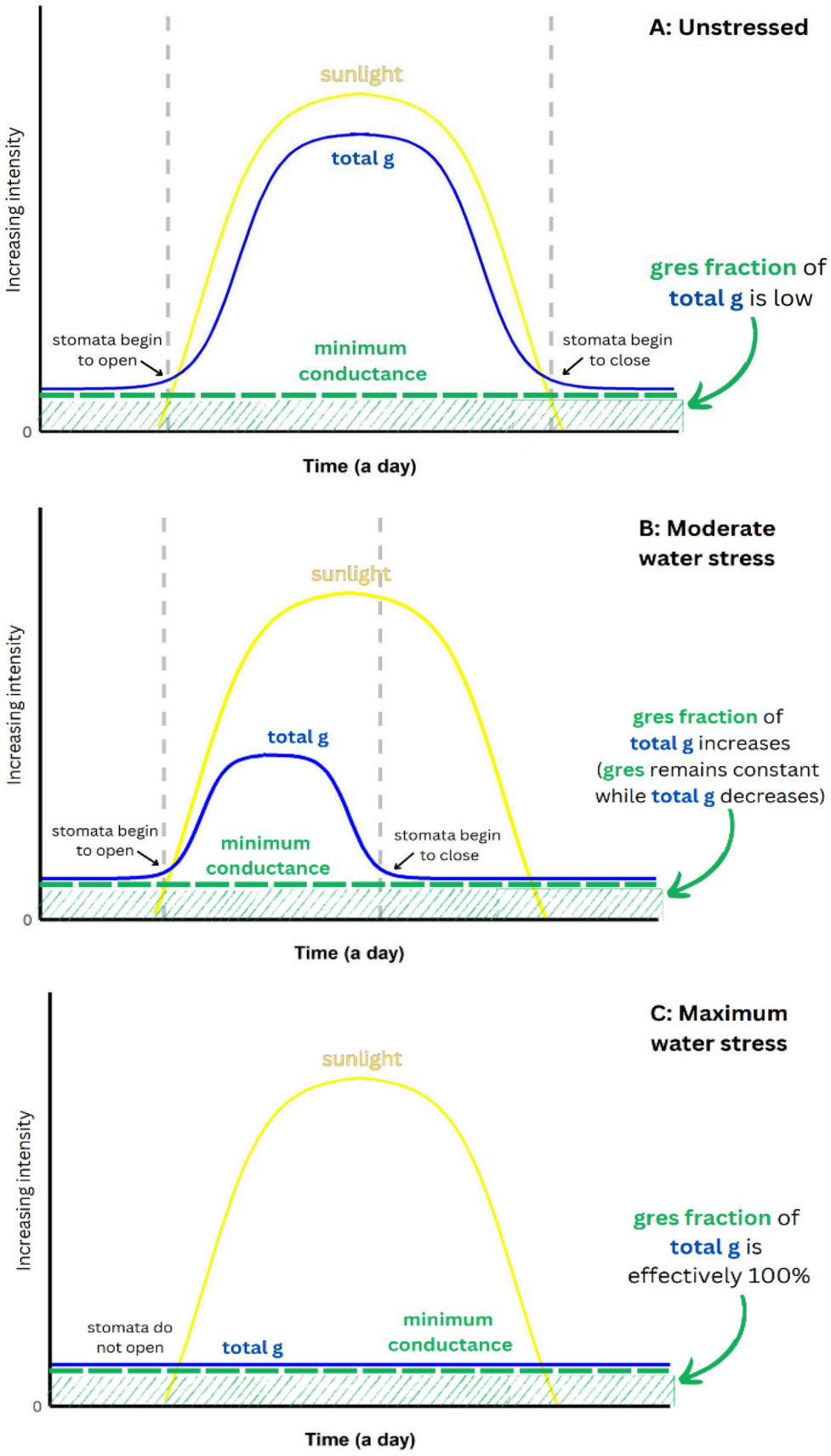

Figure 5: Conceptual representation of the contribution of g_{res} to total conductance (g), the g_{res} fraction, under differing water stress levels. g_{res} has the biggest impact on total g of the plant when stomata are fully closed under high water stress.

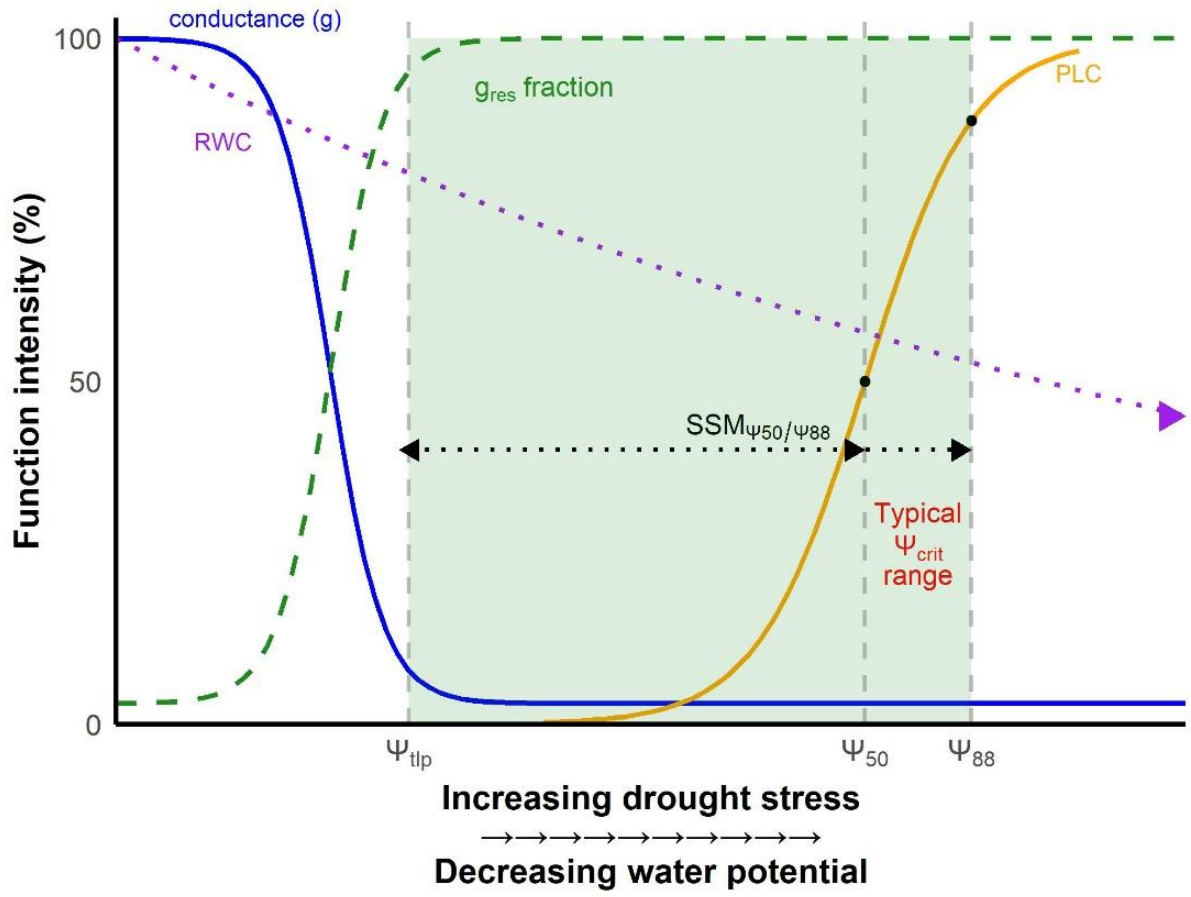

Figure 6: Conceptual representation of the physiological processes occurring during a drought event. Conductance (g) decreases as stomata close. Relative water content (RWC) decreases as the plant loses water under increasing drought stress. After a certain period, embolism will be induced, and conductivity of xylem will decrease (percent loss conductivity – PLC increase) until it reaches Ψ_{crit}. g_{res} fraction is highest after Ψ_{tlp} (a proxy for Ψ_{gs90}) and controls water losses after this point across the SSM. Water loss mitigation does not matter post-death, showing that g_{res} matters most over the SSM.

3.2 Practical implications of requiring SSM

To obtain the point of stomatal closure (Ψ_{gs90}), one could calculate it empirically from stomatal conductance measurements (Petek-Petrik *et al.*, 2023). However, Ψ_{tlp} typically occurs very soon after Ψ_{gs90}. While Ψtlp is considered a plastic trait that can alter with osmotic adjustment (Bartlett *et al.*, 2014; Sorek *et al.*, 2021), multiple studies have shown these two values to occur within the same range (West and Gaff, 1976; Hinckley *et al.*, 1983; Petek-Petrik *et al.*, 2023), and so Ψ_{tlp} has previously been used as a proxy for stomatal closure. A pressure-volume curve can then be used to obtain this value. However, it is important to keep in mind that this relationship may only apply to species with strong stomatal control and that do not strongly alter leaf osmotic potential over short time scales (Meinzer *et al.*, 2014; Johnson *et al.*, 2018).

To obtain the critical water potential threshold (Ψ_{crit}), a vulnerability curve is required. Ψ_{50} or Ψ_{88} can be chosen as proxies based on whether the plant is a gymno- or angiosperm (Resco et al., 2009; Urli et al., 2013; Li et al., 2015). While other environmental or individual factors may influence these lethal thresholds, they remain helpful for determining an endpoint for the dry-down curve (the precision of this delineation is tested and shown in Fig. 9).

On the dry-down curve, the axes are RWC and time. To use Ψ_{tlp} and Ψ_{crit} to define start- and endpoints on this curve, they need to be translated to RWC_{tlp} and RWC_{crit}. The axes on a pressure-volume curve are '$\frac{1}{\Psi}$' and '$100 - RWC$'. This establishes a relationship between water potential (Ψ) and RWC which can be used to convert Ψ values to RWC values.

The proposed framework has a focus on precision. It is true that an increase in precision often necessitates an increase in sampling effort. However, determination of a precise value for g_{res} is important to establish. A better estimate of the "true" g_{res} allows us to assess how accurately other less high effort methods compare. The decision on which methods are acceptable can then be made by properly weighing up the trade-off between sampling effort and accuracy.

3.3 Other considerations:

3.3.1 Leaf area

Leaf area (LA) should be standardised to allow for comparable conductance values. However, as there are many different applications for it as a parameter, many definitions and associated methods for LA have been employed to obtain values for different purposes (Jonckheere *et al.*, 2004).

Leaf area index (LAI) is an example of such a definition. It is a dimensionless variable representing LA, originally described based on a single side of the leaf and ground surface area (Watson, 1947). Due to the complication introduced by the structures of non-flat leaves, it has been redefined several times, including by considering projected area (Bolstad and Gower, 1990; Smith, 1991). This has been done to obtain a suitable definition which has a physical and biological significance (Chen and Black, 1992), i.e. a definition that links physical form with biological function. LAI's current definition aims to define area of total interception, as this physically represents the area of the leaf intercepting radiation from the sun and has biological connotations for gas exchange surface area (Jonckheere *et al.*, 2004).

In a similar way, it stands to reason that the LA definition in the context of minimum conductance should have relevance in these ways. As such, it would likely be best to quantify total conducting area. This would incorporate all area covered by stomata, area covered by the cuticle, and any other surface through which water can be lost, such as wounds or bark. Many studies on simple leaves use double-sided LA (Blackman *et al.*, 2019; Billon *et al.*, 2020), a simple doubling of vertically scanned area, as this is a sensible proxy for total LA for these leaf shapes. When using a planimetric method, this means that for complex morphologies with more 3D leaf structures, and for area determination of small branches, scanned LA would need to be transformed in unique ways, based on logical assumptions about morphology. While all LA determination methods have shortcomings, it is encouraged for a specific method to be chosen according to the context of use (Jonckheere *et al.*, 2004). Thus, in the experiments in this study based on diverse leaf morphologies, the total leaf area has been estimated using logical assumptions, as in Chapter 2 (see Table S1).

As mentioned, prior, an inconsistency in LA estimation has been whether LA was measured pre- (fresh LA) or post-dry-down (dry LA). When deciding whether to measure fresh LA or dry LA, we thus turn again to the value with a biological meaning, one which more closely represents the conducting area through which the sample is losing water. While this is complicated by the fact that leaves will shrink during the dry-down process, I argue that ultimately quantifying fresh LA for use in the g_{res} and g_{min} equation is preferable. This value more closely represents the conducting area during the period before the plant has reached Ψ_{crit} than the dry LA obtained well past plant mortality.

3.3.2 Comparability of gres and gmin

For species with non-excisable or small leaves, a measure of g_{res} will be obtained from the mass loss method instead of a g_{min} measure. It has been shown that the g_{bark} contribution to g_{res} can be quite small to the point where g_{min} and g_{res} are not statistically different (Billon *et al.*, 2020). However, for species which display hydraulic segmentation wherein leaf and stem have divergent vulnerabilities to embolism and are often drought-deciduous (Wolfe, Sperry and Kursar, 2016; Blackman *et al.*, 2019; Levionnois *et al.*, 2021), distinguishing between g_{res} and g_{bark} is important. Water loss is mediated by g_{res} (i.e., $g_{min} + g_{bark}$), but when leaves are shed, water loss instead becomes mediated by g_{bark} only.

However, for non-drought-deciduous species, we would like to be able to compare g_{res} to g_{min} to ascertain whether g_{res} can be used as proxy for g_{min} (and vice versa). This would be particularly helpful when assessing existing datasets. To do this, we need to know whether g_{res} is statistically different from g_{min}.

3.3.3 Environmental measurement conditions

It is of course important to measure temperature and humidity throughout the experiment. Measurement temperature may have effects on cuticular permeability (Kerstiens, 1996; Riederer and Muller, 2008; Fernández *et al.*, 2017; Schuster, Burghardt and Riederer, 2017) which may differ unpredictably based on species, and should thus be carefully considered based on context of the experiment. It may also induce rapid dry-down sections due to mechanical advantage decreasing data quality, however this should be handled by fitting the exponential decay model from Eqn. 6 to the data and using the values generated along that smoothed curve. Chapter 2 showed that this model fitted the data with a high R^2 (see also Table 4 and 5), thus reducing noise.

Wind can increase measured conductance if it removes the air boundary layer surrounding the leaf. Wind conditions should thus be kept consistent during the experiment. An apparatus such as the DroughtBox (Billon *et al.*, 2020) is well suited for this purpose.

3.4 Aim

Stomatal Margin Retention Index (SMRI) is a newly created index for quantifying time taken to cross the stomatal safety margin (SSM) (Petek-Petrik *et al.*, 2023), and requires a measurement of g_{res} or g_{min} to calculate it. It has been shown to be a particularly strong predictor of plant time to death but has only been tested on gymnosperms and requires further testing. Therefore, the proposed framework was applied on three species from the Cape Floristic Region (CFR) which represent diverse and prominent growth forms within the region (Skelton *et al.*, 2023).

The aims of this chapter were to 1) compare g_{res} and g_{min} calculated across the SSM to those without this delineation, 2) assess whether g_{res} and g_{min} are statistically different for a non-drought-deciduous species, 3) assess whether measurement temperature had an effect on g_{res} and g_{min}, or on SMRI, and 4) pick up on any other shortcomings or notable consequences of the proposed framework. Additionally, the actual values for g_{res} or g_{min} and SMRI of the three study species were of interest and are discussed in Chapter 4.

3.5 Methods

3.5.1 Study area and study species

Sampling was carried out at Jonaskop in the Riviersonderend Mountains (33° 56′ 30.45″ S and 19° 31′ 34.18″ E, 980 m elevation above sea level), a mountainous sclerophyllous shrubland (fynbos) community within the CFR. Annual rainfall at the site is 411mm, of which 66% occurs in winter (Agenbag *et al.*, 2008; Skelton *et al.*, 2023). Vegetation on the sandy, nutrient-leached soil is typical of the fynbos, being dominated by a low open canopy of proteoids, with an understorey comprised primarily of ericoid shrubs and reed-like restioids (Agenbag *et al.*, 2008). These three vegetation types are morphologically diverse, representing the dominant families and growth forms within the Fynbos biome. The selected study species fell within these families and were *Protea repens* (L.) L. (Proteaceae), *Erica monsoniana* L.f. (Ericaceae), and *Cannomois congesta* Mast. (Restionaceae). They were also chosen because previous work (Skelton *et al.*, 2023; West *et al.*, 2024) and ongoing work (MSc and PhD research by fellow students) has been carried out on them, making them well understood representative species.

The weather station at the Jonaskop field site.

3.5.2 Xylem vulnerability to embolism

Data for xylem vulnerability to embolism (expressed as Ψ_{88}) were obtained from the raw data of Skelton *et al.*, 2023 obtained at Jonaskop on the same three species during 2012-2014 using the optical method (Brodribb, Bienaimé and Marmottant, 2016; Brodribb *et al.*, 2016, 2017; Skelton *et al.*, 2018).

3.5.3 Minimum conductance

3.5.3.1 Sampling

Sample collection for minimum conductance at Jonaskop occurred on 2 July 2024. For *E. monsoniana*, and *C. congesta*, seven individuals were collected, of which six were used, with one serving as a backup. An extra set of seven were collected for *P. repens*, for a total of 14 samples with two backups.

All samples were taken from healthy-looking individuals at the base of a branch of the plant and kept hydrated with the stem in water, allowing for rehydration, and stored at 10°C until experimentation began (this was Run 3, and began on 4 Jul). Each individual plant had four samples taken from it, one to be used in each of four temperature treatments (discussed below). Fully expanded shoots were selected and cut at the base of a node. Flowers were avoided where possible but were removed if present. Cuts were sealed with contact adhesive.

For *Protea repens,* both individual leaves and fully expanded shoots were selected. This was done to determine whether there was a significant difference in g_{min} obtained when using leaves (as traditionally described in the MLD method) and g_{res} obtained when using shoots (a necessity for most species investigated in this study due to small size).

3.5.3.2 Experiments

Similarly to the experiments performed in Chapter 2, several temperature treatments were performed at 20°C, 35°C, and 40°C. The experiments for 20°C, 35°C, and 40°C were performed in temperature controlled phytotron chambers (see Table S2). An additional treatment attempted at 25°C was performed in a constant temperature room, but ultimately had to be excluded due to failed temperature control and non-standardised wind speed.

For each treatment for each species, six samples from different individuals were imaged using a scanner (Epson Perfection V850 Pro) in order to obtain leaf area planimetrically. The ImageJ program (Schneider, Rasband and Eliceiri, 2012) was used to obtain one-sided leaf area in the same way as in Chapter 2.

For certain samples, leaf area was taken post-desiccation as it was easier to obtain accurately when leaves could be removed. In these cases, scans of extra samples were taken pre- and post-desiccation. The percent loss in leaf area over the dry-down process was then determined on a per-species basis and used to empirically set a calibration factor that was applied to the relevant scans (see Table S1). Dry-down measurements then proceeded in the same way as in Chapter 2, this time using three-place decimal balances (OHAUS Carat Series TAJ203), and relative water content (RWC) was obtained.

3.5.4 Pressure-volume curves

3.5.4.1 Sampling

To obtain Ψ_{tlp} from pressure-volume (p-v) curves for *E. monsoniana*, *P. repens,* and *C. congesta*, samples were collected from Jonaskop on 14 November, 25 November, and 2 December 2024 respectively.

For each species, six individuals were collected. All samples were taken at the base of a branch of the plant and kept in a humid, airtight environment (sealed plastic bags with moist paper-towel) while in transit. As allowing overnight rehydration may cause osmotic changes to TLP (Meinzer et al., 2014), there is a trade-off to consider between this drawback and technical difficulties when measuring samples where water potential has already fallen far below zero. As the specimens were collected during the beginning of the hot, dry summer season, it was decided that rehydration was required in this instance. Plants were thus kept in the dark at 10°C overnight to rehydrate. On the following morning, p-v curve procedure began. Each individual plant had one twig taken from it, resulting in a maximum of six curves per species. Fully expanded shoots were selected and cut at the base of a node. Flowers were avoided where possible but, if present, were removed prior to removal of twig from sample.

3.5.4.2 Procedure

Turgor loss point (Ψ_{tlp}) values were obtained using a pressure-bomb following the methods of Tyree and Hammel, 1972. Water potential was obtained using a portable pressure-chamber (PMS Instrument Company Model 1505D Pressure Chamber Instrument), with weight being measured using a three-place decimal balance (OHAUS Carat Series TAJ203) immediately afterwards. Samples were then left to dry on the benchtop. Measurements were repeated at intervals of approximately 15 minutes to begin but intervals were extended based on rate of dry-down for a given species and as water potential began to decline more slowly over time. Samples were bagged to pause dry-down if required due to handling multiple samples at once. Measurements continued until at least three points had been obtained after Ψ_{tlp}.

3.5.5 Data analysis

Data was collected, collated and analysed in R (R Core Team, 2020) as in Chapter 2, using the same packages. All temperature and humidity data were collected without error. Again, an exponential decay function of the form found in Eqn. 6 was fitted to each curve.

Critical water potential (Ψ_{crit}) values at Ψ_{50} and Ψ_{88} were extracted for each species from Skelton *et al.*, 2023. Pressure-volume curves were used to obtain the relative water content (RWC) at the relevant water potential thresholds, i.e. at turgor loss point (RWC_{tlp}) and at Ψ_{crit} ($RWC_{\Psi 88}$ in this case) (Skelton *et al.*, 2023), for each species. Using these fitted RWC (y) values from the model, the parameters necessary for g_{res} or g_{min} calculation were generated at RWC_{tlp} and $RWC_{\Psi 88}$.

Values for g_{res} and g_{min} were then calculated using the slope between RWC_{tlp} and $RWC_{\Psi 88}$ (i.e., across $SSM_{\Psi 88}$) (see Fig. 7 for visual demonstration of slope limits). Stomatal Margin Retention Index (SMRI) was then computed as the stomatal safety margin (SSM) divided by g_{res} or g_{min}. In addition, separate values for g_{res} and g_{min} were calculated using different RWC intervals, namely the slope between RWC_{tlp} and $RWC_{\Psi 50}$ (across $SSM_{\Psi 50}$), the slope after RWC_{tlp}, the slope between $RWC_{100\%}$ and $RWC_{\Psi 88}$, as well as over the whole dry-down slope. The endpoint had to be such that endpoint+A >100 due to how the models were fit, else 'NAs' were produced. Thus, for those points, the data were excluded. Specimens with a RWC below zero were also excluded from analysis.

Using base R functions, multiple one-way ANOVAs were run comparing g_{res} and g_{min}, and $SMRI_{\Psi 88}$ values within both species and temperature levels. Several Tukey HSD posthoc tests were then performed to determine significance between the different components within each level.

3.6 Findings

In all figures and tables which follow throughout the remainder of the thesis, significance thresholds were $p < 0.05$ and error bars are 95% confidence intervals.

3.6.1 Effect of slope selection:

3.6.1.1 Results

As expressed before, model fit was very good with 97.22% of the R^2 values were over 0.95, and 100% were over 0.90 (Fig. 8, see also Table 4).

The g_{res} and g_{min} values calculated using different slope intervals (Fig. 9) show a consistent clustering pattern across all species and almost all temperatures.

The values obtained over the SSM were very similar whether using Ψ_{50} or Ψ_{88} as the Ψ_{crit} value. As all species were angiosperms, Ψ_{88} was thus used in all analysis going forward. Additionally, values calculated using the slope before Ψ_{88} were tightly aligned with the SSM-limited values.

The second cluster was those values calculated across the whole slope and those calculated using the slope after TLP. These clearly diverged from the first cluster of three, except perhaps in *P.repens* leaves.

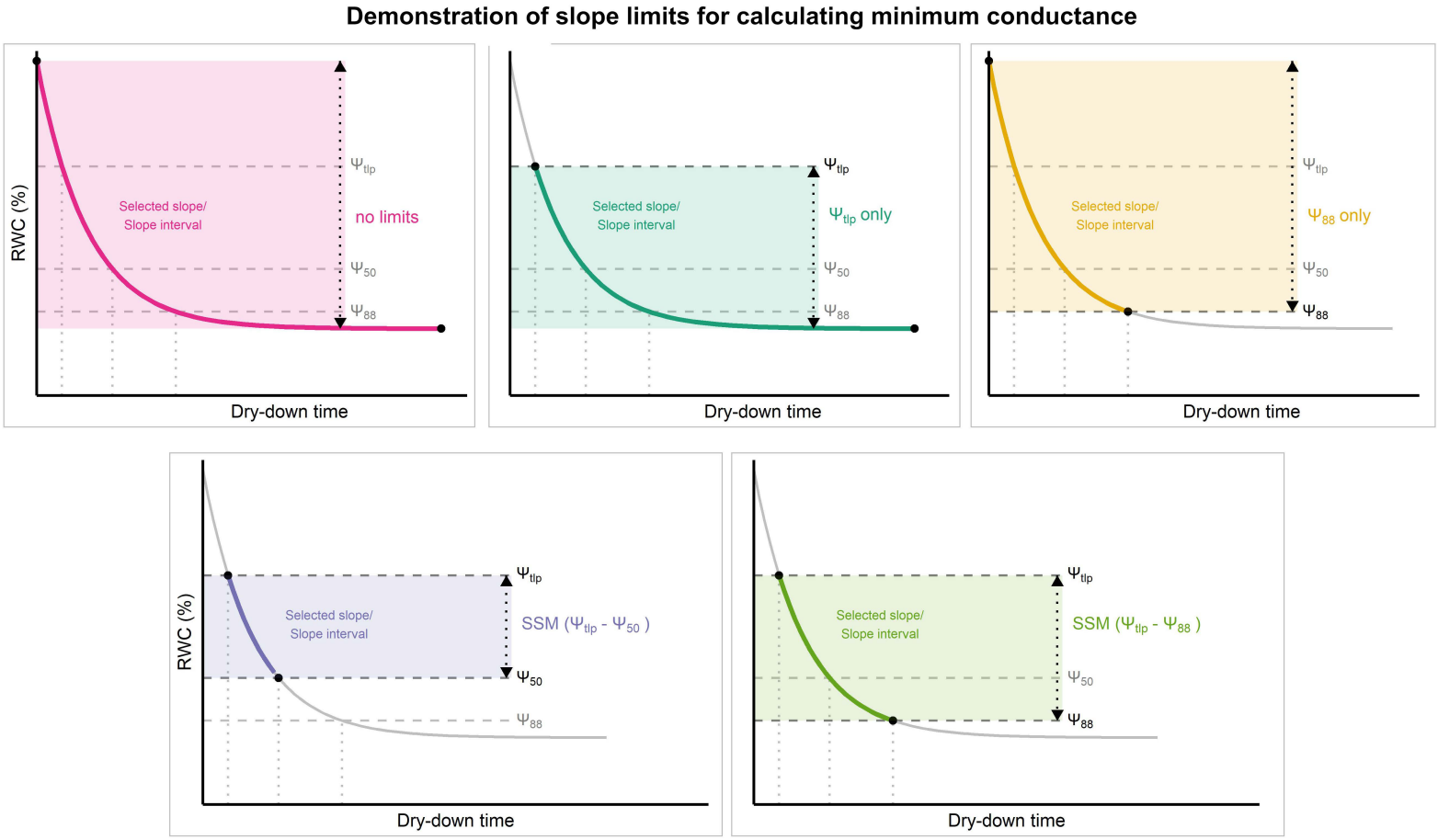

Figure 7: Relative water content (RWC) decreases with dry-down time. g_{res} and g_{min} values are calculated using RWC values on the slope between different water potential (Ψ) values. The slope intervals used will be: 1) "no limits", i.e. the whole dry-down slope, 2) "Ψ_{tlp} only", i.e. after turgor loss point, 3) "Ψ_{88} only", i.e. before Ψ_{88}, 4) "SSM (Ψ_{tlp} - Ψ_{50})", i.e. the stomatal safety margin (SSM) defined between Ψ_{tlp} & Ψ_{50}, and 5) "SSM (Ψ_{tlp} - Ψ_{88})", the SSM defined between Ψ_{tlp} & Ψ_{88}.

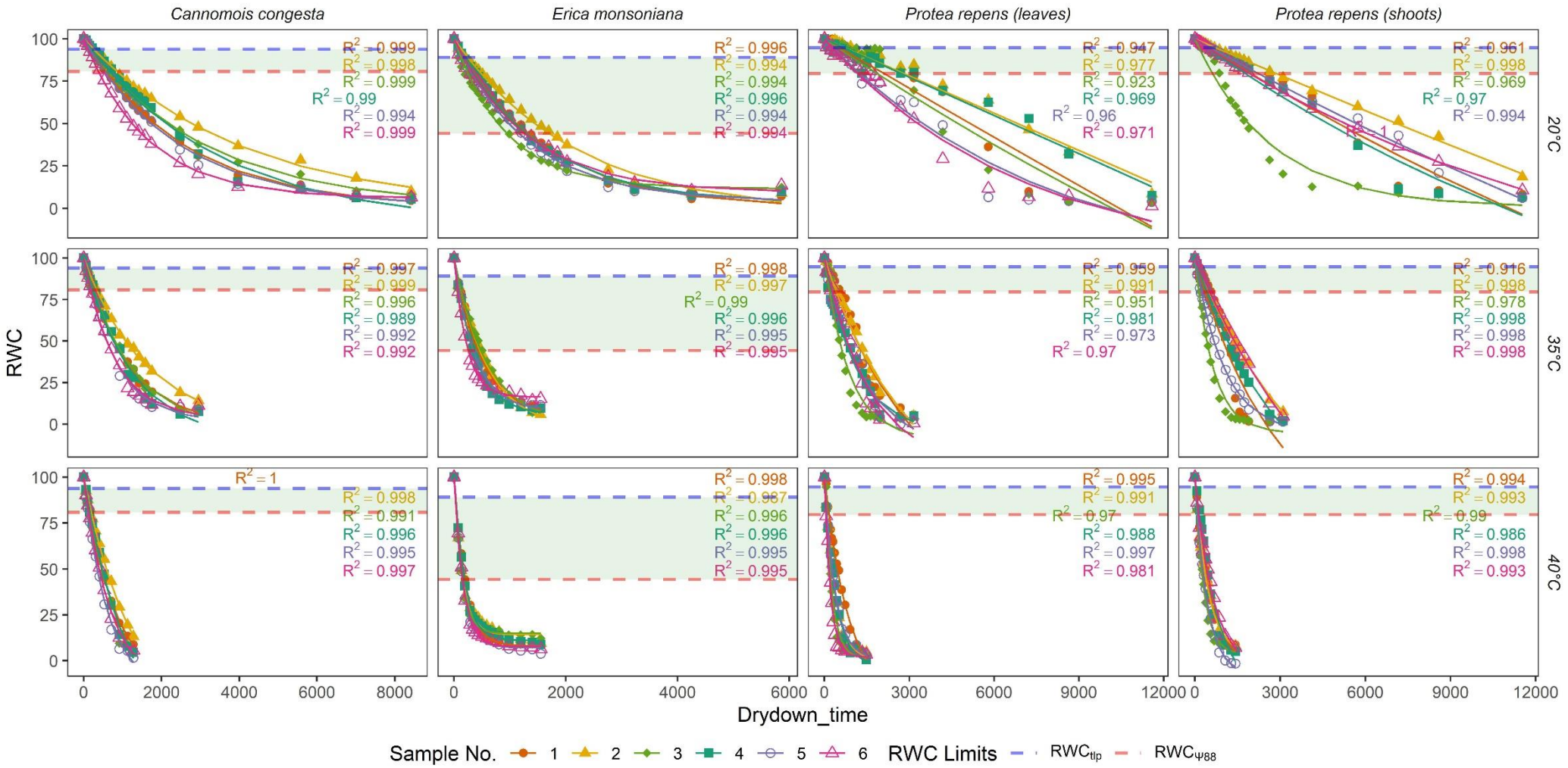

Figure 8: Dry-down curves showing the decrease in relative water content (RWC) with time in Run 3 study species, fitted with the saturating model (Eqn. 6).

Associated R^2 values are displayed. Eqn. 6: $y = A * e^{-k*x} + (100 - A)$

Blue dashed lines represent the RWC_{tlp}, while red dashed lines represent the $RWC_{\Psi 88}$. The green shaded area represents the $SSM_{\Psi 88}$ over which the linear slope section was defined.

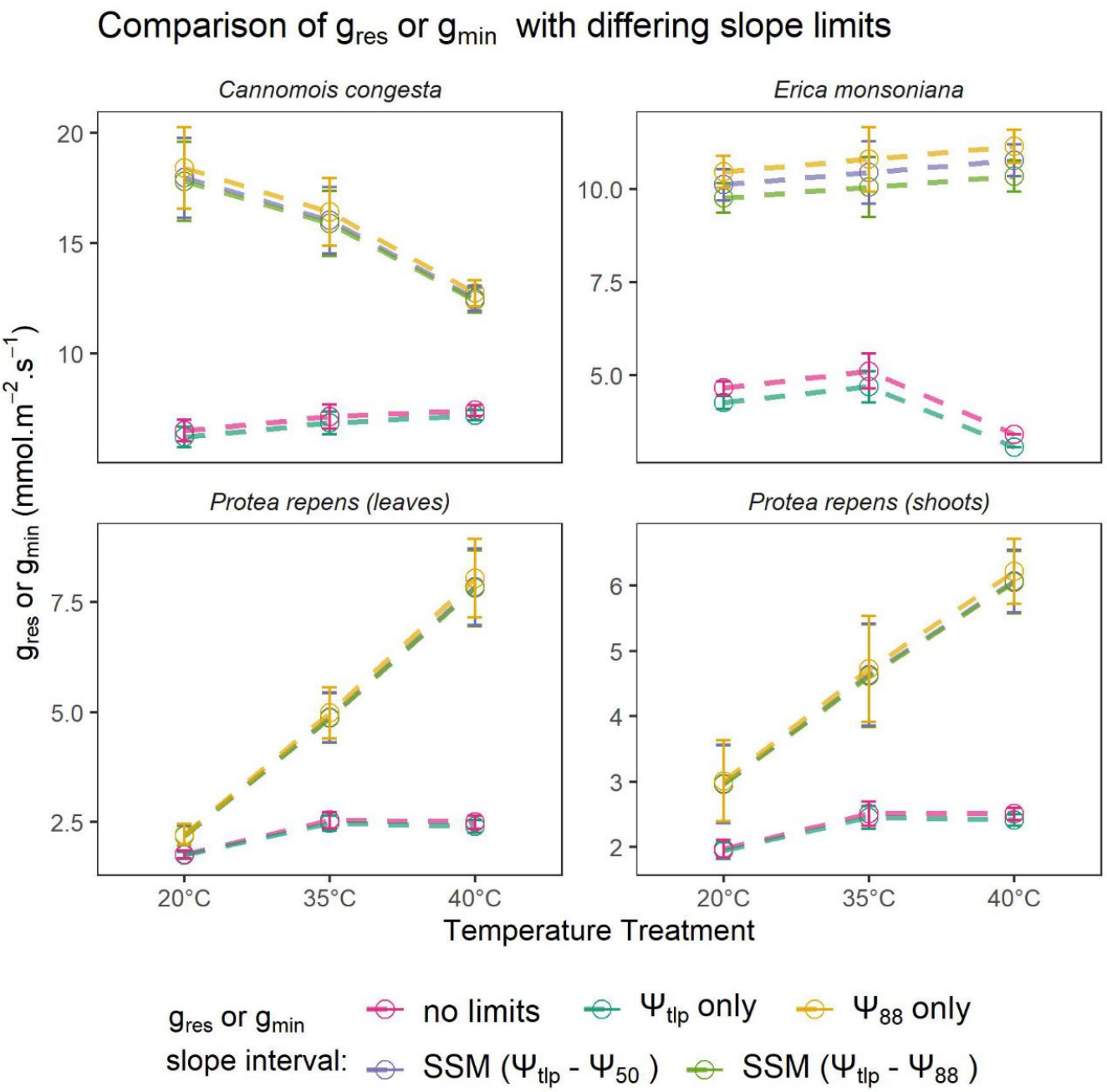

Figure 9: g_{res} and g_{min} values calculated using different limits on the start- and endpoints defined for the interval defining the linear portion of the slope used in the g_{res} or g_{min} calculation.

3.6.1.2 Discussion

The obvious clustering in minimum conductance values of those where Ψ_{crit} was used for calculation (Fig. 9: yellow, purple, and green points) and those where it wasn't (Fig. 9: pink, and teal points) emphasises the importance of selecting a linear slope portion as shown in Chapter 2. Thus, including a measure of Ψ_{crit} seems essential for accurate calculation.

However, the extreme similarity between minimum conductance values calculated between Ψ_{50} and Ψ_{88} seems to indicate that conductance values are not particularly sensitive to what value is chosen for Ψ_{crit}, so long as it is placed a good distance away from the definitive end of the dry-down curve. In other words, there seems to be some leeway when trying to pinpoint the end of the section being used to calculate minimum conductance, the so-called "linear section" of the curve. Rather, there is a window instead of a fixed point. Additionally, the inclusion of TLP in the calculation did not seem to significantly change the calculated minimum conductance values.

This suggests several things. Firstly, for species commonly reported in the literature with so-called 'linear' dry-down slopes, the linear portion of the slope identified by eye may be perfectly defendable as an accurate enough estimate for functional assessment when a modelled curve is fitted to the data. This is because a curve section that appears somewhat linear must automatically exclude the very end of the dry-down. Further statistical comparison in future studies comparing those methods to the ones proposed in this study are required to confirm this notion.

Secondly, for dry-down slopes with any shape, it may be possible that a less precise proxy for Ψ_{tlp} and Ψ_{crit} may be used and would generate statistically similar values for minimum conductance. For example, if RWC_{tlp} and RWC_{crit} which are used in the framework could be estimated from global databases, they could be used. Theoretically, RWC averages could be refined based on growth form, or habitat, or other tags that narrow the range and improve the RWC average, although this comes with its own challenges (see 3.7 - Critiques and Improvements). It may even be defendable to forgo using Ψ_{tlp} as it seemed to have little effect on outputted values (Fig. 9).

What can be said for certain is that it should be considered standard practice to report which values were used to calculate g_{res} and g_{min}. When Ψ_{tlp} and Ψ_{crit} data are available, g_{res} and g_{min} should ideally be measured over the SSM. The context in which g_{res} and g_{min} will be measured most commonly seems to be for modelling time to death where data for the SSM parameters will likely be collected anyway. Under this scenario, improving the accuracy of the conductance estimates and allowing for the methods to be applied to a broader range of species is a step forward in utilising minimum conductance in hydraulic studies.

3.6.2 Effect of measurement temperature:

3.6.2.1 Results

3.6.2.1.1 g_{res} and g_{min}

There does not seem to be a significant temperature effect on g_{res} (Fig. 10). Any observable patterns were not significant. For g_{min} measured from *P. repens* leaves, g_{min} appeared to decrease with an increase in temperature, however there was only a significant difference between the temperature extremes (20°C and 40°C).

3.6.2.1.2 Stomatal Margin Retention Index (SMRI)

In *C. congesta* and *E. monsoniana*, $SMRI_{\Psi 88}$ did not differ significantly with measurement temperature (Fig. 11). However, for *P. repens*, SMRI trended downwards with increasing temperature. This pattern was significant in shoots except between 35°C and 40°C. For *P. repens* leaves, only the temperature extremes (20°C and 40°C) were significantly different from each other.

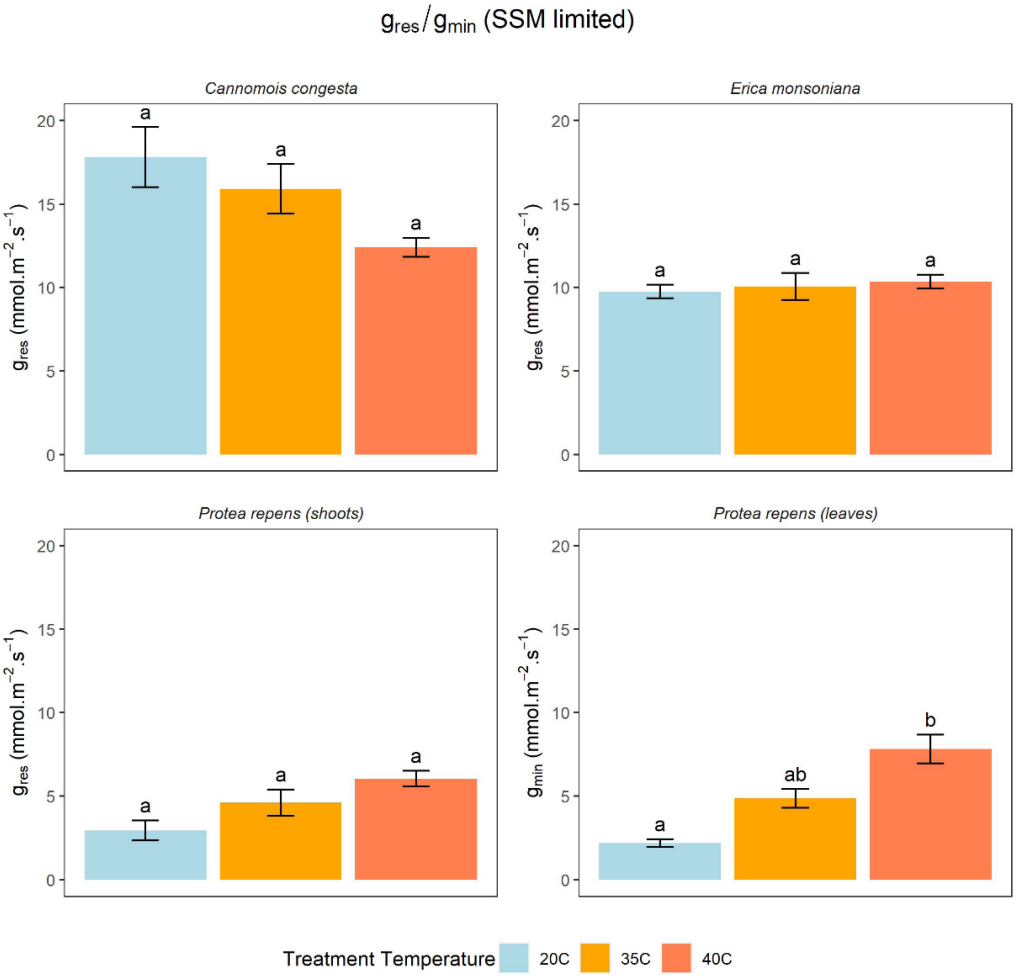

Figure 10: SSM limited g_{res} and g_{min}, i.e., measured across the SSM_{88}, at different temperatures for the study species shown. Arranged by species and comparisons made between temperatures.

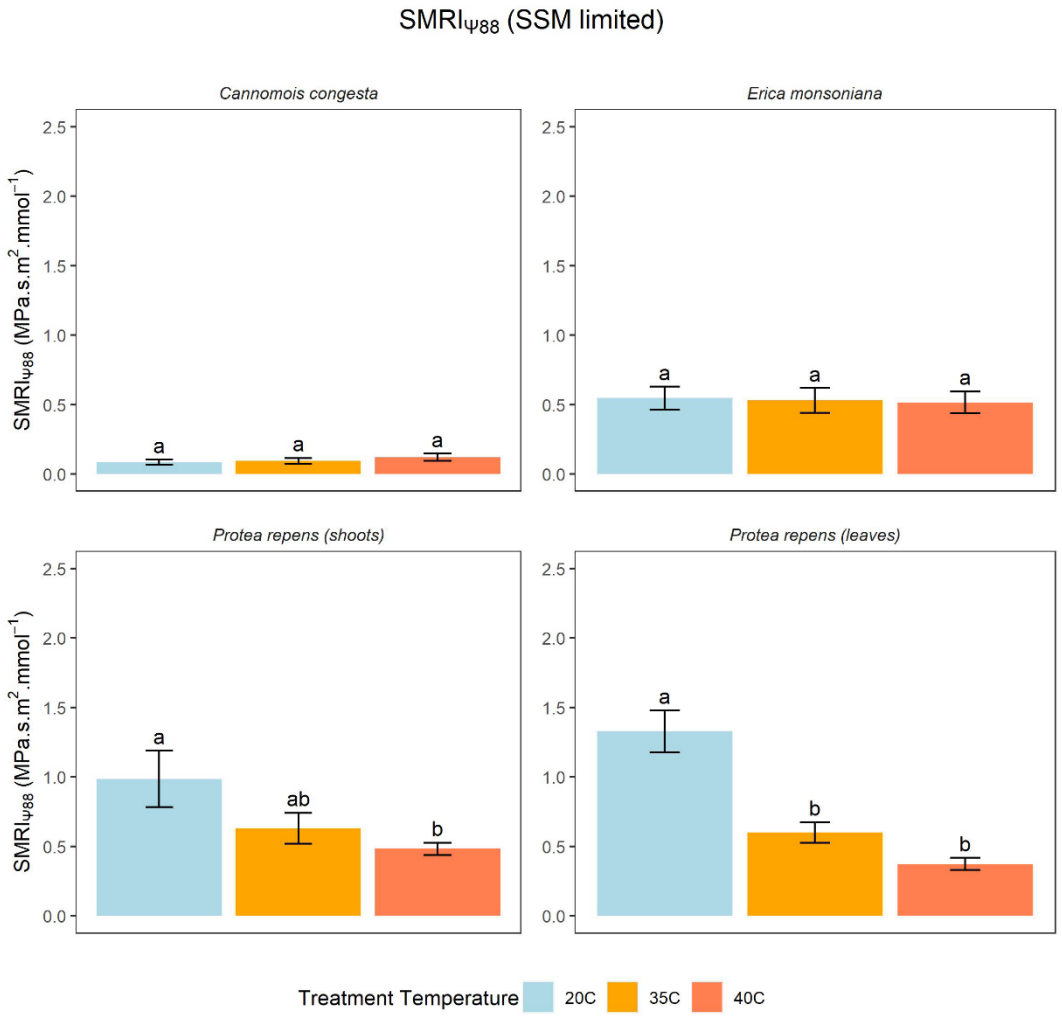

Figure 11: SSM limited SMRI, i.e., calculated using g_{res} or g_{min} measured across the SSM_{88}, at different temperatures for the study species shown. Arranged by species and comparisons made between temperatures.

3.6.2.2 Discussion

3.6.2.2.1 g_{res} and g_{min}

While there was no strong temperature effect on minimum conductance values, patterns were still observable for *P. repens* and *C. congesta* (Fig. 10). Values for *P. repens* tended to increase with temperature. This small change may be linked to increased contributions from g_{cuti} as the cuticular wax becomes more permeable at higher temperatures. As wax composition differs between species, this could also explain why barely any pattern was observed in *E. monsoniana*. Values for *C. congesta* tended to decrease with increased temperature, and it is unclear what could be causing this pattern.

These results suggest that the temperature at which g_{res} and g_{min} measurements are taken does not seem to be important for accurate determination of these values. Thus, suggesting values

from the literature obtained under different temperatures may likely be statistically comparable. However, this doesn't seem to be the whole picture as shown by Fig. 11.

3.6.2.2.2 Stomatal Margin Retention Index (SMRI)

As SSM is fixed and SMRI is a function of g_{res} or g_{min}, the patterns in Fig. 11 are roughly an inverse of the g_{res} and g_{min} patterns (Fig. 10). However, as alluded to above, the significance of SMRI trends differs from that of g_{res} and g_{min}. While the SMRI of *C. congesta* and *E. monsoniana* are unaffected by temperature, several temperatures in *P. repens* were significantly different.

This calls into question the suggestion above that g_{res} and g_{min} values measured at different temperatures can actually be considered comparable when those values are being integrated into more complex values and models.

However, let us return to the consideration from above that cuticular wax permeance may be involved in creating the observed trends in g_{res} and g_{min}. It has been shown that measurement temperature can have a more complex interaction with g_{res} and g_{min}, rapidly increasing with temperature (Eamus *et al.*, 2008), and that this can be highly species specific (Schuster *et al.*, 2016). Further investigation is required to confirm whether cuticular wax permeance differences are the cause of different patterns for the three species in this study, but it seems a likely candidate. Considering this, it seems then that understanding the effect of measurement temperature on g_{res} and g_{min} of a particular species likely also requires knowledge about cuticular wax permeance. Thus, it is recommended that measurements of g_{res} and g_{min} be conducted at the temperature of interest. For example, if a species faces high temperatures or heat waves in the field, it would be logical to conduct g_{res} and g_{min} measurements at the expected temperature range that the plant will be exposed to.

3.6.3 Comparability of g_{res} and g_{min}

The lack of a significant difference between g_{min} measured on *P. repens* leaves and g_{res} measured on *P. repens* shoots (values can be seen in Tables 6A & 7A and Figs. 9 & 10, but see Chapter 4, Fig. 14 and Fig. 15 for a visual comparison with significance lettering) is helpful when attempting to use the modified framework for using the MLD method on shoots for species with non-excisable leaves where it is not plausible to measure g_{min} on the leaves directly. *P. repens* occurs in the same locale as the other species measured and is non-drought-deciduous. If g_{min} (leaves only) and g_{res} (leaves + stem) do not differ significantly in *P. repens*, then it gives us some confidence to believe that g_{res} measured in species with non-excisable

leaves is not significantly different to the g_{min} of the leaves alone. Thus, for the purposes of quantifying measures of minimum conductance going forward, it may be defendable to compare g_{res} for non-drought-deciduous species to g_{min} from other species. However, to increase our confidence in this assertion, this comparison should be carried out across other species, and g_{min} should be measured directly on these other species (see 3.7 - Critiques and Improvements). In drought-deciduous species, it is still important to distinguish between g_{res}, g_{min}, and g_{bark} when using minimum conductance in a model of time-to-death (Blackman *et al.*, 2019).

TABLE 6A: Minimum conductance measured for study species (mean ±se)

Species	**Temperature**	**g_{res} or $g_{min\psi 88}$ (mmol m^{-2} s^{-1})**
Cannomois congesta	20°C	17.81 ±1.80
	35°C	15.90 ±1.49
	40°C	12.41 ±0.56
Erica monsoniana	20°C	9.76 ±0.40
	35°C	10.06 ±0.80
	40°C	10.35 ±0.42
Protea repens (leaves)	20°C	2.19 ±0.23
	35°C	4.87 ±0.56
	40°C	7.82 ±0.86
Protea repens (shoots)	20°C	2.96 ±0.60
	35°C	4.62 ±0.78
	40°C	6.05 ±0.48

TABLE 7A: Stomatal margin retention index (SMRI) of study species (mean ±se)

Species	Temperature	$SMRI_{\psi 88}$ (MPa s m^2 $mmol^{-1}$)
Cannomois congesta	20°C	0.084 ±0.02
	35°C	0.094 ±0.02
	40°C	0.121 ±0.03
Erica monsoniana	20°C	0.546 ±0.08
	35°C	0.530 ±0.09
	40°C	0.515 ±0.08
Protea repens (leaves)	20°C	1.328 ±0.15
	35°C	0.599 ±0.07
	40°C	0.373 ±0.04
Protea repens (shoots)	20°C	0.986 ±0.20
	35°C	0.630 ±0.11
	40°C	0.482 ±0.04

3.7 Critiques and Improvements

3.7.1 Measuring g_{min} with non-excisable leaves

Measurements of g_{min} for species with non-excisable leaves are not directly obtainable due to said leaves. These values would be helpful for determining the comparability of g_{min} and g_{res}. However, as $g_{res} = g_{min} + g_{bark}$, it is possible to directly measure g_{bark} on sections of a twig and then indirectly calculate g_{min} for these species. Unfortunately, this simple step was not realised at the time of experimentation. Going forward, this would be a desirable comparison to make.

3.7.2 Initial RWC

Even though specimens were allowed to rehydrate prior to the beginning of the dry-down process, it is possible that during sample preparation and scanning that RWC fell below 100% and thus the initial weight value recorded was taken slightly below 100% RWC. In future, measuring weight prior to sample preparation would allow one to calculate the true RWC at the initial dry-down weight measurement. The exponential decay function (Eqn. 6) could be modified to not be forced to intersect the y-axis at 100% RWC.

3.7.3 Wind speed

Disturbance or removal of the boundary layer of air surrounding the leaf will allow for an increased conductance at the leaf surface. When dealing with low magnitude conductance such

as g_{res} and g_{min}, this increase can make a significant contribution to the total measured. The DroughtBox (Billon *et al.*, 2020) aimed to standardise the measurement conditions, which included a fan to homogenise wind conditions. I have also seen recommendations that wind be applied, but with no guidance on wind strength (Sack and Scoffoni, 2010). The wind effect has seemingly not been considered much outside of just maintaining stable conditions.

In retrospect, it seems preferable to add a wind component as this closer represents what a plant would experience in situ. Going forward, it seems important to give some consideration to wind conditions during the measurement process, whether these be standardised or based on an individual species' environment. Assessing the effects of a change in wind conditions could also be important for future study.

3.7.4 Leaf Area

Determination of the leaf area (LA) using purely a planimetric method invites some inaccuracies when attempting to account for 3D structure and branch architecture. This was done to avoid the very high sampling effort and additional complications of obtaining double-sided leaf area for tiny leaved species with their many leaves, as well as avoid having to sample dry leaf area and converting.

However, another method commonly used for LA determination is the gravimetric method. This method constructs an empirical relationship between leaf dry mass and leaf fresh area by taking a sub-sample of the total sample and finding the LA using planimetric methods. The dry mass of that sub-sample is then obtained to construct a LA-to-dry-mass ratio (leaf mass per area, LMA). One can then find the dry weight of the whole sample and obtain the LA of that sample using the LMA ratio (Jonckheere *et al.*, 2004). While incredibly helpful when determining LA for large samples, one must be careful when considering branches. LA and area of the stem (bark area, BA) should be calculated separately. LMA ratios will not be accurate when pooling leaf and stem areas, or weights. This is because they have different densities and without partitioning the planimetric area into leaf or stem contributions, averaged LMA will not correctly represent the weight contribution of each component. BA may instead be calculated based on the shape and dimensions of the stem, for example assuming the shape of a cone (Billon *et al.*, 2020). Thus, for obtaining total leaf area, the gravimetric method may be both lower effort and more accurate especially when working on shoots or leaves with non-standard morphologies. Regardless of the methods used, it is important to be transparent.

3.7.5 RWC as a proxy for Ψ_{tlp} and Ψ_{crit}

The ability to avoid measuring Ψ_{tlp} and Ψ_{crit} while still obtaining an accurate enough and biologically relevant minimum conductance estimate would be ideal. Pressure-volume curves used to obtain Ψ_{tlp} and vulnerability curves used to obtain Ψ_{crit} are both high effort, time-intensive processes with low throughput, as well as their own set of methods to consider. If more linear slopes can be determined by eye and more non-linear slopes can be determined using global RWC values as a proxy, this would allow g_{res} and g_{min} to be measured simply and accurately and increase throughput. It would allow for species such as those in Run 1 and 2 to have a proper g_{res} or g_{min} assigned to them without needing 13+ p-v curves and vulnerability curves.

How promising are these prospects? For more linear slopes, a comprehensive comparison between 'by eye' slope selection and SSM slope selection is required. For more non-linear slopes, we are faced with an issue. Unfortunately, data for RWC_{tlp} and especially RWC_{crit} are rare in the current literature. While RWC_{tlp} has been shown to have a relatively narrow range (70%-96.8%) (Bartlett, Scoffoni and Sack, 2012), this is based on a very small subset of plant species (n = 89). RWC_{crit} when recorded seems to display a much broader range (Martinez-Vilalta *et al.*, 2019). In this study, the range was as much as 36% across only three species (Table 8). Even when these RWC values are reported, these data are also not easily comparable due to them being recorded for leaves only or due to inconsistencies in definition of RWC or mortality (Martinez-Vilalta *et al.*, 2019). This might make it more difficult and effort-intensive to acquire minimum conductance measurements for species with steep non-linear slopes. Those species seem to more commonly be those where g_{res} was measured on shoots due to non-excisable leaves (Fig. 3). This is a growth form more common in arid species, which may be at higher risk under warming climate conditions.

However, in a context where effects of anthropogenic climate change are already occurring and time is of the essence, the trade-off between accuracy and throughput could very well be argued to favour throughput. Perhaps using existing rough estimates from the literature for RWC_{tlp} and RWC_{crit} is better than nothing. Maybe breaking down the available data by environment, by habit or phylogenetically will reveal some more promising patterns to allow for RWC at these thresholds to act as a proxy. Again, further investigation is required to assess how these methods compare to those estimated using the full SSM.

Chapter 4:
Minimum conductance and SMRI of CFR species

The Cape Floristic Region (CFR) is of great interest as a biodiversity hotspot. Obtaining measures of drought resilience in its most characteristic functional types has been the research focus of several studies (Jacobsen *et al.*, 2007, 2009; Skelton, West and Dawson, 2015; Skelton *et al.*, 2023; West *et al.*, 2024). To further this pursuit, minimum conductance (g_{res} or g_{min}) and stomatal margin retention index ($SMRI_{\Psi crit}$) were quantified for three of these species, using the framework proposed in Chapter 3.

4.1 Study Species

The three study species mentioned in Chapter 3, are both morphologically diverse and are representative of the typical mountain fynbos families, namely Proteaceae, Ericaceae, and Restionaceae. This study aimed to build off existing knowledge on these species (Skelton *et al.*, 2023; West *et al.*, 2024) and further understanding of their hydraulic behaviour.

The Common Sugarbush, *Protea repens* (L.) L. (Proteaceae) is a broad-leaved, woody proteoid shrub which is one of the most ubiquitous species across the CFR. *Erica monsoniana* L.f. (Ericaceae), a.k.a. Snow Heath is a small- to medium-sized, small leaved woody ericoid shrub, while the Overberg Fountainreed, *Cannomois congesta* Mast. (Restionaceae), is a reed-like graminoid with upright culms. While these latter two species are not as widespread, they represent the widespread genera of *Erica* and *Cannomois* respectively.

4.1.2 Current understanding of ecology and hydrology

To understand drought strategy amidst these diverse co-occurring species, it is critical to understand the environmental context they exist within.

In these species, water relations and rooting structure have been shown to play important roles in how drought conditions are dealt with (West *et al.*, 2012; Skelton *et al.*, 2023). Consistent with other proteoids (Higgins, Lamb and van Wilgen, 1987; West *et al.*, 2012), *P. repens* is thought to be quite deep-rooted. This is in contrast to ericoids like *E. monsoniana* which have been shown to be generally shallow-rooted (Higgins, Lamb and van Wilgen, 1987; West *et al.*, 2012) and sensitive to moisture levels in shallow soil layers (Skelton *et al.*, 2023). Restionaceae such as *C. congesta* instead have shallow rhizomatous roots forming a base above-ground from which culms grow (Bell, Stock and Linder, 2000).

Based purely on measured values for Ψ_{50} and Ψ_{88}, *E. monsoniana* seem to be able to tolerate the most negative water potentials, followed by *P. repens* (Skelton et al., 2023), with *C. congesta* having the least resistant xylem (Skelton et al., 2023; West et al., 2024). Prior measurements of the SSM mirror these patterns.

In an in-situ study of these three species over the course of two summers (Skelton *et al.*, 2023), *E. monsoniana*'s predawn and midday water potentials fell by the most over the driest period, before making a full recovery of function following a rainfall event. Neither *P. repens* nor *C. congesta* showed decreases in their WPs anywhere close to that of *E. monsoniana*. The current understanding is that *E. monsoniana* commonly experiences drought in the shallow soil-layer which it tolerates, whilst *P. repens* is not-sensitive to this drought as it uses its deep roots to access deep soil water reserves (common within the fractured sandstone substrate commonly found in the Fynbos biome). The lack of sensitivity to shallow soil drought despite its short roots in *C. congesta* has been attributed to the unique anatomies of the Restionaceae that seem to be adapted for a very different style of water acquisition. It is known that the bases of restio culms can capture and store significant amounts of water from dew and cloud cover (Marloth, 1903, 1905; Nagel, 1956), with the lignified reed-like culms channelling dew down towards the exposed base of the plant which acts as a sort of sponge. In this way, it is currently believed that restio species may be significantly decoupled from presiding soil-surface moisture conditions, avoiding the full brunt of shallow soil drought using a different mechanism than *P. repens* (West *et al.*, 2012, 2024).

4.1.3 Predictions for minimum conductance and SMRI

Given what we know about the three species' diverging hydraulic strategies, it is possible to make predictions of which species will have the tightest control over its g_{res} and g_{min} values in order to moderate it's time to death under uniform drought conditions (represented by SMRI), and thus what rough magnitude g_{res} and g_{min} values would lead to that result.

It is hypothesised that neither *P. repens* nor *C. congesta* will have the strongest control over their g_{res} and g_{min} as they are not sensitive to shallow-layer soil drought. Therefore, regulating minimum conductance seems to be of less importance to them than to *E. monsoniana*, which deos experience shallow-layer soil drought. It is thus expected to have a tighter control to ensure it does not reach Ψ_{crit} under drought period, regulating its tolerance strategy. Therefore, taking SSM into consideration, it is expected that SMRI will be lowest in *C. congesta* (poorer

control + smallest SSM), highest in *E. monsoniana* (best control + large SSM), with *P. repens* falling in the middle (poorer control + intermediate length SSM).

4.2 Aim

The aim of this chapter is to 1) determine the length of the Stomatal Safety Margin (SSM) for the three study species using existing Ψ_{crit} data and own Ψ_{tlp} data, 2) determine and compare their g_{res} or g_{min} values, 3) incorporate these minimum conductance values and SSM to calculate $SMRI_{\Psi 88}$ and obtain an idea of which species are most vulnerable to drought effects, and 4) explain how the obtained results interact with morphology, life-history, or other aspects of these study species within the context of the CFR, adding to our understanding of these representative species.

4.3 Assessing minimum conductance & SMRI across species:

These results were obtained from measurements acquired from the same investigation as in Chapter 3 (referred to as 'Run 3'). As such, the methods for p-v curves, and g_{res} and g_{min} measurements can be found in Chapter 3.

4.3.1 Results

4.3.1.1 Stomatal Safety Margin parameters

Data for Table 8 & Fig. 12 was sourced from Skelton *et al.*, 2023 (Ψ_{88} & RWC_{88}) and from pressure-volume measurements conducted in Chapter 3 (Ψ_{tlp} & RWC_{tlp}, see Fig. 13 for p-v curves). $SSM_{\Psi 88}$ was calculated as the difference between these two parameters. We can see in Fig. 12 that while TLPs all fall within quite a narrow range of ~0.64 MPa, Ψ_{88} values have a much larger range of ~4.34 MPa. This supports what has been reported in the literature (Bartlett, Scoffoni and Sack, 2012; Martinez-Vilalta *et al.*, 2019). This large range leads to diverse sizes in SSMs, with *Erica monsoniana* having the longest at ~5.33 MPa, followed by *Protea repens* with a SSM at ~2.91 MPa, just over half the length of that of *E. monsoniana*. *Cannomois congesta* then has the shortest SSM at ~1.50 MPa.

It is worth mentioning that some measured water potentials at TLP seemed to be less negative than expected based on prior measurements (Skelton *et al.*, 2023; West *et al.*, 2024) and anecdotal observation. This could be due to sample collection coinciding with a delayed spring growing period after an especially long winter in 2024. Observationally, shoots were still fairly young, and thus would not yet have fully developed xylem. Based on the lack of sensitivity to small changes in the endpoint used for g_{res} and g_{min} calculation (Fig. 10), I do not believe these seasonally induced inaccuracies compromise the findings of this chapter much, if at all.

TABLE 8: ***Hydraulic thresholds for study species (mean ±se)***

Species	Ψ_{TLP} (MPa)	RWC_{TLP}	Ψ_{88} (MPa)	$RWC_{\Psi 88}$ (%)	$SSM_{\Psi 88}$ (MPa)
Cannomois congesta	-1.17 ±0.12	93.82 ±0.81	-2.67 ±0.30	80.76 ±1.03	1.50 ±0.32
Erica monsoniana	-1.68 ±0.04	89.03 ±1.33	-7.01 ±0.78	44.20 ±1.58	5.33 ±0.78
Protea repens	-1.04 ±0.12	94.68 ±0.11	-3.95 ±0.06	79.52 ±0.08	2.91 ±0.13

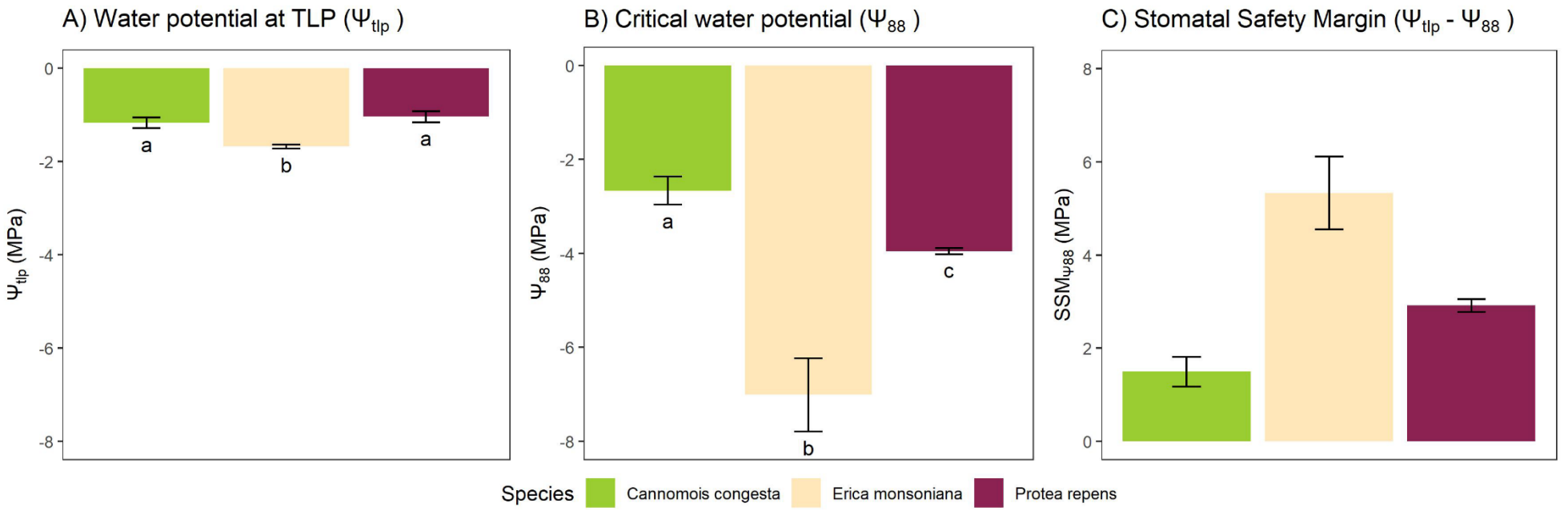

Figure 12: Hydraulic thresholds for the study species: A) Ψ_{tlp} the water potential at turgor loss point, B) Ψ_{88} the water potential at 88% embolism, and C) the difference between them, the stomatal safety margin ($SSM_{\Psi 88}$).

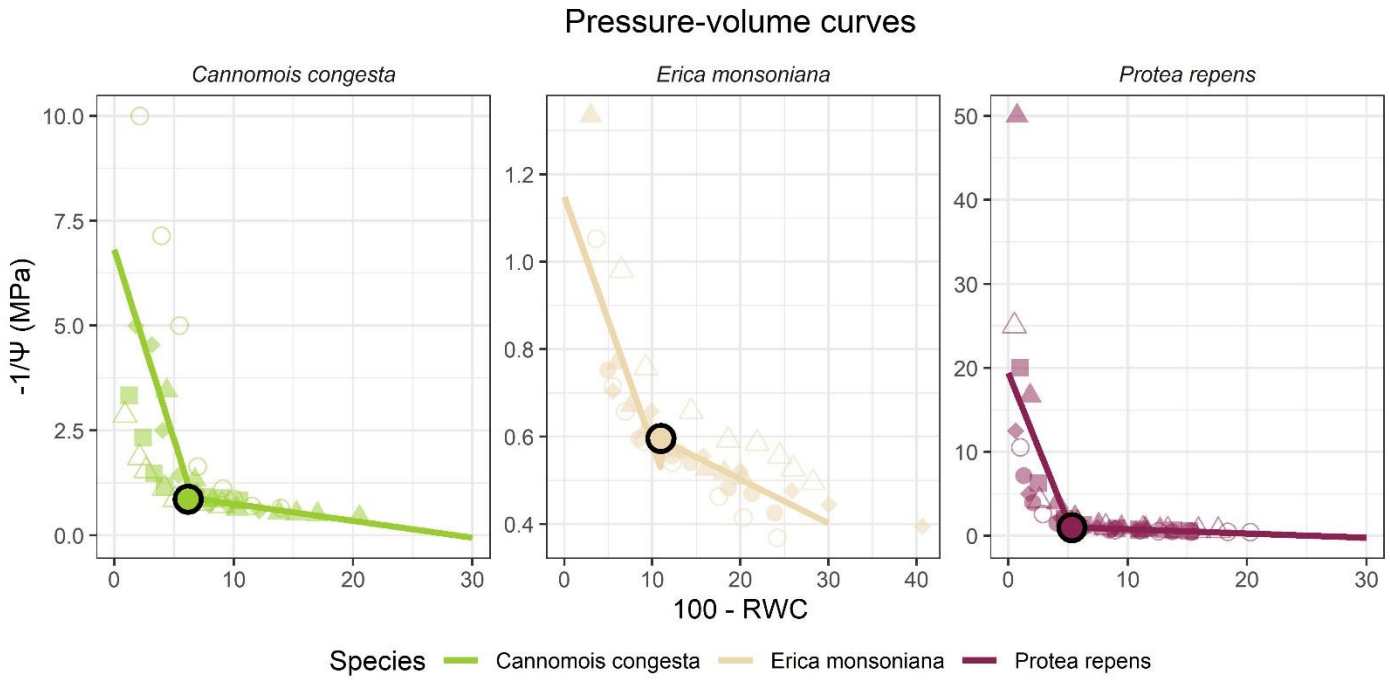

Figure 13: Average pressure-volume (p-v) curves for the three study species. Slopes and turgor loss points were obtained by averaging each value separately. Varied point shapes represent data from different individuals.

4.3.1.2 Minimum conductance (g_{res} and g_{min})

Tables 6B and 7B, and Figs. 13 & 14 contain the same data as Tables 6A and 7A, and Figs. 9 &10 in Chapter 3 respectively, but rearranged such that values can be more easily compared within species.

At all temperatures *C. congesta* displayed the highest minimum conductance (Fig. 14), which was only non-significant when comparing to *E. monsoniana* at 40°C. A mostly significant trend is seen in *E. monsoniana* having larger g_{res} than *P. repens*, especially at lower temperatures due to an apparent increase in *P. repens* g_{res} and g_{min} as temperature rose. This difference was still present, but non-significant at 35°C and specifically compared to *P. repens* shoots at 40°C.

The overall trend was that the highest minimum conductance was found in *C. congesta*, followed by *E. monsoniana*, and finally *P. repens*, although the latter two were similar.

4.3.1.3 Stomatal Margin Retention Index (SMRI)

When it came to outputting $SMRI_{\Psi 88}$, at all temperatures, *C. congesta* significantly displayed the lowest values. *E. monsoniana* had statistically and visually similar SMRI to *P. repens* at all temperatures, except at 20°C where *E. monsoniana* had the significantly lower value.

TABLE 6B: Minimum conductance measured for study species (mean ±se)

Temperature	Species	$g_{res\ or}\ g_{min\psi 88}$ (mmol m^{-2} s^{-1})
20°C	*Cannomois congesta*	17.81 ±1.80
	Erica monsoniana	9.76 ±0.40
	Protea repens (leaves)	2.19 ±0.23
	Protea repens (shoots)	2.96 ±0.60
35°C	*Cannomois congesta*	15.90 ±1.49
	Erica monsoniana	10.06 ±0.80
	Protea repens (leaves)	4.87 ±0.56
	Protea repens (shoots)	4.62 ±0.78
40°C	*Cannomois congesta*	12.41 ±0.56
	Erica monsoniana	10.35 ±0.42
	Protea repens (leaves)	7.82 ±0.86
	Protea repens (shoots)	6.05 ±0.48

TABLE 7B: Stomatal margin retention index (SMRI) of study species (mean ±se)

Temperature	Species	$SMRI_{\psi 88}$ (MPa s m^2 $mmol^{-1}$)
20°C	*Cannomois congesta*	0.084 ±0.02
	Erica monsoniana	0.546 ±0.08
	Protea repens (leaves)	1.328 ±0.15
	Protea repens (shoots)	0.986 ±0.20
35°C	*Cannomois congesta*	0.094 ±0.02
	Erica monsoniana	0.530 ±0.09
	Protea repens (leaves)	0.599 ±0.07
	Protea repens (shoots)	0.630 ±0.11
40°C	*Cannomois congesta*	0.121 ±0.03
	Erica monsoniana	0.515 ±0.08
	Protea repens (leaves)	0.373 ±0.04
	Protea repens (shoots)	0.482 ±0.04

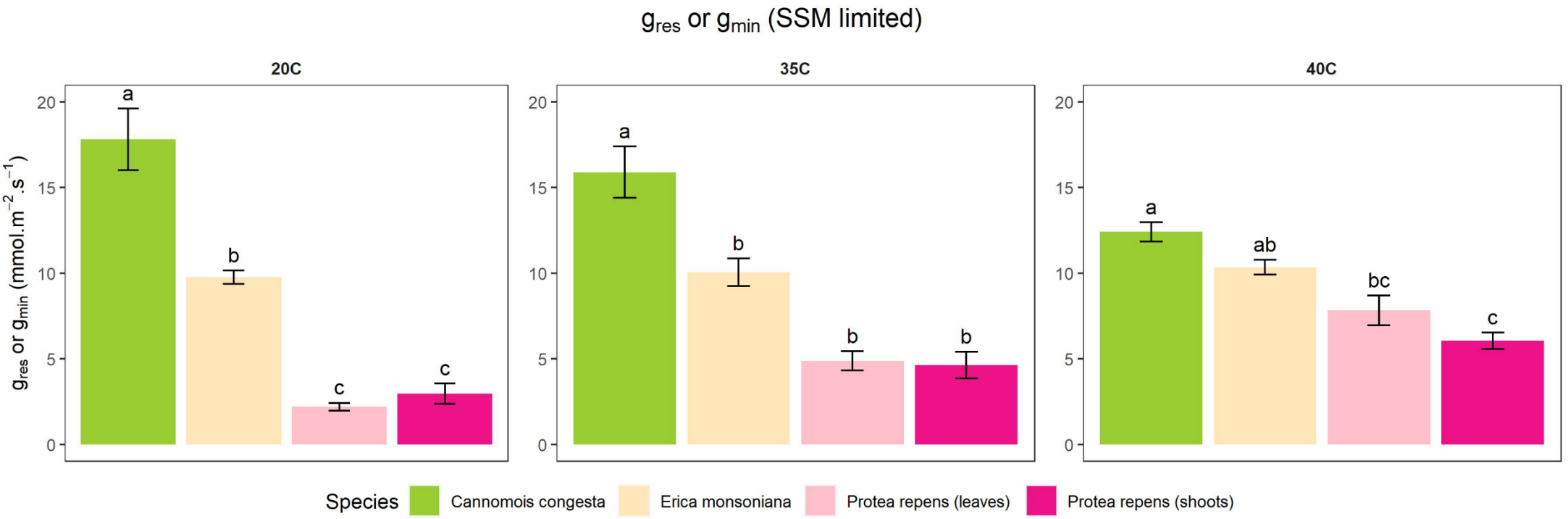

Figure 14: SSM limited g_{res} and g_{min}, i.e., measured across the SSM_{88}, at different temperatures for the study species shown. Arranged by temperature and comparisons made between species.

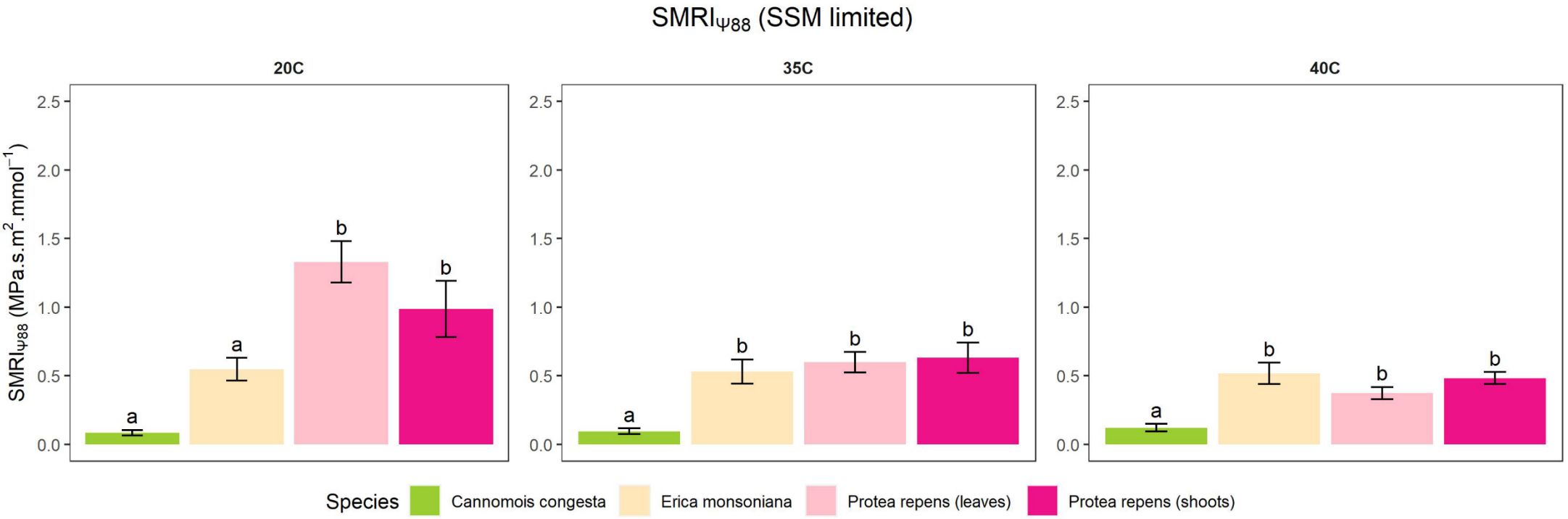

Figure 15: SSM limited $SMRI_{\Psi 88}$, i.e., calculated using g_{res} and g_{min} measured across the SSM_{88}, at different temperatures for the study species shown. Arranged by temperature and comparisons made between species.

4.3.2 Discussion

4.3.2.1 Contextualising results to existing literature

4.3.2.1.1 g_{res} and g_{min}

Comparison to existing values should be done with caution due to the array of concerns addressed in this study, however it can still be helpful on the broader scale. Existing literature was compiled by Duursma *et al.* 2019, and 221 species had acceptable g_{min} (as it was termed there) values which comprise the most complete set of trait values in the literature. All following g_{res} and g_{min} values are in mmol m^{-2} s^{-1}.

Average g_{min} across studies was 4.9 (Duursma *et al.*, 2019). With a g_{res} and g_{min} in the range of 2.19 to 7.82 (Table 6B), *P. repens* has a mean minimum conductance that falls within the average range. *E. monsoniana* with g_{res} in the range of 9.76 to 10.35 is above average. *C. cannomois* is a fair bit above-average with g_{res} in the range 12.41 to 17.81, however it is not amongst the most extreme recorded values which can supposedly reach minimum conductance values greater than 30. These three species thus represent a pretty good dispersion about the mean of the global g_{res} and g_{min} values recorded so far.

4.3.2.1.2 SMRI

SMRI is a newly defined index (Petek-Petrik *et al.*, 2023), reported in MPa s m^2 $mmol^{-1}$. This index was tested on four gymnosperm (specifically conifer) species and was thus reported as $SMRI_{\Psi 50}$. Three of these species were embolism resistant, namely *Cupressus sempervirens* L.*,* *Juniperus communis* L.*,* and *Tetraclinis articulata* (Vahl) Mast., with the latter being regarded as the most embolism-resistant species in the Northern hemisphere. The remaining species was *Taxodium distichum* (L.) Rich, considered to be embolism sensitive.

The highly resistant *T. articulata* had an SMRI of 6.06 ± 0.58. The more moderately resistant species *C. sempervirens* and *J. communis* had SMRIs of 2.07 ± 0.34 and 3.14 ± 0.26 respectively. The embolism sensitive *T. distichum* had an SMRI of 0.18 ± 0.03.

In comparison *P. repens* and *E. monsoniana* had $SMRI_{\Psi 88}$ values ranging from ~50% to 25% of the magnitude of the standard resistant conifers (Table 7B). This implies that neither species are particularly embolism resistant. This matches prior findings (Skelton *et al.*, 2023; West *et al.*, 2024) and is not surprising as the locale (Jonaskop) in which these specimens were collected is not considered particularly arid and is frequented by cloud due to its altitude. *C. congesta* displayed an SMRI ranging from ~65% to 45% of that of the most sensitive conifer, *T. distichum*. This implies that it is incredibly sensitive to embolism, consistent with what has

been found previously (Skelton *et al.*, 2023; West *et al.*, 2024). Adding more SMRI values to the literature would help to further contextualise these results.

4.3.2.2 Contextualising results between co-occurring species

4.3.2.2.1 Erica monsoniana and *Protea repens*

When we look simply at Ψ_{crit} (Ψ_{88} in this case), *E. monsoniana* has the most embolism resistant xylem and largest SSM (Fig. 12). However, when combined with its higher rate of g_{res}, we see that it in fact has a similar range of SMRI to *P. repens* (Fig. 15). Thus, these two species have arrived at a similar level of drought resistance (reduction in sensitivity based on SMRI) by way of diverging hydraulic strategies. Thus, we must reject the hypothesis that *E. monsoniana* has the lowest g_{res} and that *P. repens* would have a lower g_{res} and g_{min} than *E. monsoniana*.

While this denies expectations for *E. monsoniana*, it is not implausible that such a large SSM may be sufficient of an adaptation to tolerate the level of drought commonly experienced in-situ. However, *P. repens* seems to be conservative with its water loss under drought despite what appears to be extensive buffering from deep-soil water stores. While it has a shorter SSM, it was not observed approaching close to Ψ_{crit} to the extent *E. monsoniana* was, even in a particularly dry summer (2012/2013) (Skelton *et al.*, 2023).

To try and make sense of this, it is worth considering the consequences of hydraulic failure on each species' overall survival strategy. If a mature individual of *E. monsoniana* were to die of hydraulic failure, this loss is at least partially offset by the fact that ericoids release seed regularly and recruit from the seedbank. It is likely that this individual has already released seed that has been incorporated into the seedbank. These seeds will then recruit/will have already recruited under favourable conditions. It has successfully passed on its genes to the next generation. *P. repens* on the other hand is serotinous, like most other proteoids, and keeps its seeds held within the canopy to be released when fire occurs. The parent plant likely dies (*P. repens* is considered a reseeder) but the seeds are released and are adapted to thrive in the comparatively nutrient-rich and competition-free post-fire environment. If the parent plant were to die prematurely from hydraulic failure, the seeds would be released under normal conditions and would have a much lower recruitment success. In this way, the consequences of hydraulic failure seem to be more severe for *P. repens* than for *E. monsoniana*, perhaps explaining why *P. repens* seems to be more conservative with its combination of SMRI and reliance on deep water.

It is also worth considering the distributions of these species. The fynbos biome is considered a biodiversity hotspot and much of this can be attributed to the existence of many refugia-type localised habitats which can host narrow-range endemic species (Keppel *et al.*, 2015). Many of these habitats are localised hotspots with increased water availability such as wetlands, seeps, riverbanks, bogs, and vleis. *P. repens* is however a generalist and is common across many fynbos landscapes (Manning, Goldblatt and Manning, 2012), likely being adapted to thrive in a wider range of moisture and soil conditions by tapping into deep water reserves. It could thus be less tuned to specific environmental conditions at a given site, and rather employ more conservative strategies to ensure survival across many habitats. *E. monsoniana* on the other hand has a narrower distribution (Manning, Goldblatt and Manning, 2012) and is present in sites where conditions presumably match its preferred moisture conditions (otherwise it would not have persisted there historically). Therefore, while on paper they have similar SMRIs, both experience soil drought events at the local scale. *P. repens* seems to avoid drought under a variety of presiding climates through deep rooting and good control of its minimum conductance. *E. monsoniana* is more specialised, having only persisted in areas where the shallow soil drought does not cause it to become locally extinct, likely through some combination of drought tolerant xylem, increased uptake of cloud moisture to buffer drought effects, and ability to regenerate from seed when drought is too severe.

4.3.2.2.2 Cannomois congesta

C. congesta has both a narrow SSM (Fig. 12) and high g_{res} (Fig. 14), resulting in a very small SMRI compared to the other two species (Fig. 15), matching our hypothesis. This SMRI is also very small compared to the other species recorded so far. This further emphasises that *C. congesta* must not be reliant on soil-moisture and remarkably avoids drought effects via cloud-moisture.

In combination with this buffering effect, many Restionaceae species are associated with wet-habitats or are restricted to niche locales present within their greater range based on wetness. This may help explain low drought resistance traits in *C. congesta* and species with similar hydraulic niches. However, further studies of Restionaceae species with differing hydraulic niches, including arid-adapted species, is required to further understand the extent to which they face risk as different water sources deplete, and whether these patterns change under climate change conditions (Skelton *et al.*, 2023).

4.3.2.3 Significance of findings

While the g_{res} or g_{min} and SMRI values reported above are important for understanding the species occurring within the CFR, they also highlight how adaptive capacity for dealing with drought can arise through a diverse and complex set of interacting traits. *E. monsoniana* with its large SSM but high g_{res} arriving at similar SMRI values to *P. repens* shows the importance of minimum conductance as one of these interacting traits that needs to be considered in models of predicting tHF. The extreme low values of *C. congesta* show how unique morphologies and life-histories may also interact with tHF in unexpected ways.

Chapter 5:
Synthesis of findings and final framework recommendations

5.1 Summary of minimum conductance assessment and framework

The minimum conductance has been shown to be a particularly important addition to models of time to hydraulic failure (tHF) in plants, which themselves are essential for understanding the sensitivity and adaptive capacity of plants vulnerable to climate change effects.

The methods for estimation and the very definition of minimum conductance have been assessed and were found wanting for standardisation, reproducibility, and widespread applicability in Chapter 2.

Building upon this, Chapter 3 proposed a framework for determining minimum conductance (carefully referred to as either g_{res} for shoots or g_{min} for leaves) based upon physiological theory, as well as making general recommendations for standardisation and consistency of methods. This framework recommends measuring either g_{res} or g_{min} over the stomatal safety margin (SSM). This framework was then applied on characteristic Cape Floristic Region (CFR) families (Proteaceae, Ericaceae, and Restionaceae) in order to assess its function further in Chapter 4. Several considerations came to light and were considered in the final recommendations for application of the framework presented below.

5.2 Final recommendations for framework application

Having now tested the framework on both species with and without excisable leaves, insight has been obtained on how it should be implemented going forward when measuring minimum conductance in the form of both g_{res} and g_{min}. I now make a recommendation on methods to use to maintain consistency in important measured traits underlying minimum conductance.

5.2.1 Sampling

From personal experience, samples with low mass combined with a less sensitive decimal balance resulted in reduced sensitivity to mass changes and created unnecessary noise in the data such that models were a worse fit. It is desirable for your balance to be able to detect mass decreases in your sample at short time intervals. Therefore, I recommend using a three-place decimal balance and samples heavier than 0.3g. Consider using a more sensitive balance if needing to detect even smaller mass changes.

5.2.2 Leaf area

The leaf area (LA) quantified should be total conducting area as this is what is important in the context of g_{min} (Jonckheere *et al.*, 2004). For simple flat leaves, this can be simply double-sided LA measured planimetrically. For more complex and/or small leaves, potentially in combination with branches, this will be a more complex assessment. While one could replicate the logical transformation methods of this paper, I'd recommend attempting gravimetric methods to calculate bark and leaf area separately. If using the planimetric method, LA should be taken when fresh, when possible. If not possible due to using shoots, dry area can be taken. A calibration should then be set up using a separate sample to determine the average percent change in LA from a wet sample to a dry one. This calibration can then be applied to the measured dry leaf areas to obtain an estimate of fresh leaf area.

5.2.3 VPD and temperature conditions

If an exponential decay curve (Eqn. 6) is fitted to the data, it seems that the measurement temperature does not have a significant effect on data quality (Table 5). Therefore, the measurement temperature chosen should be relevant to the goal of the study. Humidity should be relatively constant. Both temperature and humidity should be monitored throughout the course of the experiment. Keep in mind that higher temperatures induce faster dry-downs, thus data sampling frequency should ideally be shortened at higher temperatures.

5.2.4 Wind presence

Even a small amount of unintentional wind was shown to significantly affect the results of one treatment in Run 3 such that it had to be excluded. Therefore, wind conditions are important and should be kept constant. Further consideration should be given to what the best wind conditions for determining g_{res} or g_{min} should be, i.e., whether they should be minimised (as in this study) or whether they should be representative of the plant's wind conditions in situ. The DroughtBox stands out as a helpful standardisation tool for controlling not only wind, but also temperature and VPD conditions while constantly measuring weight loss within the chamber.

5.2.5 RWC determination

I recommend taking a weight measurement immediately after a sample is to begin preparation in order to acquire a more accurate relative water content (RWC) value. Adjust the curve equation accordingly.

5.2.6 *Fitting of exponential decay function*

I recommend fitting the exponential decay function to dry-down curves in order to obtain a continuous slope which can be delimited at any interval and is not dependent on sampling density or skewed by outliers at the extremes. While the model showed great success in this study (Tables 4 & 5), it is recommended to assess one's own success of model fitting using the R^2 and keep an eye out for non-logical data (e.g. negative RWCs due to measurement error). The equation of the curve fitted should be $y = A * e^{-k*x}$, as when following the RWC recommendation above, the curve won't pass through 100% RWC.

5.2.7 g_{res} *vs* g_{min}

It is important to use the correct terms when quantifying minimum conductance. Use 'g_{min}' when using leaves, and use 'g_{res}' when using shoots. When applying the minimum conductance to measures such as SMRI or other assessments of tHF, presence of leaf-shedding behaviour will alter which minimum conductance (g_{res} or g_{bark}) is acting along the SSM and this will need to be considered (see Blackman *et al.*, 2019).

5.2.8 *Slope selection interval*

The strength of the framework presented in this thesis is the ability to determine g_{res} and g_{min} over a biologically relevant interval, namely the stomatal safety margin (SSM). Therefore, when the data for the starting point (Ψ_{tlp} or Ψ_{gs90}) and endpoint (Ψ_{crit}) of the SSM are available, I recommend using the p-v curve to obtain RWC_{tlp} and RWC_{crit}, which can then be used to select the linear portion of the slope for g_{res} or g_{min} determination. Presence of RWC_{crit} appears to be influential on outputted minimum conductance values, more so than RWC_{tlp}, and should be prioritised when obtaining both is not possible. Regardless of interval used, future values should be explicit about the section of the curve used to calculate minimum conductance.

5.3 Minimum conductance and SMRI findings in CFR

Chapter 4 not only acted as an assessment of the framework, but also explored how the minimum conductance data obtained for *Protea repens* (Proteaceae), *Erica monsoniana* (Ericaceae), and *Cannomois congesta* (Restionaceae) contributed to our current understanding of drought in these diverse families within the Cape Floristic Region. Values of g_{res} or g_{min} and SMRI showed a diverse set of values for both parameters when compared to the broader literature. These values added evidence to support the existing ideas of the adaptive strategies used by these co-occurring species, while also expanding knowledge on what components form

these strategies. *P. repens* being a deep-rooted species, seems to be decoupled from shallow soil drought, but was shown to be surprisingly conservative with its minimum conductance perhaps due to generalist adaptations and increased consequences of hydraulic failure. The idea that *E. monsoniana* copes with shallow surface droughts through a large SSM was supported, although it seems that it relies on its resistant xylem more than controlled minimum conductance, perhaps due to niche dependence and a reseeding strategy which does not result in extinction due to drought death. It also seems that low minimum conductance is not a strategy *C. congesta* uses to deal with its small SSM and shallow roots. It seems highly probable that it is decoupled from soil-moisture and is instead strongly reliant on cloud moisture for survival.

These findings allowed a reassessment and reframing of current ideas, thus revealing the importance of a holistic understanding of drought strategies and the necessity for inclusion of minimum conductance not only in models of tHF, but also in theoretical understanding of drought dynamics.

5.4 Further study

Looking forward, the main goal would be to remove the reliance of calculating g_{res} or g_{min} on SSM parameters, as these are effort intensive to obtain. This could be done either by showing that other methods are capable of matching the accuracy of the SSM method or by finding a proxy for the SSM parameters.

In this study it was shown that perhaps there exists a window for the selected endpoint of the linear slope of the dry-down curve for g_{res} and g_{min} determination that does not cause a significant difference in final outputted g_{res} or g_{min} value (Fig. 9). Therefore, when SSM data are not present, it may be defendable to assess the linear section by eye. However, further testing would be required over a selection of dry-down curves to confirm that this method is an accurate enough estimate of g_{res} and g_{min}.

If SSM data is not present, it may also be possible to obtain a rough estimate of g_{res} and g_{min} using average global values for RWC_{tlp} and RWC_{crit}. Further investigation is required to assess how accurate these are and whether refining RWC threshold values by habitat or growth form could narrow the range of values.

Alternatively, it may be possible to extract some parameter from the fitted exponential decay function (Eqn. 6), such as A or k, and link it to some biological meaning. This

parameter would then be closely correlated with final g_{res} or g_{min}, and thus removing the necessity of having the SSM parameters. This angle seems promising, however, further investigation is required to identify if such a biological meaning exists and the extent of the correlation.

Finally, assessing SMRI as a parameter further using these findings could be implemented in future by determining how well it predicts the tHF of these species.

5.5 Conclusion

Obtaining values for g_{res} or g_{min} has shown to be crucial for understanding vulnerability of plant species to drought. I hope that by more clearly defining these terms and by providing standardised and reproducible methods for their estimation on a variety of morphologically diverse species, more studies will consider this important parameter and improve our understanding and predictions for species at risk of being lost to climate changes.

Appendix: Supplementary Tables

TABLE S1 Leaf area transformations applied to approximate total surface area from 2D scans

Calibration factor was obtained for certain species where it was only possible to obtain proper scans of leaf area (LA) after they had undergone the dry-down experiment (dry LA). Calibration factor was obtained from several separate samples by scanning both fresh LA and dry LA, then dividing the fresh LA by the dry LA. Anatomy correction formula was obtained through logical deductions of leaf shape and coverage outlined in the Motivation column. Final transformation factor was then obtained by multiplying the two previous columns together. Final LA was then calculated as the measured LA (dry or fresh) multiplied by the final transformation factor.

TABLE S1	**Leaf area transformations applied to approximate total surface area from 2D scans**				
Species	**Site**	**Calibration factor**	**Anatomy correction formula**	**Final transformation factor**	**Motivation**
Dicerothamnus rhinocerotis	Drie Kuilen, Renosterveld	1	1*2 = 2	2	Double-sided as twigs were separated to prevent overlap.
Oedera squarrosa	Drie Kuilen, Renosterveld	1.443975	(0.65*4) + 0.35*2) *2 = 4	5.775899	Half of the total leaves (roughly 65% of visible area) are side-on and are curled, with only a quarter of the leaf visible: Half of abaxial side and all of the adaxial side is hidden. A quarter of the leaves are front facing and are half obscured. The other quarter are completely hidden and should have leaf area equal to the front side. Stem takes up small area.
Ruschia multiflora	Drie Kuilen, Renosterveld	2.156046	1*3 = 3	6.468138	Leaves had 3 faces and stem was thick.
Passerina obtusifolia	Drie Kuilen, Renosterveld	1.578746	(0.65*2) + (0.35*2) *2 = 2.7	4.262613	Half of the total leaves (roughly 65% of visible area) are side-on, with only half of the leaf visible. A quarter of the leaves are front facing and are half obscured. The other quarter are completely hidden and should have leaf area equal to the front side. Stem takes up small area. Minimal leaf overlap.
Protea laurifolia	Drie Kuilen, Renosterveld	1.12303	1*2 = 2	2.24606	Double-sided as simple leaf shape
Microdon polygaloides	Drie Kuilen, Renosterveld	1	(1*2) + (0.35*2) = 2.7	2.7	Overlap is minimum, so all visible leaves are roughly half obscured. A quarter of total leaves which are fully obscured.
Wahlenbergia nodosa	Drie Kuilen, Renosterveld	1	(0.5*2) *2 + (0.5*3) = 3.5	3.5	Roughly 50% of the visible area is front-on leaves of which 50% of each leaf's abaxial surface is obscured and 100% of their adaxial surface is obscured. For each front-on leaf, there are roughly 2 side-on leaves. Those side-on leaves have roughly a third of their area shown when directly side-on.

					Leaf positionings rotate around the stem, but co-occurring increase and decrease in obfuscation should cancel each other out.
Clutia rubricaulis	Drie Kuilen, Renosterveld	1	(0.65*1.25) *2 + (0.35*3) = 2.675	2.675	Roughly 65% of the visible area is front-on leaves of which 20% of each leaf's abaxial surface is obscured and 100% of their adaxial surface is obscured. For each front-on leaf, there are roughly 2 side-on leaves. Those side-on leaves have roughly a third of their area shown when directly side-on. Leaf positionings rotate around the stem, but co-occurring increase and decrease in obfuscation should cancel each other out.
Lobostmon decorus	Drie Kuilen, Fynbos	2.15665	1*2 = 2	4.313299	Double-sided as simple leaf shape
Aspalathus shawii	Drie Kuilen, Fynbos	1	(1*2) *2 *2 = 8	8	A lot of leaves. Any visible area on the front is roughly 50% obscured by other leaves and has a hidden side. Roughly half the total leaves are also entirely obscured.
Selago dolosa	Drie Kuilen, Fynbos	1	(0.5*2) + (0.5*3) = 2.5	2.5	Roughly 50% of the visible area is front-on leaves of which 100% of their adaxial surface is obscured. For each front-on leaf, there are roughly 2 side-on leaves. Those side-on leaves have roughly a third of their area shown when directly side-on. Leaf positionings rotate around the stem, but co-occurring increase and decrease in obfuscation should cancel each other out.
Agathosma capensis	Drie Kuilen, Fynbos	1	(0.65*2) + (0.35*3) = 2.35	2.35	Roughly 65% of the visible area is front-on leaves of which 100% of their adaxial surface is obscured. For each front-on leaf, there are roughly 2 side-on leaves. Those side-on leaves have roughly a third of their area shown when directly side-on. Leaf positionings rotate around the stem, but co-occurring increase and decrease in obfuscation should cancel each other out.
Protea lorifolia	Drie Kuilen, Fynbos	1	1*2 = 2	2	Double-sided as simple leaf shape
Protea repens	Drie Kuilen, Fynbos	1	1*2 = 2	2	Double-sided as simple leaf shape
Cannomois congesta	Jonaskop	1	1*2 = 2	2	Double-sided as simple cylindrical shape
Erica monsoniana	Jonaskop	1	1*2*2 = 4	4	Roughly 50% of leaves are visible from the side. Doubling this area gives the two-sided area of 50% of the leaves. Doubling this area gives the two-sided area for the remaining 50% of the leaves.
Protea repens (shoots)	Jonaskop	1.139242	1*2 = 2	2.278483	Double-sided as simple leaf shape
Protea repens (leaves)	Jonaskop	1	1*2 = 2	2	Double-sided as simple leaf shape

TABLE S2: Environmental parameters within chambers (mean ±se)

Run	Site	Treatment Temperature	Measured Temperature (°C)	Relative Humidity (%)	VPD (kPa)
1	Drie Kuilen	20°C	19.72 ±0.01	57.91 ±0.02	0.97 ±0.00
		25°C	25.75 ±0.01	50.24 ±0.03	1.65 ±0.00
		35°C	34.87 ±0.01	39.56 ±0.07	3.38 ±0.00
		40°C	39.69 ±0.04	47.14 ±0.06	3.85 ±0.01
2	Drie Kuilen	20°C	19.54 ±0.01	60.67 ±0.05	0.89 ±0.00
		25°C	25.78 ±0.01	53.93 ±0.04	1.53 ±0.00
		35°C	34.68 ±0.02	42.78 ±0.04	3.17 ±0.00
		40°C	39.69 ±0.04	47.14 ±0.06	3.85 ±0.01
3	Jonaskop	20°C	20.06 ±0.02	63.34 ±0.03	0.86 ±0.00
		35°C	35.46 ±0.02	53.74 ±0.06	2.67 ±0.00
		40°C	40.38 ±0.03	23.56 ±0.15	5.76 ±0.02

References

Ackerly, D. (2004) 'Functional Strategies of Chaparral Shrubs in Relation to Seasonal Water Deficit and Disturbance', *Ecological Monographs*, 74(1), pp. 25–44. Available at: https://doi.org/10.1890/03-4022.

Adams, H.D. *et al.* (2017) 'A multi-species synthesis of physiological mechanisms in drought-induced tree mortality', *Nature Ecology & Evolution*, 1(9), pp. 1285–1291. Available at: https://doi.org/10.1038/s41559-017-0248-x.

Agenbag, L. *et al.* (2008) 'Diversity and species turnover on an altitudinal gradient in Western Cape, South Africa: baseline data for monitoring range shifts in response to climate change', *Bothalia*, 38(2). Available at: https://doi.org/10.4102/abc.v38i2.287.

Allen, C.D. *et al.* (2010) 'A global overview of drought and heat-induced tree mortality reveals emerging climate change risks for forests', *Forest Ecology and Management*, 259(4), pp. 660–684. Available at: https://doi.org/10.1016/j.foreco.2009.09.001.

Allsopp, N., Colville, J.F. and Verboom, G.A. (2014) *Fynbos: Ecology, Evolution, and Conservation of a Megadiverse Region*. Oxford University Press.

Anderegg, L.D.L., Anderegg, W.R.L. and Berry, J.A. (2013) 'Not all droughts are created equal: translating meteorological drought into woody plant mortality', *Tree Physiology*, 33(7), pp. 672–683. Available at: https://doi.org/10.1093/treephys/tpt044.

Anfodillo, T., Di Bisceglie, D.P. and Urso, T. (2002) 'Minimum cuticular conductance and cuticle features of Picea abies and Pinus cembra needles along an altitudinal gradient in the Dolomites (NE Italian Alps)', *Tree Physiology*, 22(7), pp. 479–487. Available at: https://doi.org/10.1093/treephys/22.7.479.

Auguie, B. and Antonov, A. (2017) 'gridExtra: Miscellaneous Functions for "Grid" Graphics'. Available at: https://cran.r-project.org/web/packages/gridExtra/index.html (Accessed: 11 September 2024).

Bartlett, M.K. *et al.* (2014) 'Global analysis of plasticity in turgor loss point, a key drought tolerance trait', *Ecology Letters*, 17(12), pp. 1580–1590. Available at: https://doi.org/10.1111/ele.12374.

Bartlett, M.K. *et al.* (2016) 'The correlations and sequence of plant stomatal, hydraulic, and wilting responses to drought', *Proceedings of the National Academy of Sciences*, 113(46), pp. 13098–13103. Available at: https://doi.org/10.1073/pnas.1604088113.

Bartlett, M.K., Scoffoni, C. and Sack, L. (2012) 'The determinants of leaf turgor loss point and prediction of drought tolerance of species and biomes: a global meta-analysis', *Ecology letters*, 15(5), pp. 393–405.

Bell, T.L., Stock, W.D. and Linder, H.P. (2000) 'Ecophysiological investigations of the distribution of Poaceae and Restionaceae in the Cape Floristic Region, South Africa', in *Grasses: Systematics and Evolution: Systematics and Evolution*. Csiro Publishing.

Bengtson, C., Larsson, S. and Liljenberg, C. (1978) 'Effects of Water Stress on Cuticular Transpiration Rate and Amount and Composition of Epicuticular Wax in Seedlings of Six Oat Varieties', *Physiologia Plantarum*, 44(4), pp. 319–324. Available at: https://doi.org/10.1111/j.1399-3054.1978.tb01630.x.

Billon, L.M. *et al.* (2020) 'The DroughtBox: A new tool for phenotyping residual branch conductance and its temperature dependence during drought', *Plant, Cell & Environment*, 43(6), pp. 1584–1594. Available at: https://doi.org/10.1111/pce.13750.

Blackman, C.J. *et al.* (2016) 'Toward an index of desiccation time to tree mortality under drought', *Plant, Cell & Environment*, 39(10), pp. 2342–2345. Available at: https://doi.org/10.1111/pce.12758.

Blackman, C.J. *et al.* (2019) 'Desiccation time during drought is highly predictable across species of Eucalyptus from contrasting climates', *New Phytologist*, 224(2), pp. 632–643. Available at: https://doi.org/10.1111/nph.16042.

van Blerk, J.J. *et al.* (2021) 'Does a trade-off between growth plasticity and resource conservatism mediate post-fire shrubland responses to rainfall seasonality?', *New Phytologist*, 230(4), pp. 1407–1420.

Bolstad, P.V. and Gower, S.T. (1990) 'Estimation of leaf area index in fourteen southern Wisconsin forest stands using a portable radiometer', *Tree Physiology*, 7(1-2-3–4), pp. 115–124. Available at: https://doi.org/10.1093/treephys/7.1-2-3-4.115.

Brodribb, T.J. *et al.* (2016) 'Visual quantification of embolism reveals leaf vulnerability to hydraulic failure', *New Phytologist*, 209(4), pp. 1403–1409. Available at: https://doi.org/10.1111/nph.13846.

Brodribb, T.J. *et al.* (2017) 'Optical Measurement of Stem Xylem Vulnerability', *Plant Physiology*, 174(4), pp. 2054–2061. Available at: https://doi.org/10.1104/pp.17.00552.

Brodribb, T.J. *et al.* (2020) 'Hanging by a thread? Forests and drought', *Science*, 368(6488), pp. 261–266. Available at: https://doi.org/10.1126/science.aat7631.

Brodribb, T.J., Bienaimé, D. and Marmottant, P. (2016) 'Revealing catastrophic failure of leaf networks under stress', *Proceedings of the National Academy of Sciences*, 113(17), pp. 4865–4869. Available at: https://doi.org/10.1073/pnas.1522569113.

Brodribb, T.J. and Cochard, H. (2009) 'Hydraulic Failure Defines the Recovery and Point of Death in Water-Stressed Conifers', *Plant Physiology*, 149(1), pp. 575–584. Available at: https://doi.org/10.1104/pp.108.129783.

Bucci, S.J. *et al.* (2005) 'Mechanisms contributing to seasonal homeostasis of minimum leaf water potential and predawn disequilibrium between soil and plant water potential in Neotropical savanna trees', *Trees*, 19(3), pp. 296–304. Available at: https://doi.org/10.1007/s00468-004-0391-2.

Buckley, T.N. (2005) 'The control of stomata by water balance', *New Phytologist*, 168(2), pp. 275–292. Available at: https://doi.org/10.1111/j.1469-8137.2005.01543.x.

Campbell, G.S. and Norman, J.M. (2000) *An Introduction to Environmental Biophysics*. Springer Science & Business Media.

Cardoso, A.A. *et al.* (2018) 'Coordinated plasticity maintains hydraulic safety in sunflower leaves', *Plant, Cell & Environment*, 41(11), pp. 2567–2576. Available at: https://doi.org/10.1111/pce.13335.

Chen, J.M. and Black, T.A. (1992) 'Defining leaf area index for non-flat leaves', *Plant, Cell & Environment*, 15(4), pp. 421–429. Available at: https://doi.org/10.1111/j.1365-3040.1992.tb00992.x.

Chen, Z. *et al.* (2019) 'Prediction of temperate broadleaf tree species mortality in arid limestone habitats with stomatal safety margins', *Tree Physiology*, 39(8), pp. 1428–1437. Available at: https://doi.org/10.1093/treephys/tpz045.

Choat, B. *et al.* (2012) 'Global convergence in the vulnerability of forests to drought', *Nature*, 491(7426), pp. 752–755. Available at: https://doi.org/10.1038/nature11688.

Choat, B. *et al.* (2018) 'Triggers of tree mortality under drought', *Nature*, 558(7711), pp. 531–539. Available at: https://doi.org/10.1038/s41586-018-0240-x.

Cochard, H. *et al.* (2020) 'SurEau.c : a mechanistic model of plant water relations under extreme drought'. bioRxiv, p. 2020.05.10.086678. Available at: https://doi.org/10.1101/2020.05.10.086678.

Cochard, H. (2021) 'A new mechanism for tree mortality due to drought and heatwaves', *Peer Community Journal*, 1. Available at: https://doi.org/10.24072/pcjournal.45.

Cochard, H. and Delzon, S. (2013) 'Hydraulic failure and repair are not routine in trees', *Annals of Forest Science*, 70(7), pp. 659–661. Available at: https://doi.org/10.1007/s13595-013-0317-5.

Colville, J.F. *et al.* (2020) 'Plant richness, turnover, and evolutionary diversity track gradients of stability and ecological opportunity in a megadiversity center', *Proceedings of the National Academy of Sciences*, 117(33), pp. 20027–20037.

Cowling, R.M. *et al.* (2005) 'Rainfall reliability, a neglected factor in explaining convergence and divergence of plant traits in fire-prone mediterranean-climate ecosystems', *Global ecology and biogeography*, 14(6), pp. 509–519.

Cowling, R.M. *et al.* (2015) 'Variation in plant diversity in mediterranean-climate ecosystems: The role of climatic and topographical stability', *Journal of Biogeography*, 42(3), pp. 552–564.

Cowling, R.M. *et al.* (2017) 'Levyns' Law: explaining the evolution of a remarkable longitudinal gradient in Cape plant diversity', *Transactions of the Royal Society of South Africa*, 72(2), pp. 184–201.

Creek, D. *et al.* (2020) 'Xylem embolism in leaves does not occur with open stomata: evidence from direct observations using the optical visualization technique', *Journal of Experimental Botany*, 71(3), pp. 1151–1159. Available at: https://doi.org/10.1093/jxb/erz474.

Cruiziat, P., Cochard, H. and Améglio, T. (2002) 'Hydraulic architecture of trees: main concepts and results', *Annals of Forest Science*, 59(7), pp. 723–752. Available at: https://doi.org/10.1051/forest:2002060.

Dai, A. (2013) ‘Increasing drought under global warming in observations and models’, *Nature Climate Change*, 3(1), pp. 52–58. Available at: https://doi.org/10.1038/nclimate1633.

Dawson, T.P. *et al.* (2011) ‘Beyond predictions: biodiversity conservation in a changing climate’, *Science*, 332(6025), pp. 53–58.

Dayer, S. *et al.* (2020) ‘The sequence and thresholds of leaf hydraulic traits underlying grapevine varietal differences in drought tolerance’, *Journal of Experimental Botany*. Edited by H. Griffiths, 71(14), pp. 4333–4344. Available at: https://doi.org/10.1093/jxb/eraa186.

DeLucia, E.H. and Berlyn, G.P. (1984) ‘The effect of increasing elevation on leaf cuticle thickness and cuticular transpiration in balsam fir’, *Canadian Journal of Botany*, 62(11), pp. 2423–2431. Available at: https://doi.org/10.1139/b84-331.

Delzon, S. and Cochard, H. (2014) ‘Recent advances in tree hydraulics highlight the ecological significance of the hydraulic safety margin’, *The New Phytologist*, 203(2), pp. 355–358.

Deng, Z. (2015) ‘EXAMINATION OF HYDRODYNAMIC SOIL- PLANT WATER RELATIONS WITH A NEW SPAC MODEL AND REMOTE SENSING EXPERIMENTS’.

Dixon, H.H. and Joly, J. (1997) ‘XII. On the ascent of sap’, *Philosophical Transactions of the Royal Society of London. (B.)*, 186, pp. 563–576. Available at: https://doi.org/10.1098/rstb.1895.0012.

Drake, J.E. *et al.* (2018) ‘Trees tolerate an extreme heatwave via sustained transpirational cooling and increased leaf thermal tolerance’, *Global Change Biology*, 24(6), pp. 2390–2402. Available at: https://doi.org/10.1111/gcb.14037.

Duursma, R.A. *et al.* (2019) ‘On the minimum leaf conductance: its role in models of plant water use, and ecological and environmental controls’, *New Phytologist*, 221(2), pp. 693–705. Available at: https://doi.org/10.1111/nph.15395.

Dynesius, M. and Jansson, R. (2000) ‘Evolutionary consequences of changes in species’ geographical distributions driven by Milankovitch climate oscillations’, *Proceedings of the National Academy of Sciences*, 97(16), pp. 9115–9120.

Eamus, D. *et al.* (2008) ‘Comparing model predictions and experimental data for the response of stomatal conductance and guard cell turgor to manipulations of cuticular conductance, leaf-to-air vapour pressure difference and temperature: feedback mechanisms are able to account

for all observations', *Plant, Cell & Environment*, 31(3), pp. 269–277. Available at: https://doi.org/10.1111/j.1365-3040.2007.01771.x.

Elzhov, T.V. *et al.* (2023) 'minpack.lm: R Interface to the Levenberg-Marquardt Nonlinear Least-Squares Algorithm Found in MINPACK, Plus Support for Bounds'. Available at: https://cran.r-project.org/web/packages/minpack.lm/index.html (Accessed: 11 September 2024).

Fernández, V. *et al.* (2017) 'Physico-chemical properties of plant cuticles and their functional and ecological significance', *Journal of Experimental Botany*, 68(19), pp. 5293–5306. Available at: https://doi.org/10.1093/jxb/erx302.

Flexas, J. and Medrano, H. (2002) 'Drought-inhibition of Photosynthesis in C3 Plants: Stomatal and Non-stomatal Limitations Revisited', *Annals of Botany*, 89(2), pp. 183–189. Available at: https://doi.org/10.1093/aob/mcf027.

Graves, S. and Dorai-Raj, H.-P.P. and L.S. with help from S. (2024) 'multcompView: Visualizations of Paired Comparisons'. Available at: https://cran.r-project.org/web/packages/multcompView/index.html (Accessed: 11 September 2024).

Grolemund, G. and Wickham, H. (2011) 'Dates and Times Made Easy with lubridate', *Journal of Statistical Software*, 40, pp. 1–25. Available at: https://doi.org/10.18637/jss.v040.i03.

Heinsoo, K. and Koppel, A. (1998) 'Minimum epidermal conductance of Norway spruce (Picea abies) needles: influence of age and shoot position in the crown', *Annales Botanici Fennici*, 35(4), pp. 257–262.

Herrick, G.T. and Friedland, A.J. (1991) 'Winter desiccation and injury of subalpine red spruce', *Tree Physiology*, 8(1), pp. 23–36. Available at: https://doi.org/10.1093/treephys/8.1.23.

Hewitson, B.C. and Crane, R.G. (2006) 'Consensus between GCM climate change projections with empirical downscaling: precipitation downscaling over South Africa', *International Journal of Climatology: A Journal of the Royal Meteorological Society*, 26(10), pp. 1315–1337.

Higgins, K.B., Lamb, A.J. and van Wilgen, B.W. (1987) 'Root systems of selected plant species in mesic mountain fynbos in the Jonkershoek Valley, south-western Cape Province',

South African Journal of Botany, https://doi.org/10.1016/S0254-6299(16)31438-7.53(3), pp. 249–257. Available at:

Hinckley, T.M. *et al.* (1983) 'Drought relations of shrub species: assessment of the mechanisms of drought resistance', *Oecologia*, 59(2), pp. 344–350. Available at: https://doi.org/10.1007/BF00378860.

Hochberg, U. *et al.* (2018) 'Iso/Anisohydry: A Plant–Environment Interaction Rather Than a Simple Hydraulic Trait', *Trends in Plant Science*, 23(2), pp. 112–120. Available at: https://doi.org/10.1016/j.tplants.2017.11.002.

Hygen, G. (1951) *Studies in Plant Transpiration I. | Physiologia Plantarum | EBSCOhost*. Available at: https://doi.org/10.1111/j.1399-3054.1951.tb07515.x.

Jacobsen, A.L. *et al.* (2007) 'Xylem density, biomechanics and anatomical traits correlate with water stress in 17 evergreen shrub species of the Mediterranean-type climate region of South Africa', *Journal of Ecology*, 95(1), pp. 171–183. Available at: https://doi.org/10.1111/j.1365-2745.2006.01186.x.

Jacobsen, A.L. *et al.* (2009) 'Water stress tolerance of shrubs in Mediterranean-type climate regions: Convergence of fynbos and succulent karoo communities with California shrub communities', *American Journal of Botany*, 96(8), pp. 1445–1453. Available at: https://doi.org/10.3732/ajb.0800424.

James, A.T., Lawn, R.J. and Cooper, M. (2008) 'Genotypic variation for drought stress response traits in soybean. I. Variation in soybean and wild Glycine spp. for epidermal conductance, osmotic potential, and relative water content', *Australian Journal of Agricultural Research*, 59(7), pp. 656–669. Available at: https://doi.org/10.1071/AR07159.

Jentsch, A., Kreyling, J. and Beierkuhnlein, C. (2007) 'A new generation of climate-change experiments: events, not trends', *Frontiers in Ecology and the Environment*, 5(7), pp. 365–374. Available at: https://doi.org/10.1890/1540-9295(2007)5[365:ANGOCE]2.0.CO;2.

Johnson, D.M. et al. (2018) 'Leaf hydraulic parameters are more plastic in species that experience a wider range of leaf water potentials', Functional Ecology, 32(4), pp. 894–903. Available at: https://doi.org/10.1111/1365-2435.13049.

Jonckheere, I. *et al.* (2004) 'Review of methods for in situ leaf area index determination', *Agricultural and Forest Meteorology*, 121(1–2), pp. 19–35. Available at: https://doi.org/10.1016/j.agrformet.2003.08.027.

Jordan, G.J. and Brodribb, T.J. (2007) 'Incontinence in aging leaves: deteriorating water relations with leaf age in Agastachys odorata (Proteaceae), a shrub with very long-lived leaves', *Functional Plant Biology*, 34(10), pp. 918–924. Available at: https://doi.org/10.1071/FP07166.

Kassambara, A. (2023) 'ggpubr: "ggplot2" Based Publication Ready Plots'. Available at: https://cran.r-project.org/web/packages/ggpubr/index.html (Accessed: 11 September 2024).

Keppel, G. *et al.* (2012) 'Refugia: identifying and understanding safe havens for biodiversity under climate change', *Global ecology and biogeography*, 21(4), pp. 393–404.

Keppel, G. *et al.* (2015) 'The capacity of refugia for conservation planning under climate change', *Frontiers in Ecology and the Environment*, 13(2), pp. 106–112.

Kerstiens, G. (1996) 'Cuticular water permeability and its physiological significance', *Journal of Experimental Botany*, 47(12), pp. 1813–1832. Available at: https://doi.org/10.1093/jxb/47.12.1813.

Klein, T. (2014) 'The variability of stomatal sensitivity to leaf water potential across tree species indicates a continuum between isohydric and anisohydric behaviours', *Functional Ecology*, 28(6), pp. 1313–1320. Available at: https://doi.org/10.1111/1365-2435.12289.

Lens, F. *et al.* (2013) 'Embolism resistance as a key mechanism to understand adaptive plant strategies', *Current Opinion in Plant Biology*, 16(3), pp. 287–292. Available at: https://doi.org/10.1016/j.pbi.2013.02.005.

Levionnois, S. *et al.* (2021) 'Anatomies, vascular architectures, and mechanics underlying the leaf size-stem size spectrum in 42 Neotropical tree species', *Journal of Experimental Botany*, 72(22), pp. 7957–7969. Available at: https://doi.org/10.1093/jxb/erab379.

Li, S. *et al.* (2015) 'Leaf gas exchange performance and the lethal water potential of five European species during drought', *Tree Physiology*. Edited by R. Tognetti, p. tpv117. Available at: https://doi.org/10.1093/treephys/tpv117.

Malone, S.C. *et al.* (2024) 'Water, not carbon, drives drought-constraints on stem terpene defense against simulated bark beetle attack in Pinus edulis', *New Phytologist*, n/a(n/a). Available at: https://doi.org/10.1111/nph.20218.

Manning, J., Goldblatt, P. and Manning, J. (2012) *The Core Cape flora*. Pretoria: SANBI (Plants of the Greater Cape floristic region / John Manning and Peter Goldblatt, 1).

Mantova, M. *et al.* (2022) 'Hydraulic failure and tree mortality: from correlation to causation', *Trends in Plant Science*, 27(4), pp. 335–345. Available at: https://doi.org/10.1016/j.tplants.2021.10.003.

Mantova, M. *et al.* (2023) 'On the path from xylem hydraulic failure to downstream cell death', *New Phytologist*, 237(3), pp. 793–806. Available at: https://doi.org/10.1111/nph.18578.

Marloth, R. (1903) 'RESULTS OF EXPERIMENTS ON TABLE MOUNTAIN FOR ASCERTAINING THE AMOUNT OF MOISTURE DEPOSITED FROM THE SOUTH-EAST CLOUDS', *Transactions of the South African Philosophical Society*, 14(1), pp. 403–408. Available at: https://doi.org/10.1080/21560382.1903.9526032.

Marloth, R. (1905) 'RESULTS OF FURTHER EXPERIMENTS ON TABLE MOUNTAIN FOR ASCERTAINING THE AMOUNT OF MOISTURE DEPOSITED FROM THE SOUTHEAST CLOUDS', *Transactions of the South African Philosophical Society*, 16(1), pp. 97–105. Available at: https://doi.org/10.1080/21560382.1905.9526048.

Martínez-Vilalta, J. *et al.* (2014) 'A new look at water transport regulation in plants', *New Phytologist*, 204(1), pp. 105–115. Available at: https://doi.org/10.1111/nph.12912.

Martinez-Vilalta, J. *et al.* (2019) 'Greater focus on water pools may improve our ability to understand and anticipate drought-induced mortality in plants', *New Phytologist*, 223(1), pp. 22–32. Available at: https://doi.org/10.1111/nph.15644.

Martínez-Vilalta, J. and Garcia-Forner, N. (2017) 'Water potential regulation, stomatal behaviour and hydraulic transport under drought: deconstructing the iso/anisohydric concept', *Plant, Cell & Environment*, 40(6), pp. 962–976. Available at: https://doi.org/10.1111/pce.12846.

Martin-StPaul, N., Delzon, S. and Cochard, H. (2017) 'Plant resistance to drought depends on timely stomatal closure', *Ecology Letters*, 20(11), pp. 1437–1447. Available at: https://doi.org/10.1111/ele.12851.

McDowell, N. *et al.* (2008) 'Mechanisms of plant survival and mortality during drought: why do some plants survive while others succumb to drought?', *New Phytologist*, 178(4), pp. 719–739.

McDowell, N.G. *et al.* (2022) 'Mechanisms of woody-plant mortality under rising drought, CO2 and vapour pressure deficit', *Nature Reviews Earth & Environment*, 3(5). Available at: https://doi.org/10.1038/s43017-022-00272-1.

Meinzer, F.C. et al. (2014) 'Dynamics of leaf water relations components in co-occurring iso- and anisohydric conifer species', Plant, Cell & Environment, 37(11), pp. 2577–2586. Available at: https://doi.org/10.1111/pce.12327.

Meinzer, F.C. *et al.* (2016) 'Mapping "hydroscapes" along the iso- to anisohydric continuum of stomatal regulation of plant water status', *Ecology Letters*, 19(11), pp. 1343–1352. Available at: https://doi.org/10.1111/ele.12670.

Mucina, L. and Rutherford, M.C. (2006) *The vegetation of South Africa, Lesotho and Swaziland*. South African National Biodiversity Institute.

Nagel, J.F. (1956) 'Fog precipitation on table mountain', *Quarterly Journal of the Royal Meteorological Society*, 82(354), pp. 452–460. Available at: https://doi.org/10.1002/qj.49708235408.

Nardini, A. and Salleo, S. (2000) 'Limitation of stomatal conductance by hydraulic traits: sensing or preventing xylem cavitation?', *Trees*, 15(1), pp. 14–24. Available at: https://doi.org/10.1007/s004680000071.

Petek-Petrik, A. *et al.* (2023) 'Drought survival in conifer species is related to the time required to cross the stomatal safety margin', *Journal of Experimental Botany*, p. erad352. Available at: https://doi.org/10.1093/jxb/erad352.

Pineda-García, F., Paz, H. and Meinzer, F.C. (2013) 'Drought resistance in early and late secondary successional species from a tropical dry forest: the interplay between xylem resistance to embolism, sapwood water storage and leaf shedding', *Plant, Cell & Environment*, 36(2), pp. 405–418. Available at: https://doi.org/10.1111/j.1365-3040.2012.02582.x.

Pivovaroff, A.L. *et al.* (2016) 'Multiple strategies for drought survival among woody plant species', *Functional Ecology*, 30(4), pp. 517–526. Available at: https://doi.org/10.1111/1365-2435.12518.

R Core Team (2020) 'R: The R Project for Statistical Computing'. Available at: https://www.r-project.org/ (Accessed: 11 September 2024).

Resco, V. *et al.* (2009) 'Drought-induced hydraulic limitations constrain leaf gas exchange recovery after precipitation pulses in the C3 woody legume, Prosopis velutina', *New Phytologist*, 181(3), pp. 672–682. Available at: https://doi.org/10.1111/j.1469-8137.2008.02687.x.

Riederer, M. and Muller, C. (2008) *Annual Plant Reviews, Biology of the Plant Cuticle*. John Wiley & Sons.

Sack, L. and Holbrook, N.M. (2006) 'LEAF HYDRAULICS', *Annual Review of Plant Biology*, 57(Volume 57, 2006), pp. 361–381. Available at: https://doi.org/10.1146/annurev.arplant.56.032604.144141.

Sack, L. and Scoffoni, C. (2010) *Minimum epidermal conductance (gmin, a.k.a. cuticular conductance)*, *PROMETHEUS*. Available at: https://prometheusprotocols.net/function/gas-exchange-and-chlorophyll-fluorescence/stomatal-and-non-stomatal-conductance-and-transpiration/minimum-epidermal-conductance-gmin-a-k-a-cuticular-conductance/ (Accessed: 2 September 2024).

Salomón, R.L. *et al.* (2017) 'Stem hydraulic capacitance decreases with drought stress: implications for modelling tree hydraulics in the Mediterranean oak Quercus ilex', *Plant, Cell & Environment*, 40(8), pp. 1379–1391. Available at: https://doi.org/10.1111/pce.12928.

Schneider, C.A., Rasband, W.S. and Eliceiri, K.W. (2012) 'NIH Image to ImageJ: 25 years of image analysis', *Nature Methods*, 9(7), pp. 671–675. Available at: https://doi.org/10.1038/nmeth.2089.

Scholz, F.G. *et al.* (2011) 'Hydraulic Capacitance: Biophysics and Functional Significance of Internal Water Sources in Relation to Tree Size', in F.C. Meinzer, B. Lachenbruch, and T.E. Dawson (eds) *Size- and Age-Related Changes in Tree Structure and Function*. Dordrecht: Springer Netherlands, pp. 341–361. Available at: https://doi.org/10.1007/978-94-007-1242-3_13.

Schuster, A.-C. *et al.* (2016) 'Effectiveness of cuticular transpiration barriers in a desert plant at controlling water loss at high temperatures', *AoB PLANTS*, 8, p. plw027. Available at: https://doi.org/10.1093/aobpla/plw027.

Schuster, A.-C., Burghardt, M. and Riederer, M. (2017) 'The ecophysiology of leaf cuticular transpiration: are cuticular water permeabilities adapted to ecological conditions?', *Journal of Experimental Botany*, 68(19), pp. 5271–5279. Available at: https://doi.org/10.1093/jxb/erx321.

Sinclair, T.R. and Ludlow, M.M. (1986) 'Influence of Soil Water Supply on the Plant Water Balance of Four Tropical Grain Legumes', *Functional Plant Biology*, 13(3), pp. 329–341. Available at: https://doi.org/10.1071/pp9860329.

Skelton, R.P. *et al.* (2018) 'Low Vulnerability to Xylem Embolism in Leaves and Stems of North American Oaks', *Plant Physiology*, 177(3), pp. 1066–1077. Available at: https://doi.org/10.1104/pp.18.00103.

Skelton, R.P. *et al.* (2023) 'Consistent responses to moisture stress despite diverse growth forms within mountain fynbos communities', *Oecologia*, pp. 1–17.

Skelton, R.P., West, A.G. and Dawson, T.E. (2015) 'Predicting plant vulnerability to drought in biodiverse regions using functional traits', *Proceedings of the National Academy of Sciences*, 112(18), pp. 5744–5749. Available at: https://doi.org/10.1073/pnas.1503376112.

Smith, N.J. (1991) 'Predicting Radiation Attenuation in Stands of Douglas-Fir', *Forest Science*, 37(5), pp. 1213–1223. Available at: https://doi.org/10.1093/forestscience/37.5.1213.

Sorek, Y. *et al.* (2021) 'An increase in xylem embolism resistance of grapevine leaves during the growing season is coordinated with stomatal regulation, turgor loss point and intervessel pit membranes', *New Phytologist*, 229(4), pp. 1955–1969. Available at: https://doi.org/10.1111/nph.17025.

Sperry, J.S. (1995) '5 - Limitations on Stem Water Transport and Their Consequences', in B.L. Gartner (ed.) *Plant Stems*. San Diego: Academic Press (Physiological Ecology), pp. 105–124. Available at: https://doi.org/10.1016/B978-012276460-8/50007-2.

Sperry, J.S. (2004) 'Coordinating stomatal and xylem functioning – an evolutionary perspective', *New Phytologist*, 162(3), pp. 568–570. Available at: https://doi.org/10.1111/j.1469-8137.2004.01072.x.

Sperry, J.S., Donnelly, J.R. and Tyree, M.T. (1988) 'A method for measuring hydraulic conductivity and embolism in xylem', *Plant, Cell & Environment*, 11(1), pp. 35–40. Available at: https://doi.org/10.1111/j.1365-3040.1988.tb01774.x.

Tadross, M., Jack, C. and Hewitson, B. (2005) 'On RCM-based projections of change in southern African summer climate', *Geophysical Research Letters*, 32(23).

Tardieu, F. *et al.* (1997) 'Will increases in our understanding of soil-root relations and root signalling substantially alter water flux models?', *Philosophical Transactions of the Royal*

Society of London. Series B: Biological Sciences, 341(1295), pp. 57–66. Available at: https://doi.org/10.1098/rstb.1993.0091.

Tardieu, F. and Simonneau, T. (1998) 'Variability among species of stomatal control under fluctuating soil water status and evaporative demand: modelling isohydric and anisohydric behaviours', *Journal of Experimental Botany*, 49, pp. 419–432.

Trenberth, K.E. (2011) 'Changes in precipitation with climate change', *Climate Research*, 47(1–2), pp. 123–138. Available at: https://doi.org/10.3354/cr00953.

Trifilò, P. *et al.* (2015) 'Diurnal changes in embolism rate in nine dry forest trees: relationships with species-specific xylem vulnerability, hydraulic strategy and wood traits', *Tree Physiology*. Edited by F. Meinzer, 35(7), pp. 694–705. Available at: https://doi.org/10.1093/treephys/tpv049.

Tyree, M.T. and Hammel, H.T. (1972) 'The Measurement of the Turgor Pressure and the Water Relations of Plants by the Pressure-bomb Technique', *Journal of Experimental Botany*, 23(74), pp. 267–282.

Tyree, M.T. and Zimmermann, M.H. (2002) *Xylem Structure and the Ascent of Sap*. Springer Science & Business Media.

Urli, M. *et al.* (2013) 'Xylem embolism threshold for catastrophic hydraulic failure in angiosperm trees', *Tree Physiology*, 33(7), pp. 672–683. Available at: https://doi.org/10.1093/treephys/tpt030.

Volaire, F. (2018) 'A unified framework of plant adaptive strategies to drought: Crossing scales and disciplines', *Global Change Biology*, 24(7), pp. 2929–2938. Available at: https://doi.org/10.1111/gcb.14062.

Watson, D.J. (1947) 'Comparative Physiological Studies on the Growth of Field Crops: I. Variation in Net Assimilation Rate and Leaf Area between Species and Varieties, and within and between Years', *Annals of Botany*, 11(41), pp. 41–76.

West, A.G. *et al.* (2012) 'Diverse functional responses to drought in a Mediterranean-type shrubland in South Africa', *New Phytologist*, 195(2), pp. 396–407.

West, A.G. *et al.* (2024) 'Assessing vulnerability to embolism and hydraulic safety margins in reed-like Restionaceae', *Plant Biology*, 26(4), pp. 633–646. Available at: https://doi.org/10.1111/plb.13644.

West, D.W. and Gaff, D.F. (1976) ‘The Effect of Leaf Water Potential, Leaf Temperature and Light Intensity on Leaf Diffusion Resistance and the Transpiration of Leaves of Malus sylvestris’, *Physiologia Plantarum*, 38(2), pp. 98–104. Available at: https://doi.org/10.1111/j.1399-3054.1976.tb04866.x.

Wickham, H. *et al.* (2019) ‘Welcome to the Tidyverse’, *Journal of Open Source Software*, 4(43), p. 1686. Available at: https://doi.org/10.21105/joss.01686.

Wickham, H., François, R., *et al.* (2023) ‘dplyr: A Grammar of Data Manipulation’. Available at: https://cran.r-project.org/web/packages/dplyr/index.html (Accessed: 11 September 2024).

Wickham, H., Bryan, J., *et al.* (2023) ‘readxl: Read Excel Files’. Available at: https://cran.r-project.org/web/packages/readxl/index.html (Accessed: 11 September 2024).

Wilke, C.O. (2024) ‘cowplot: Streamlined Plot Theme and Plot Annotations for “ggplot2”’. Available at: https://cran.r-project.org/web/packages/cowplot/index.html (Accessed: 11 September 2024).

Wolfe, B.T., Sperry, J.S. and Kursar, T.A. (2016) ‘Does leaf shedding protect stems from cavitation during seasonal droughts? A test of the hydraulic fuse hypothesis’, *New Phytologist*, 212(4), pp. 1007–1018. Available at: https://doi.org/10.1111/nph.14087.

Ziegler, C. *et al.* (2023) ‘Large leaf hydraulic safety margins limit the risk of drought-induced leaf hydraulic dysfunction in Neotropical rainforest canopy tree species’, *Functional Ecology*, 37(6), pp. 1717–1731. Available at: https://doi.org/10.1111/1365-2435.14325.

Ziegler, C. *et al.* (2024) ‘Residual water losses mediate the trade-off between growth and drought survival across saplings of 12 tropical rainforest tree species with contrasting hydraulic strategies’, *Journal of Experimental Botany*, 75(13), pp. 4128–4147. Available at: https://doi.org/10.1093/jxb/erae159.

Zufferey, V. *et al.* (2011) ‘Diurnal cycles of embolism formation and repair in petioles of grapevine (Vitis vinifera cv. Chasselas)’, *Journal of Experimental Botany*, 62(11), pp. 3885–3894. Available at: https://doi.org/10.1093/jxb/err081.